Molecular and ecological investigations of Caribbean sponge diseases

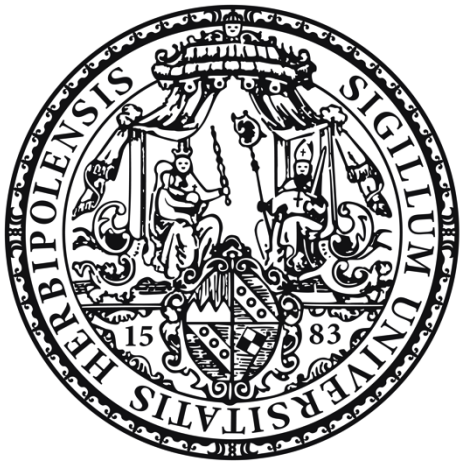

Molekulare und ökologische Untersuchungen zu Krankheiten Karibischer Meeresschwämme

Dissertation for a Doctoral Degree

at the Graduate School of Life Sciences,

Julius-Maximilians-Universität Würzburg,

Section: Infection & Immunity

Submitted by

Hilde Gabriele Angermeier

from

Ansbach

Würzburg, May 2011

Submitted on:

Members of the Promotionscommittee:

Chairperson: Prof. Dr. Thomas Müller

Primary Supervisor: Prof. Dr. Ute Hentschel Humeida

Supervisor (Second): Prof. Dr. Georg Krohne

Supervisor (Third): Prof. Dr. Joseph R. Pawlik

Supervisor (Fourth): Prof. Dr. Micha Ilan

Date of Public Defence:

Date of Receipt of Certificates:

Affidavit

I hereby declare that my thesis entitled “Molecular and ecological investigations of Caribbean sponge diseases” is the result of my own work. I did not receive any help or support from commercial consultants. All sources and / or materials applied are listed and specified in the thesis.

Furthermore, I verify that this thesis has not yet been submitted as part of another examination process neither in identical nor in similar form.

Würzburg, May 2011 (Hilde Angermeier)

Eidesstattliche Erklärung

Hiermit erkläre ich an Eides statt, die Dissertation „Molekulare und ökologische Untersuchungen zu Krankheiten Karibischer Meeresschwämme“ eigenständig, d.h. insbesondere selbstständig und ohne Hilfe eines komerziellen Promotionsberaters, angefertigt und keine anderen als die von mir angegebenen Quellen und Hilfsmittel verwendet zu haben.

Ich erkläre außerdem, dass die Dissertation weder in gleicher noch in ähnlicher Form bereits in einem anderen Prüfungsverfahren vorgelegen hat.

Würzburg, May 2011 (Hilde Angermeier)

Acknowledgments

Subsequently, I want to express my deepest gratitude to the following persons:

Prof. Ute Hentschel Humeida for sparking my passion for marine sponges by sending me in August 2006 to a joint summer academy of BIOTECmarin and the Marie Curie Research Training Network, where I had the chance to get first time my hands wet in a scientific sense during sponge work inside and outside the Limski channel. Already during my diploma thesis her intriguing stories on bleaching of the giant barrel sponge *X. muta* fascinated me, so that I applied for a scholarship of the **Graduate School of Life Sciences (GSLS) at the University of Würzburg**. Prof. Hentschel Humeida gave me, based on this stipend, vast opportunities to participate at research expeditions for in situ field work on Caribbean sponge diseases. In addition, I was amply given the chance to take part at sponge summer schools and to present my projects at various international symposia such as the 8th World Sponge Conference 2010 or the EURO Symposium 2011 of the International Society for Reef Studies (ISRS). Prof. Hentschel's always positive attitude and trust encouraged me and strengthened together with the growings tasks my personality strongly.

Prof. Georg Krohne for being an inspiring second supervisor full of scientific passion as well as his team **Daniela Bunsen and Claudia Gehrig** for excellent assistance within the departement of electron microscopy.

Prof. Joseph Pawlik (UNCW, USA) for being an exemplar third supervisor, with whom it was a great pleasure to collaborate with on bleaching of the giant barrel sponge *X. muta* and the erect rope sponge *A. compressa*. He invited me twice to research expeditions throughout the Bahamas onboard the RV Seward Johnson (HBOI) and once to field-work at NOAA´s Undersea Research Center (NURC). Thus, I gratefully acknowledge as well the underlying **marine operations personnel** at NURC and onboard the RV Seward Johnson for their excellent support. In addition, I thank **S.E. McMurray** (UNCW) and **Prof. Christopher Finelli** (UNCW) for their professional assistance with the *X. muta* story in the field and beyond.

Prof. Micha Ilan (Tel Aviv University, Israel) for being a fascinating fourth supervisor and a great consultant whenever we met. He conferred his passion for marine life and science on me.

Prof. Niels Lindquist and Prof. Christopher Martens (University of North Carolina at Chapel Hill (UNC-CH), USA) for their friendliness of hosting me during their research expedition to NURC in September 2009 and for providing me with constructive ideas whenever needed.

Usama R. Abdelmohsen for his help with high performance liquid chromatography (HPLC), **Volker Glöckner** for his overall support especially during field work, **Franziska Lampmann** for her molecular efforts during the *A. compressa* studies and **Janine Kamke** for her excellent assistance with phylogenetic tree construction.

My colleagues and friends of the last years: **Dr. Sheila Pimentel-Elardo**, **Dr. Alexander Siegl**, **Dr. Susanne Schmitt**, **Dr. Kristina Bayer**, **Dr. Naseem Muhammad**, **Paula Tabares**, **Lucas Moitinho e Silva**, **Christine Gernert**, **Odette Szasz** and **Eva Reisberg**.

Additionally, **my colleagues** from the Research Center for Infectious Diseases (ZINF) & the Institute for Molecular Infection Biology (IMIB) as well as from the Julius-von-Sachs-Institute at the Julius-Maximilians-University of Würzburg, Germany.

Prof. Dr. Dr. Jörg Hacker and **Prof. Dr. Markus Riederer** for their scientific hospitality.

Prof. Tyler Smith (University of the Virgin Islands, USA) and **Lauren Siba** (Misool Eco Resort, Indonesia) for sharing information on the most recent disease outbreaks affecting *Xestospongia* species within the Caribbean and the Indo-Pacific.

Frank Michels (UW-PSD) for assistance with image editing of the underwater photographs.

Above all, I want to thank my **family and friends** for making me the person that I am and in particular **my parents**, Barbara & Johann Angermeier, for their infinite support and faith into my dreams.

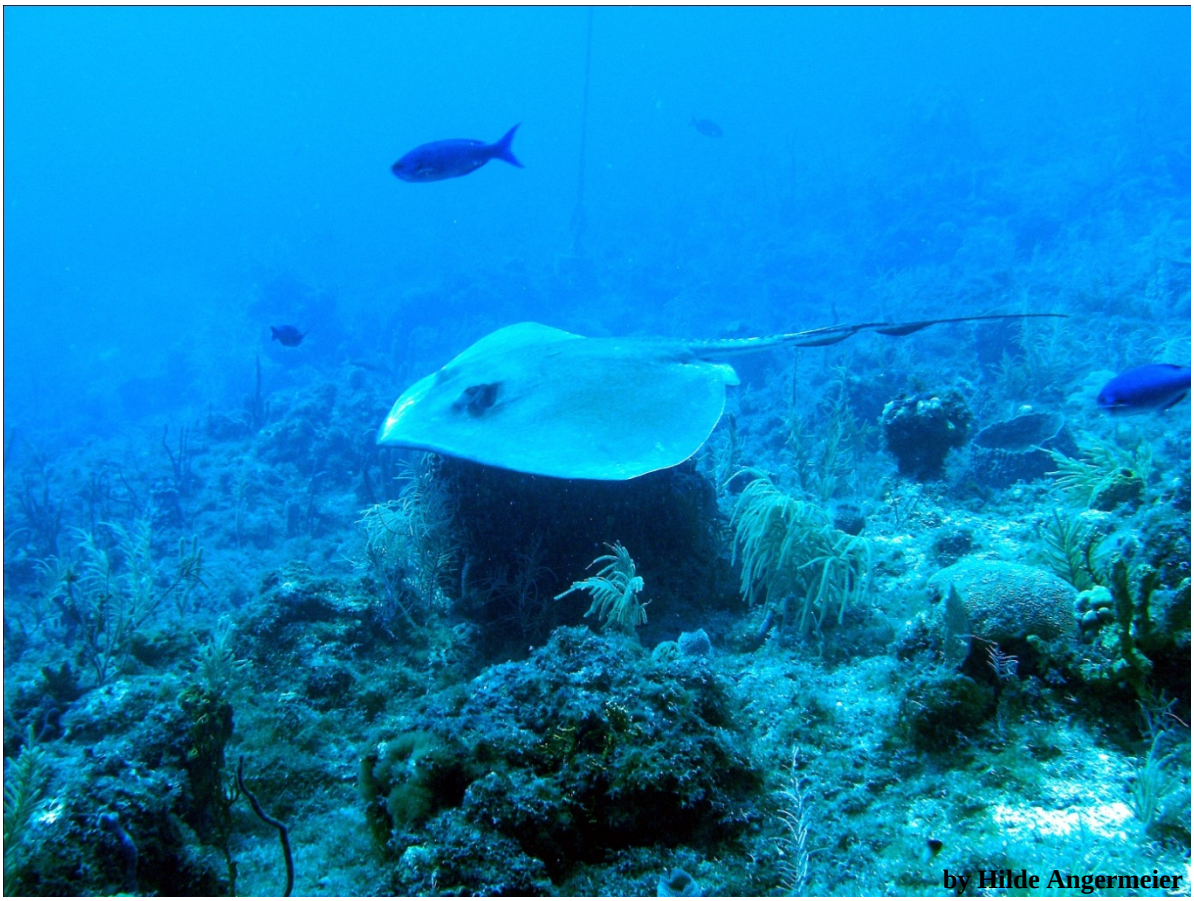

Das Herz gleicht ganz dem Meere
hat Ebbe, Sturm und Flut
und manche schöne Perle,
die in der Tiefe ruht…

(Unbekannter Autor)

Für Meine Eltern,
Barbara & Johann Angermeier

Table of contents

I. Summary

While beneficial sponge-microbe associations have received much attention in recent years, less effort has been undertaken to investigate the interactions of sponges with potentially pathogenic microorganisms. Thus, the aim of this study was to examine two selected Caribbean disease conditions, termed “Sponge Orange Band” and “Sponge White Patch”, via ecological and molecular methods. Sponge Orange Band (SOB) disease affects the prominent Caribbean barrel sponge *Xestospongia muta* that is counted among the high-microbial-abundance (HMA) sponges, whereas Sponge White Patch (SWP) disease affects the abundant rope sponge *Amphimedon compressa* that belongs to the low-microbial-abundance (LMA) sponges.

Sponge Orange Band disease is characterized by gradual discoloration of the sponge’s surface tissue ranging from healthy brown to bleached white. It is frequently accompanied by an orange band-like transition zone. The disease leads to visual degradation and results in the collapse of the entire sponge within only up to six weeks. Electron microscopy revealed that the color loss is accompanied by massive destruction of the pinacoderm leaving only spicules and detritus behind. Chlorophyll *a* content as determined by spectrophotometry and the characteristic *X. muta* secondary metabolites as measured by HPLC were significantly lower in bleached than in healthy tissues. Denaturing gradient gel electrophoresis (DGGE) using cyanobacteria-specific 16S rDNA primers revealed a distinct shift in that the *Synechococcus/Prochlorococcus* clade of sponge symbionts was absent in the bleached tissues while several clades of unspecific cyanobacteria, including lineages associated with coral disease (i.e., *Leptolyngbya*), had invaded. DGGE using eubacteria-specific 16S rDNA primers revealed no evidence for the appearance of what might be considered a bacterial pathogen. Moreover, the eubacterial community profiles of diseased individuals were highly variable, unlike to those of healthy sponges. Terminatory, underwater infection experiments were conducted by transplanting bleached cores into healthy *X. muta* individuals which were then monitored regularly by Scuba diving for up to eleven days. No visual signs of disease developed, rather the surfaces around the tissue implants started to heal up.

On the contrary, Sponge White Patch disease affects the naturally dark red rope sponge *Amphimedon compressa.* It is characterized by distinctive white patches that are found irregularly on diseased individuals. However, no transition zone occurs. Affected sponges

seem to recover by discharge of diseased tissue. In winter 2007 up to 1/5th of an individual was shown to be infested by disease at Dry Rocks Reef, Florida, afflicting as much as 18% of the entire *A. compressa* population. Electron microscopy revealed severe degradation within the bleached tissues as well as the presence of spongin-boring bacteria solely within the white but not the red parts, either healthy or affected. Profiling microbial community changes by DGGE revealed a fairly consistent banding pattern within healthy *A. compressa* sponges and the red parts of SWP-diseased individuals. This consistent profile had shifted within the white parts of diseased individuals by the presence of additional bands. Thus, we isolated bacterial strains from the white patches of diseased *A. compressa* individuals into pure culture via collagen-containing media and compared their microbial fingerprints via DGGE to the one obtained from the white patch material. Suitable strains of interest were injected during in situ infection trials. In addition, underwater infection experiments were performed by the attachment of diseased tissue to healthy *A. compressa* sponges. Both trials did not evoke a disease phenotype. It thus seems that SWP disease of *A. compressa* is neither contagious nor due to microbial infection.

In conclusion, I have documented for both Caribbean sponge diseases, Sponge Orange Band affecting the HMA-sponge *X. muta* as well as Sponge White Patch affecting the LMA-sponge *A. compressa*, a disease progression going along with massive tissue destruction as well as loss of the characteristic microbial signatures. Even though new bacteria were shown to colonize the bleached areas, the infection trials revealed in both cases no indication for the involvement of a microbial pathogen as an etiologic agent of disease leaving us still in the dark about the cause of Sponge Orange Band as well as Sponge White Patch disease.

Zusammenfassung

Während gewinnbringende Assoziationen von Schwämmen mit Mikroorganismen in den letzten Jahren viel Aufmerksamkeit erhalten haben, wurde weit weniger in die Interaktion von Schwämmen mit möglicherweise pathogenen Mikroben investiert. Somit war es das Ziel dieser Studie zwei ausgewählte Karibische Schwammkrankheiten namens „*Sponge Orange Band*“ und „*Sponge White Patch*“ mittels ökologischer und molekularer Methoden zu untersuchen. Die *Sponge Orange Band* (SOB) Erkrankung befällt den bedeutenden karibischen Fass-Schwamm *Xestospongia muta*, der zu den bakterienhaltigen (HMA) Schwämmen gezählt wird, während die *Sponge White Patch* (SWP) Erkrankung den häufig vorkommenden Seil-Schwamm *Amphimedon compressa* betrifft, der zu den bakterienarmen (LMA) Schwämmen gehört. Für die Erkrankung *Sponge Orange Band* ist eine graduelle Entfärbung des Oberflächengewebes vom gesunden Braun zum gebleichten Weiß charakteristisch. Eine Übergangszone, die an eine orange Bande erinnert, ist eine häufige Begleiterscheinung. Die Krankheit führt zur sichtbaren Degeneration und resultiert innerhalb von nur sechs Wochen im Zusammenbruch des gesamten Schwammes. Elektronenmikroskopie bewies, dass der Farbverlust mit einer massiven Zerstörung des Pinacoderms einher geht, die nur Spiculae und Detritus zurück lässt. Sowohl der mittels Spektrophotometrie ermittelte Chlorophyll *a* Gehalt als auch die *X. muta* spezifischen Sekundärmetabolite, die anhand von HPLC nachgewiesen wurden, wiesen beide signifikant niedrigere Werte in gebleichten als in gesunden Geweben auf. Denaturierende Gradienten Gelelektrophorese (DGGE) mit Cyanobakterien-spezifischen 16S rDNA Primern verriet eine abrupte Verschiebung. Sie bestand darin, dass die *Synechococcus/Prochlorococcus* Klade der Schwammsymbionten in den gebleichten Geweben fehlte, wohingegen sie durch einige Kladen unspezifischer Cyanobakterien, inklusive mit Korallenkrankheiten assoziierte Bakterienstämme (wie zum Beispiel *Leptolyngbya*), ersetzt war. DGGE mit Eubakterien-spezifischen 16S rDNA Primern erbrachte keinen Beweis für das Vorhandensein eines möglicherweise bakteriellen Pathogens. Darüber hinaus waren die Profile der eubakteriellen Gemeinschaft innerhalb kranker Individuen höchst variabel, ganz im Gegensatz zu denen gesunder Schwämme. Abschließend wurden Infektionsexperimente unter Wasser durchgeführt, indem gebleichte Gewebskerne in gesunde *X. muta* Individuen transplantiert wurden. Diese wurden regelmäßig mittels SCUBA Tauchgängen über einen Zeitraum von bis zu elf Tagen kontrolliert. Es entwickelten sich keine sichtbaren Krankheitssymptome, stattdessen schien das Oberflächengewebe um die Fremdtransplantate herum zu heilen.

Die Erkrankung *Sponge White Patch* im Gegensatz befällt den natürlicherweise tiefroten Seilschwamm *Amphimedon compressa*. Sie ist charakterisiert durch unverkennbare weiße Flecken, die sich unregelmäßig auf den kranken Individuen verteilen. Jedoch tritt keine Übergangszone auf. Befallene Schwämme scheinen sich von der Krankheit zu erholen, indem sie das kranke Gewebe abstoßen. Folgende Werte wurden im Winter 2007 für das Dry Rocks Riff in Florida ermittelt: die gesamte *A. compressa* Population war zu 18% von der Krankheit befallen und ein einzelnes Individuum mit bis zu einem Fünftel seiner Biomasse. Elektronenmikroskopie stellte eine hochgradige Zerstörung innerhalb der gebleichten Gewebe dar und verwies auf das Vorhandensein von Spongin-bohrenden Bakterien. Diese waren allerdings nur innerhalb der weißen und nicht innerhalb der roten Bereiche lokalisiert, davon unabhängig ob letztere zu einem gesunden oder zu einem betroffenen Schwamm gehörten. Veränderungen innerhalb der bakteriellen Schwammgemeinschaft wurden anhand von DGGE-Profilen festgehalten. Die gesunden *A. compressa* Schwämme und die roten Bereiche SWP-erkrankter Individuen wiesen ein ziemlich konstantes Bandenmuster auf. Dieses einheitliche Profil hatte sich allerdings in den weißen Bereichen der kranken Schwämme durch die Anwesenheit zusätzlicher Banden verlagert. Deshalb isolierten wir aus den weißen Stellen kranker *A. compressa* Individuen bakterielle Stämme, die wir anhand von Kollagen-enthaltenden Medien in Reinkultur brachten und deren mikrobielle Fingerabdrücke wir mittels DGGE mit denen des weißen Schwammgewebes verglichen. Ausgewählte Stämme mit geeignetem Profil wurden während in situ Infektionsversuchen in gesunde Schwammindividuen injiziert. Zusätzlich wurde in Unterwasser-Infektionsexperimenten krankes Gewebe an gesunden *A. compressa* Schwämmen befestigt. Beide Versuche verursachten keinen der Krankheit entsprechenden Phänotyp. Das heißt, dass die SWP-Erkrankung von *A. compressa* weder ansteckend noch von einer mikrobiellen Infektion hervorgerufen zu sein scheint.

Abschließend ist anzumerken, dass ich für beide Karibischen Schwammkrankheiten, sowohl für *Sponge Orange Band* des HMA-Schwammes *X. muta* als auch für *Sponge White Patch* des LMA-Schwammes *A. compressa*, einen Krankheitsverlauf beschreiben konnte, der mit massiver Gewebszerstörung und dem Verlust charakteristischer mikrobieller Signaturen einhergeht. Obwohl ich zeigen konnte, dass zusätzliche Bakterienarten die gebleichten Schwammbereiche kolonisieren, lieferten meine Infektionsversuche in beiden Fällen keinen Beweis für die Beteiligung eines mikrobiellen Pathogens als Krankheitserreger. Somit liegen die eigentlichen Auslöser der Erkrankungen *Sponge Orange Band* als auch *Sponge White Patch* noch immer im Dunkeln.

II. Introduction

1. Marine sponges - the phylum *Porifera*

1.1 Taxonomy

The phylum *Porifera* comprises all freshwater as well as marine sponges and owns its name to R. E. Grant, who derived it in the nineteenth century from the Latin words “porus” and “ferre” which describe the pore-bearing characteristics of these suspension-feeding animals (Brusca and Brusca, 1990). First fossil records of sponges were detected in South Chinese rock deposits of Precambrian times dating back some 580 million years ago. They underline the importance of this phylum during the metazoan evolution and rank them among the evolutionarily most deeply-branching multicellular organisms (Li *et al.*, 1998). In general, sponges are sessile, filter-feeding animals, which use flagellated cells, termed choanocytes, to create a water current throughout their bodies, which are comprised of a complex water canal system (Bergquist, 1978; Brusca and Brusca, 1990). Though sponges are counted among the metazoa, they lack a nervous system, muscle- and sensory cells as well as real organs. Instead, they are equipped with a unique bauplan that is characterized by variable reproductive modes as well as cellular totipotency and mobility balancing the lack of true tissues and organs. However, their unicellular grade of complexity, the presence of sponge-specific flagella-bearing choanocytes as well as their response towards environmental stimuli all point towards a direct ancestry of sponges from protozoa during the onset of the metazoan evolution. As a consequence, the sponges are grouped among the diploblastic Parazoa, which are a neighbouring group of the Eumetazoa (Lévi, 1970; Bergquist, 1985; Brusca and Brusca, 1990; Willmer, 1990; Wehner and Gehring, 1995; Fieseler *et al.*, 2004). However, the fact that in sponges also genes and proteins were detected that fulfill functions in multicellular animals and that are highly homologous to the ones of higher animals, underlines the important role this phylum plays in evolution (Müller, 1998; Böhm *et al.*, 2000; Müller *et al.*, 2002).

The *Porifera* are divided into three classes: the Calcarea (calcareous sponges), the Hexactinellida (glass sponges) and the Demospongiae (demosponges). The latter is the most comprehensive and variable class covering about 95% of all sponge species (Brusca and Brusca, 1990). About 6000 living species of the *Porifera* are currently described, but the true diversity is estimated to be rather around 15 000 species. Sponges can be detected from

tropical to subtropical coral reefs over temperate waters until even polar regions and from shallow depths until the deep sea (Hooper and van Soest, 2002). Remarkably, 150 species of Demospongiae are constricted to freshwater rivers and lakes (Bergquist, 1978; Brusca and Brusca, 1990).

A typical sponge is normally vase-shaped. However, its morphotype is often adapted to the conditions of the environment. For example where the water current is strong, sponges are frequently in shapes of lobes, tubes, vases and golf-balls or even of an encrusting type. In contrast, where the current is low, sponges are fan-shaped or have a branched structure. The size of sponges spans from only few millimeters to over one meter in height and diameter (Humann, 1992; Jung, 1996). In addition, representatives of the *Porifera* can possess all kinds of colors. I have personally observed them to range from white over yellow, orange, red, violet, blue and green to brown, black and grey. Even fluorescent and polymorphic species can be detected (Jung, 1996). An overview of the great diversity in sponge shape, size and coloration that I encountered in the Caribbean Sea is shown in Figure 1.

1.2 Morphology

Sponges possess a basic bauplan (Bergquist, 1978; Simpson, 1984; Brusca and Brusca, 1990). They consist out of two epithelia: an outer pinacoderm comprised of pinacocytes lining their surface and an inner choanoderm built up by choanocytes, which are responsible for the uptake of nutrition via pino- and phagocytosis into vesicles by flagella and microvilli. Endopinacocytes are a special type of pinacocytes that are covering the surface of the water channels within the sponge. The mesohyl of the sponge is its main component and determines its weight and size. It is located in between the pinacoderm and the choanoderm. Digestion, the uptake of nutrition and the disposal of waste- or reproductive products as well as the secretion of the sponge skeleton takes place therein. The mesohyl is composed of a colloidal fluid called mesogloea that harbours collagen fibers, spicules and numerous amoebocytes. The latter can take over various cellular forms and functions. With the exception of one family of carnivorous, prey-catching sponges, all representatives of the phylum *Porifera* are sessile filter feeders pumping thousands of litres of seawater per day through the aquiferous canals that are embedded within the sponge body (Simpson, 1984). The beating of the choanocytes promotes the flow of seawater through numerous ostia into the pinacoderm

(Brusca and Brusca, 1990). Only food particles of 0.1 to 50µm in size can be taken up by the sponge due to the limited width of the ostia. Particles of 2-5µm in size are phagocytozed di-

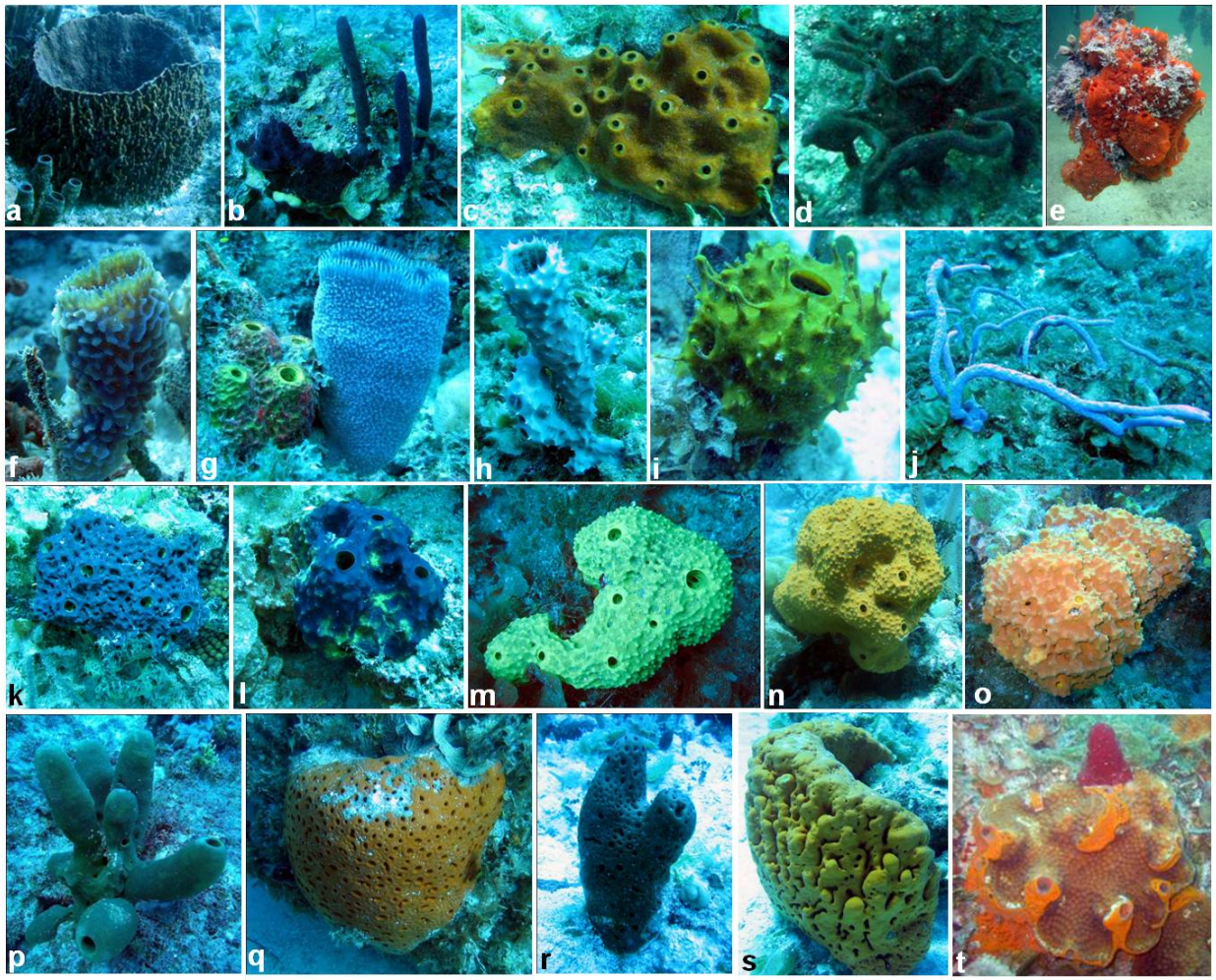

Fig. 1. An overview of the diversity within the phylum *Porifera*: The barrel sponge *Xestospongia muta* (a), the rope sponge *Amphimedon compressa* (b), the encrusting sponge *Ectyoplasia ferox* (c), the vase sponge *Cribrochalina vasculum* (d), the mangrove sponge *Tedania ignis* (e), the tube sponges *Callyspongia plicifera* (f), *Niphates digitalis* (g), *Callyspongia vaginalis* (h), *Aplysina fistularis* (i), the rope sponge *Aplysina cauliformis* (j), the five differently colored morphotypes of the lobular sponge *Aiolochroia crassa* (k-o) as well as the marine tube- or lobular sponges *Agelas conifera* (p), *Agelas clathrodes* (q), *Agelas dispar* (r) and *Agelas cerebrum* (s) as well as the boring sponge *Mycale laevis* (t).

rectly by archaeocytes lining the water channels. If they are 0.1-0.2 µm in size, they can enter the sponge and are taken up by choanocytes (Brusca and Brusca, 1990). Those filter out bacteria and cyanobacteria (Reiswig, 1971; Pile *et al.*, 1996; Pile, 1997), marine viruses (Hadas *et al.*, 2006) and bigger sized organisms like yeast cells, ciliates, flagellates and even diatoms via phagocytosis and pass them over to the archaeocytes (Frost, 1978; Imsiecke, 1993; Pile *et al.*, 1996; Ribes *et al.*, 1999). The majority of a sponge's diet is comprised of pico- (0.1-2µm in size) and nanoplankton (2-20µm in size) (Reiswig, 1971, 1975, 1990; Pile *et al.*, 1996; Pile, 1997; Ribes *et al.*, 1999; Kowalke, 2000), but also of organic matter (Reiswig, 1971) including large particles (Willenz and Van de Vyver, 1984). The digestion of sponges takes place intracellularly via phago- and pinocytosis. At the end, the sponge expels undigestable material through its osculum (Brusca and Brusca, 1990; Wehrl *et al.*, 2007). Depending on the sponge species, one to several oscula of variable size can be present.

The skeleton of a sponge stabilizes the sponge body and enlarges the surface area. It consists out of an organic and an inorganic component (Brusca and Brusca, 1990; Wehner and Gehring, 1995). Sclerocytes are responsible for the production of the inorganic component, which is comprised by calcareous or silica-containing spicules. The organic component, collagen, is provided by collencytes, lophocytes and spongocytes. One special type of collagen, called spongin, is produced by spongocytes and is located within the mesohyl, which consists mostly out of extracellular matrix. It exists exclusively in the class Demospongiae. In addition, myocytes are specialized cells within the mesohyl that regulate the contraction of the aquiferous canals or oscula. However, the most important sponge cells are the archaeocytes. They are amoeboid cells of about 5-50µm in size that can practically differentiate into any other specialized sponge cell. In addition, they are highly motile. They play an important role in the destruction of food particles via numerous enzymes, the transport of nutrients, digestion and excretion as well as in asexuell sponge reproduction. Also the system of the aquiferous canals is very essential to the sponge, as it is responsible for the nutrional uptake and the gas exchange (Brusca and Brusca, 1990; Jung, 1996). The reproduction of sponges occurs either asexually via budding or sexually via gametes (ovipar) and larvae (vivpar). Under averse conditions, some species are even capable of propagating gemmulae (Brusca and Brusca, 1990).

The members of the phylum *Porifera* have been grouped according to the complexity of their sponge bodies and choanocyte chambers into three types named asconoid, syconoid and leuconoid. The simple asconoid type possesses one big and central choanocyte chamber (Fig.

2). The syconoid type has a central cavity which is located inbetween numerous choanocyte chambers. The leuconoid type is the most common one among the *Porifera*. It is characterized by its specialized canal system. Its body complexity arises by the invagination of the choanoderm and results in numerous choanocyte chambers. Thus, it is highly efficient in providing even tall sponges with nutrients. The two model sponges investigated in this study, *Xestospongia muta* and *Amphimedon compressa*, belong both to the Demospongiae and have therefore, as all of their representatives, a leuconoid condition (Brusca and Brusca, 1990).

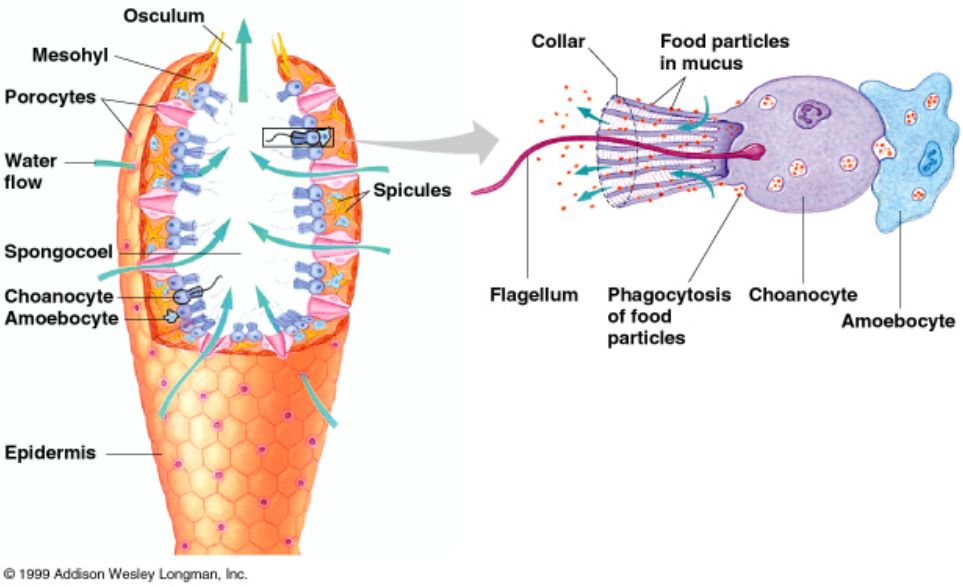

Fig. 2. Schematic cross-section through the simple body of an asconoid sponge: The choanocytes are magnified on the right hand side (© 1999 by Addison Wesley Longman, Inc.).

2. Sponges and microorganisms

Until today, the real diversity of the sponge-microbe associations is still not fully understood. Electron microscopical studies revealed at the beginning of the 1970s that numerous marine sponges live in close association with morphologically diverse microorganisms (Vacelet, 1970, 1971, 1975; Vacelet and Donadey, 1977).

As there are high disparities in microbe content within different sponge species a classification of demosponges into 'bacteriosponges' or 'high-microbial-abundance (HMA) sponges' versus 'non-bacteriosponges' or 'low-microbial-abundance (LMA) sponges' has been performed (Vacelet and Donadey, 1977; Hentschel *et al.*, 2003) (Fig. 3). Though both types coexist in the same habitat, the LMA-sponges are essentially devoid of microorganisms. The HMA-sponges in contrast harbour large and complex microbial consortia extracellularly within their mesohyl (Hill, 2004; Hentschel *et al.*, 2006; Taylor *et al.*, 2007b). The marine sponge *Aplysina cavernicola* for example was shown to consist to 38% out of bacteria (Vacelet, 1975) and to 21% of sponge cells only (Brusca and Brusca, 1990). This is in congruency with the results of Vacelet & Donadey (1977), who showed that the biomass of some HMA-sponges can consist to 40% of microorganisms. The microbes can exceed the bacterial seawater concentration by 2 to 4 orders of magnitude with 10^8-10^{10} bacteria per gram sponge wet weight (Friedrich *et al.*, 2001; Webster and Hill, 2001; Hentschel *et al.*, 2006). Interestingly, they built up a uniform and stable microbial signature within HMA-sponges irrespective of the sponge's species level or geographic distribution (Hentschel *et al.*, 2002). The LMA-sponges instead exhibit microorganisms in diversity and range of the surrounding seawater with only 10^5-10^6 bacteria per gram sponge wet weight (Hagstrom *et al.*, 2002; Hentschel *et al.*, 2006). They are typically smaller than their HMA-counterparts, what leads to the assumption that the internalized microbes of HMA-sponges are at least partly responsible for their large sizes by contributing to the biomass (Hentschel *et al.*, 2006; Wehrl, 2006). Remarkably, the bacterial load of a sponge seems to be inversely correlated with the pumping activity and thus the interior exposure to water of the sponge (Weisz *et al.*, 2008). This depends upon the surface-volume-ratio of a sponge, its choanocyte chambers, ostia sizes as well as the length and complexity of its aquiferous system (Rützler, 1985; Wilkinson, 1992). Thus, sponges with a good water supply possess only few bacteria within their mesohyl, whereas sponges with a poor water supply are densely packed with microorganisms (Vacelet and Donadey, 1977; Wilkinson, 1978). The underlying mechanism, how HMA-sponges differentiate between the vast majority of bacteria that are able to reside extracellularly within

their mesohyl without being harmed and the ones that are being digested to serve the sponge's nutritional purposes, is still unclear (Wehrl *et al.*, 2007).

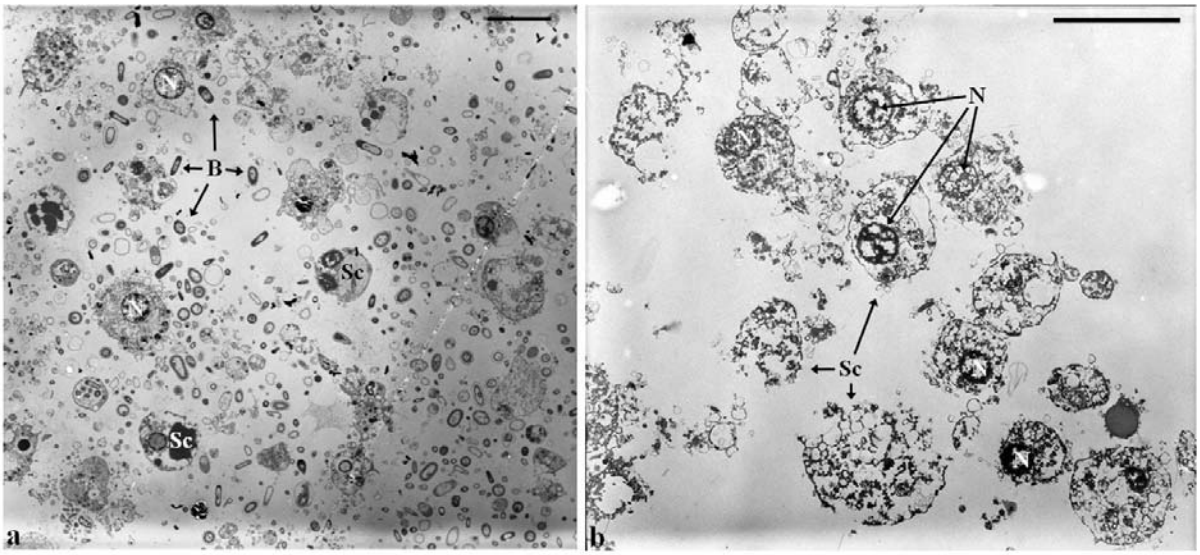

Fig. 3. Transmission electron micrographs of the high-microbial-abundance (HMA) sponge *Xestospongia muta* (a) and the low-microbial-abundance (LMA) sponge *Amphimedon compressa* (b) show abundant and diverse bacterial morphotypes (a) versus the lack of bacterial morphotypes within the two types of sponge mesohyl (b). The scale bars represent 5µm each. Abbreviations: N, nucleus; Sc, sponge cell; B, bacteria.

Typically, a microbial gradient is present within sponges of the photic zone. Their outer layers are settled by photosynthetic microorganisms like eukaryotic algae or cyanobacteria which are often, as in the case of *X. muta*, responsible for the surface coloration of the sponge (Ruetzler, 1985; Steindler *et al.*, 2005; Hentschel *et al.*, 2006; Usher, 2008). The internal mesohyl matrix is occupied by a complex consortium of extracellularly located auto- and heterotrophic bacteria. Those are infrequently also found in digestive vesicles (Wilkinson, 1978), within sponge cell nuclei (Friedrich *et al.*, 1999) or even in specialized cells termed bacteriocytes (Vacelet and Donadey, 1977; Hentschel *et al.*, 2006). Bacteria located within the latter have been even observed to replicate (Vacelet, 1971, 1975). Whether the occurrence of filamentous bacteria that are located intracellularly within sponge cell nuclei, as observed within the marine sponge *Aplysina aerophoba*, is a normal condition or whether a disease underlying one, needs to be further investigated (personal comment U. Hentschel, 2007; Vacelet, 1970; Friedrich *et al.*, 1999). Remarkably, the surfaces as well as the aquiferous canals and choanocyte chambers of healthy sponges are practically devoid of bacterial overgrowth. This

might be due to the flushing of water and might also be a result of the characteristic secondary metabolite profile that many marine sponges harbour (Brusca and Brusca, 1990; Hentschel *et al.*, 2003).

The first microscopical observations of sponge-associated bacteria were soon followed by cultivation-dependent approaches (Santavy *et al.*, 1990; Webster and Hill, 2001). However, more than 99% of all environmental microbes, including the sponge-associated ones, have been impossible to cultivate (Amann *et al.*, 1995; Rappe and Giovannoni, 2003). Thus, new molecular methods, such as 16S rRNA gene libraries, fluorescence in situ hybridizations (FISH) and analyses via restriction fragment length polymorphism (RFLP) as well as denaturing gradient gel electrophoresis (DGGE) have been employed within the last years (Taylor *et al.*, 2007b). Using universal bacterial PCR primers it was found that the sponge-associated microbial consortium differs essentially in its phylogenetic composition from the surrounding seawater (Giovannoni and Rappe, 2000; Lee *et al.*, 2011). First trials discovered a common but yet distinct sponge-specific microbial community within the phylum *Porifera* via construction of 16S rRNA gene libraries (Webster *et al.*, 2001a; Hentschel *et al.*, 2002; Taylor *et al.*, 2007b).

Until 2008, besides representatives of both archeal lineages, members of 20 bacterial phyla have been obtained from diverse sponge species (Hentschel *et al.*, 2006; Taylor *et al.*, 2007a; Webster *et al.*, 2008a; Zhu *et al.*, 2008) (Fig. 4). Those bacteria affiliated at least with 12 monophyletic, sponge-specific sequence clusters (Hentschel *et al.*, 2002), which were shown to belong to the following bacterial phyla: *Acidobacteria*, *Actinobacteria*, *Bacteroidetes*, *Chloroflexi*, *Cyanobacteria*, *Firmicutes*, *Gemmatimonadetes*, *Nitrospira*, the candidate phylum *Poribacteria*, the *Proteobacteria* including representatives of the classes *Alpha-*, *Beta/Gamma-* and *Deltaproteobacteria*, the *Spirochaetes*, the *Verrucomicrobia* as well as the so called ‘uncertain affiliation’ (Taylor *et al.*, 2007b). The latter is a group of sequences that has been derived from several sponge species. It shows highest phylogenetic similarity to the *Planctomycetes*, *Verrucomicrobia* and *Chlamydiae* (PVC) superphylum (Wagner and Horn, 2006). In generall, sponge-specific clusters have been defined by the presence of at least three 16S rRNA gene sequences within one cluster that have been obtained from different sponge species and diverse geographic locations. In addition, their sequences have to be more closely related to each other than to sequences of non-poriferan origin (Hentschel *et al.*, 2003; Siegl, 2009).

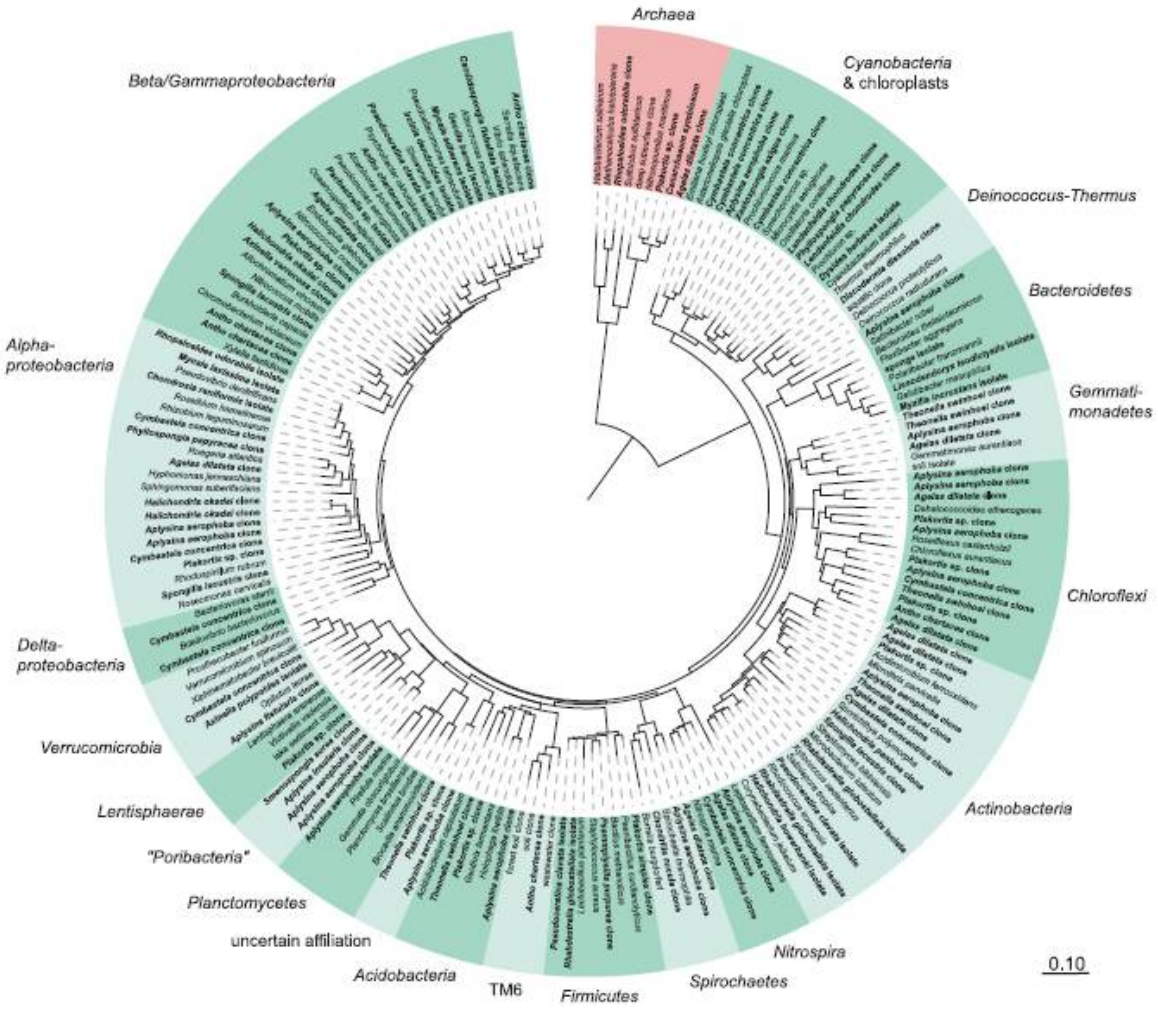

Fig. 4. 16S rRNA-based maximum likelihood phylogeny of sponge-derived archeal and bacterial phyla (in bold) obtained until 2007 (Taylor *et al.*, 2007b). Reference sequences are included. The scale bar represents 10% sequence divergence.

However, after the detection of the rare microbial biosphere newest techniques, such as 16S rRNA gene tag pyrosequencing, were also employed to research on sponge microbiology. It revealed an unparalleled bacterial diversity within Australian and Red Sea sponges. After Webster *et al.* (2009) over 250 000 sequence tags were obtained per Australian sponge species which affiliated with 23 bacterial phyla and built up 2996 operational taxonomic units (OTUs). Nearly half of the sponge-specific phyla were implying vertical transmission (Webster *et al.*, 2009). In addition, Lee *et al.* (2011) investigated with the same technology the Red Sea sponges *Hyrtios erectus*, *Stylissa carteri* and *Xestospongia testudinaria*, the latter being a close relative to my study object *X. muta*. They also detected with up to 1000 OTUs and about 2000 estimated species a high diversity within the sponge-associated bacterial community that grouped into 26 bacterial phyla (Lee *et al.*, 2011). Thus, they conclude that

sponges from the Red sea possess highly sponge- and even species-specific microbial communities that affront environmental influences. The sponge-specific bacterial phyla obtained via 16S rRNA gene library construction were to their majority confirmed by the phyla present within the Australian sponge species. However, the ones of the latter were supplemented with the phyla *Fusobacteria*, *Tenericutes*, *Deferribacteres*, *Fibrobacteres*, BRC1 and WS3 (Webster *et al.*, 2009). Lee *et al.* (2011) suggested even 30 bacterial phyla for their investigated Red Sea sponges adding on the *Chlorobi*, *Chrysiogenetes*, *Thermodesulfobacteria* and the candidate phylum OD1. In addition, they revealed first time an archeal diversity of roughly 300 species within one of their sponge species. However, so far the sponge-associated microbiota does not seem to be entirely exploited with some strains still circumventing their phylogenetic affiliation and awaiting novel molecular techniques for their elucidation (Lee *et al.*, 2011).

3. Symbiotic interactions

De Bary (1879) introduced the word 'symbiosis' as the coexistence of different organisms within the same habitat over a long period of time. In terms of the sponge-associated microbial flora, it is questionable which of the present bacteria are symbionts, commensals or even parasites. Scenarios with one-sided or reciprocal benefits and even disadvantages for both interaction partners are conceivable, especially as the microbes can serve as nutrition or slip into the roles of pathogens, commensals or stable symbionts (Siegl, 2009). However, the bacterial functions for the sponge are still largely unknown. Some well-described symbiotic traits bacteria offer their hosts are referred to in the further context.

On the one hand the bacterial transfer of nutrients to the sponge has been described repeatedly. Cyanobacteria have already been shown microscopically to pass on assimilates to their hosts (Vacelet, 1971). Furthermore, they were demonstrated to relay their metabolite glycerol to the sponge, they were located in, helping it to meet its energy requirements (Brusca and Brusca, 1990). By this means some sponge hosts are able to cover 48-80% of their energy demand via the cyanobacterial metabolism (Ruppert *et al.*, 2004). This is why cyanobacteria-containing sponge species have been shown to dominate sponge populations. Their strategy is to settle in habitats, where there is a low bacterial abundance within the seawater such as the Great Barrier Reef. There they exhibit low filtration rates of particles, as they thrive by meeting their energy requirements with the cyanobacterial assimilates (Wilkinson, 1983, 1987). Thus, comparing sponges with and without cyanobacterial

symbionts reveals their influence upon the sponge's nutritional physiology (Wilkinson *et al.*, 1988). In addition, cyanobacteria have been hypothesized to protect sponges from UV light, as they act as sun screens via their pigments and mycosporin-like amino-acids (Sara, 1971; Bandaranayake *et al.*, 1996; Shick and Dunlap, 2002).

Some sponge-associated microorganisms are even involved in the incorporation of dissolved organic matter (DOM) from the seawater into their host. In addition, they often help the sponge with recycling of its insoluable collagen via digestion (Wilkinson *et al.*, 1979; Wilkinson and Garrone, 1980; Yahel *et al.*, 2003). Certain bacterial strains are even capable of conveying novel traits to their sponge hosts such as for example nitrogen fixation (Wilkinson and Fay, 1979). The sponge's excretion of ammonium provides microbial nitrifiers a perfect substrate for their living. They remove, in exchange, its toxic metabolic by-products (Brusca and Brusca, 1990; Bayer *et al.*, 2008). Thus, both parts have a clear benefit. However, probably the most important function the bacteria have been attributed to is their involvement in the mechanical stabilization of the sponge skeleton (Wilkinson *et al.*, 1981; Rützler, 1985) (Fig. 5).

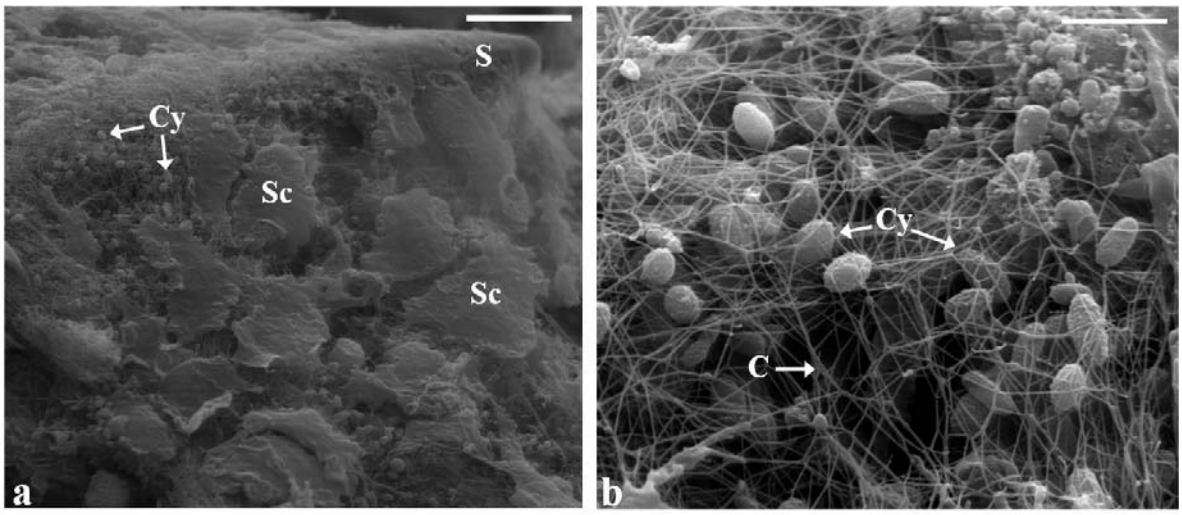

Fig. 5. Scanning electron micrographs of the marine sponge *Xestospongia muta* and its surface tissue-associated cyanobacteria (a-b). The scale bars represent 10µm (a) and 2µm (b) each. Abbreviations: S, spicule; Sc, sponge cell; Cy, cyanobacteria.

In addition, sponge-associated bacteria often play a role in the sponge's chemical defense against biofouling, pathogens and predators by the production of abundant bioactive secondary metabolites (Bakus *et al.*, 1986; Unson *et al.*, 1994; Bewley *et al.*, 1996; Hentschel

et al., 2001; Kubanek *et al.*, 2002). The latter are numerously produced in many sponge species and can be either of Poriferan (Garson *et al.*, 1998) or symbiotic (Uriz *et al.*, 1996) origin. Meanwhile it seems to be proven that often the microbes are the responsible agents for the secondary metabolite production, though it has been frequently attributed to the sponge before (Haygood *et al.*, 1999). This has at least been the case for the metabolite Swinholide A, that has meanwhile been detected within heterotrophic symbionts of the marine sponge *Theonella swinhoei* (Bewley *et al.*, 1996).

Last but not least, as another proof of symbiosis some HMA-sponge species were shown to transmit vertically parts of their associated microbial communities to their offsprings via reproductive stages. Representatives of their stable communities have been detected via novel molecular techniques within sponge oocytes, sperm cells and fertilized egg cells, embryos and larvae. This observation has been conveying those strains a symbiotic character (Usher *et al.*, 2001; Ereskovsky *et al.*, 2005; Enticknap *et al.*, 2006; Schmitt *et al.*, 2007; Sharp *et al.*, 2007; Schmitt *et al.*, 2008; Webster *et al.*, 2009). However, it is still difficult to confirm the advantages of most sponge-associated microbes for their hosts and thus any discussion on their potential functions is still in a preliminary stage. For simplification purposes I refer in my thesis to the presumed beneficial sponge-associated bacteria as ‘symbionts’, as I have been on the search for their pathogenic counterparts.

4. Aims

My PhD thesis is, in contrast to prior research on sponge-microbe interactions, devoted to the study of bacterial pathogens involved in the pathology of two Caribbean sponge diseases: Sponge Orange Band (SOB) disease affects the high-microbial-abundance (HMA) sponge *Xestospongia muta* and Sponge White Patch (SWP) disease affects the low-microbial-abundance (LMA) sponge *Amphimedon compressa*. Thus, the aim of my study was to investigate the underlying principles of both sponge diseases by taking a descriptive, ecological, histological and molecular approach. As a result a detailed description on the pathology of both sponge diseases is presented covering as well its effects on the corresponding sponge host and its associated microbiota.

III. Material and Methods

Note: All underwater photographs, pictures taken as well as all figures shown within this PhD thesis have been created by myself, Hilde Angermeier, if not mentioned differently.

1. Epidemiology of disease

1.1 The marine sponge *Xestospongia muta* as a model system

The abundant reddish-brown sponge species *Xestospongia muta* (class Demospongiae, order Haplosclerida, family Petrosiidae) ranks among the largest and most common representatives within Caribbean coral reef communities (Armstrong *et al.*, 2006). It inhabits mid-range (~15m) to deep coral reefs (~40m) within the Bahamas, Caribbean and Florida (Humann, 1992), where it thrives with highest population density, abundance and individual sponge volume at a depth of 20m (Schmahl, 1985; McMurray *et al.*, 2010). However, its geographic range has been reported to span even until Brazilian coral reefs (Collette and Rützler, 1977) and, as observed in Puerto Rico, until depth of 90m (Soest, 1980). *X. muta*'s colloquial name 'giant barrel sponge' is derived from its barrel-shaped size, which can exceed one meter in diameter and height thus comprising an extensive amount of biomass (McMurray *et al.*, 2008) (Fig. 6). Due to that and to *X. muta's* extreme longevity it is often referred to as 'redwood of the deep' (McMurray *et al.*, 2008; Holden, 2010). Besides, its representatives have already been shown to possess the following chemical compounds: unsaturated polyacetylenic brominated acids (Ashok *et al.,* 1992), the sterols Xestosterol and Mutasterol (Li *et al.,* 1980) as well as a family of chiral tetrahydrofurans termed Mutafurans A-G with antifungal activity (Morinaka *et al.*, 2007).

Fig. 6. Size demonstration: An average *Xestospongia muta* individual next to myself diving (Underwater photography by Gesine Schmidt, AWI).

The sponge body of *X. muta* is comprised of two major parts: the tan mesohyl and the reddish-brown symbiont containing surface tissue, which ranges up to 8mm deep below the sponge pinacoderm according to the surface texture at the site of tissue investigation. A schematic bauplan of the healthy *X. muta* surface demonstrates its separation into two differently colored tissue layers: a pinacodermal outer layer in shades of brown encompassing approximately 2mm and a reddish inner layer of approximately 5mm (Fig. 7), which seems to stem from the mesohyl according to visual characteristics. Both result in the total of 8mm. The sponge surface itself possesses a firm and often jagged texture (Humann, 1992) and is thus easily differentiated from the mesohyl.

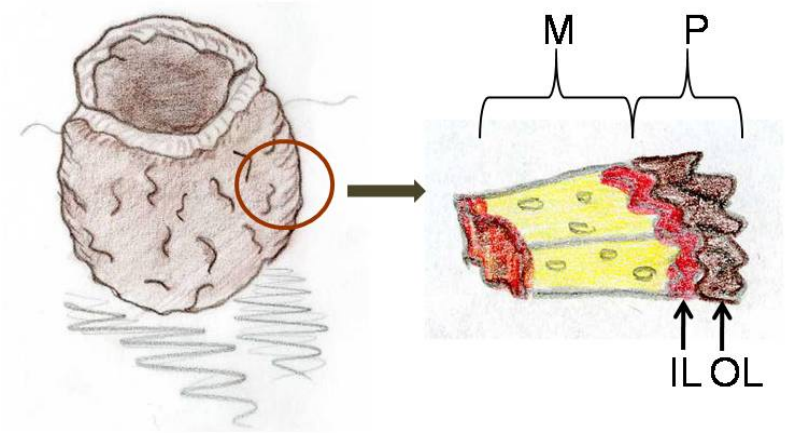

Fig. 7. Scheme of a healthy *Xestospongia muta* individual (left) and its magnified cross-section (right) to demonstrate the surface tissue composition. Abbreviations: M, mesohyl; P, pinacoderm; IL, inner layer; OL, outer layer.

1.2 Sponge Orange Band disease affecting *X. muta*

Bleaching and diseases affecting *Xestospongia muta* specimens have been reported since 1990 and were observed in Puerto Rico (Vicente, 1990), Belize and the Florida Keys (Paz, 1996; Gammill and Fenner, 2005), in Curaçao (Nagelkerken *et al.*, 2000) as well as in Cuba and at the reefs of Cozumel, Mexico (Gammill and Fenner, 2005). Meanwhile even closely related *Xestospongia* species have been observed at the Raja Ampat Archipelago in Indonesia to exhibit similar signs of disease. Bleaching of *X. muta* specimens has been documented since 1997 throughout the Bahamas and the Florida Keys on a regular level (Cowart *et al.*, 2006). It has been characterized by the loss of the sponge-specific surface coloration and has been differentiated into two different types: cyclic and fatal bleaching. Cyclic bleaching is a temporal phenomenon correlating with loss of the sponge's surface color and resulting in its

recovery within the following six month. Since 1997 25% of the *X. muta* population at Conch Reef, Florida, have been affected undergoing annual patterns of cyclic bleaching. In contrast, fatal bleaching, which is synonymous with Sponge Orange Band (SOB) disease, has been documented with a frequency rate of less than <1% within any given *X. muta* population. In addition, its intensity has been shown to vary on a yearly basis with the amount of affected individuals within a population being highly patchy. Normally no neighbouring sponge, that is close to a diseased individual, has been observed to develop symptoms of disease (McMurray *et al.*, 2008). The disease has been discovered and named in 2005 by Cowart *et al*. (2006), who found some of the reef's largest *X. muta* individuals to succumb (McMurray *et al.*, 2010). Sponge Orange Band disease is characterized by the gradual discoloration of *X. muta*'*s* normally brown surface tissue to bleached white. This process is often accompanied by an orange transition zone. Bleaching of the surface tissue has been observed to migrate over the entire sponge body in a fast path of approximately six weeks leaving the formerly brown tissue completely bleached behind. With the progression of bleaching the surface texture of the sponge body changes from hard to cotton-ball like resulting in the collapse of the entire sponge (Cowart *et al.*, 2006; Lindquist, 2008; Smith, 2009). The term 'fatal bleaching' for Sponge Orange Band disease can be explained by the entirely bleached appearance and the fatal end the majority of diseased individuals experiences, as high-rates of sponge mortality have been observed (Cowart *et al.*, 2006).

My thesis is based on Sponge Orange Band disease outbreaks, which occurred in the years 2007 and 2008 during research expeditions offshore the Bahamas at Stirrup Cays, Plana Cays and San Salvador (Fig. 9) as well as during field work at NOAA's National Undersea Research Center (NURC) offshore Key Largo within the Florida Keys National Marine Sanctuary at Conch Reef and Dixie Shoals in the years 2007 and 2009 (Fig. 10). Altogether 28 *X. muta* individuals were used in this study (see annex: Tab. 1). They were grouped into healthy (n=17) and diseased (n=11) sponges with the latter being differentiated into early and advanced stages of Sponge Orange Band disease. The most recent outbreak of Sponge Orange Band disease was documented in June 2009 by T. Smith (USVI) offshore the US Virgin Islands within the National Park St. Johns close to Puerto Rico, where hundreds of fatally bleached *X. muta* specimens were randomly detected during coral monitoring events (Fig. 9).

1.3 The marine sponge *Amphimedon compressa* as a model system

The marine sponge *Amphimedon compressa* (class Demospongiae, order Haplosclerida, family Niphatidae) is commonly called 'erect rope sponge' due to its rope-like appearance, upward growth and frequently branched body structure. However, its shape can also be encrusting or lobular. Usually, its body is in between 0.6 to 1m in size. Its pinacoderm and mesohyl are comprised of the same brilliant red that can vary from burgundy or maroon to shades of bright red or even orange. The surface texture of *A. compressa* is smooth but porous with the oscula being scattered all over the sponge. Its mesohyl is soft and flexible (Fig. 8). In general, populations of *A. compressa* can be found throughout Florida, the Bahamas and the Caribbean, where they dwell on the tops and walls of coral reefs in a depth of 10 to 20m (Humann, 1992; Zea *et al.*, 2009).

Fig. 8. Representative *A. compressa* individual at Dry Rocks Reef, Florida, exhibiting a flabellated shape and the typical brilliant red coloration.

1.4 Sponge White Patch disease affecting *A. compressa*

The first time I observed an outbreak of Sponge White Patch disease was in November 2007 at Dry Rocks Reef, Florida, during field work at NOAA's Undersea Research Center (NURC) offshore Key Largo. Additional observations followed in May and September 2009 at Conch Reef (Fig. 10). As this phenomenon had not been described before to my knowledge, I named it "Sponge White Patch (SWP) disease" due to its optical characteristics. Altogether 709 *A. compressa* individuals, grouped into either healthy (n=538) or diseased sponges (n=171), were investigated in this study (see annex: Tab. 7). In winter 2007 the frequency rate of SWP-disease has been determined at Dry Rocks Reef by inspecting 80 randomly selected squares of $1m^2$ size via SCUBA diving by counting the healthy versus the diseased *A. compressa* individuals within each of them. In addition, the amount of white versus red tissue has been measured and averaged for forty diseased sponges by volume displacement studies using a seawater-filled beaker (n=40).

Fig. 9. Caribbean collection and observation sites of Sponge Orange Band disease throughout the Bahamas, the Florida Keys and offshore the US Virgin Islands (encircled in red).

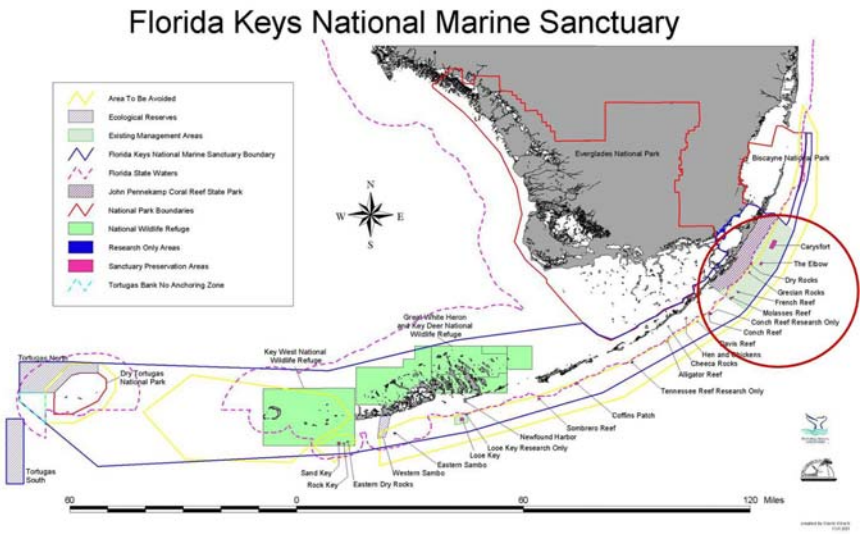

Fig. 10. Map of the Florida Keys National Marine Sanctuary highlighting the collection site at Key Largo (red).

2. Sponge collection

Xestospongia muta individuals (class Demospongiae, order Haplosclerida, family Petrosiidae) were collected throughout the Bahamas by SCUBA diving at a depth of 3 to 20m during research expeditions onboard the RV Seward Johnson (HBOI) in June 2007 and May/June 2008 (Fig. 9). Additional sampling, including *Amphimedon compressa* individuals (class Demospongiae, order Haplosclerida, family Niphatidae), occurred at the same depth within the Florida Keys National Marine Sanctuary offshore Key Largo at Conch Reef, Dixie Shoals and Dry Rocks Reef in November/December 2007 as well as May and September 2009 (Fig. 10). The samples were transferred to the surface in seawater-containing Ziploc bags to avoid contact with air and kept cool until further processing within the next hours using laboratory facilities. All samples were washed with sterile filtered artificial seawater before suitable fixation and storage for respective molecular work, chemical analysis or microscopical approaches. Altogether 28 *X. muta* individuals and 709 *A. compressa* individuals were obtained and included in this study (see annex: Tab. 1 and 7). The health states of the sponges were documented via underwater photography as well as via binocular microscopy within the laboratory.

3. Binocular microscopy

Cubes of about $1cm^3$ in size were cut from the sponge sample of interest containing sponge surface tissue as well as mesohyl. Fixation for binocular microscopy occurred in a solution of 4% formaldehyde in artificial seawater. The samples were stored until microscopy.

4. Light microscopy

During the processing of sponge samples for transmission electron microscopy semi-thin sections were produced. Those were inspected via light microscopy using the magnifications 10x, 20x, 40x and 100x applying immersion oil, if indicated.

5. Scanning electron microscopy

Cubes of about 0.5cm^3 in size were excised from sponges of interest containing surface as well as mesohyl tissue. Storage occurred at 4°C in 6.25% glutaraldehyde-phosphate-buffered solution. A five times washing procedure with Soerensen-phosphate buffer (50 mM, pH 7.4) was conducted for five minutes each. Subsequently, dehydration was performed in an increasing acetone series starting with 30% for 15min, followed by 50% for 20min, 75% for 30min, 90% for 45min and six times incubation at 100% for 30min. At the end the samples were critical point dried under pressure in 100% acetone and sputtered with gold-palladium to obtain a 30nm surface layer (5min at 25mA). Until their examination with the scanning electron microscope (Zeiss DSM 962, Oberkochen, Germany) samples were stored in a dehydrator.

6. Transmission electron microscopy

Cubes of about 1mm^3 in size were excised from the sponge surface tissues including mesohyl. Storage occurred at 4°C in 2.5% glutaraldehyde-phosphate-buffered solution. Subsequently, they were washed five times for three minutes each with cacodylate buffer (50mM, pH 7.2), were fixed with 2% buffered OsO_4 for 120min on ice and washed five times for 3min with H_2O. One % uranyl acetate was used overnight for contrasting followed by a five times washing stip with H_2O for three minutes each. Dehydration was achieved via an ethanol series on ice (30min each) starting with 30%, 50%, 70%, 90%, 96% and completed with a three times incubation in 100%. Afterwards the samples were incubated three times in propylene oxide at room temperature. They were then incubated twice in a 1:1 (vol/vol) mixture of propylene oxide-epon 812 (Serva) first for 1-2hrs and ultimately overnight. The following day the samples were incubated twice in Epon 812 for 2h followed by a final Epon incubation for 48h at 60°C. The prepared samples were sectioned with an MT-7000 ultramicrotome (RMC, Tuscon, Arizona, USA) and examined at the transmission electron microscope (Zeiss EM10, Oberkochen, Germany).

7. Epifluorescence microscopy

Tissue homogenates were made of about 1g rinsed *X. muta* sample of interest, diluted in sterile ASW, poured through a Nitex membrane to remove unground sponge tissue, filtered and stored in 3.7% paraformaldehyde. Dilutions from 10^{-1} to 10^{-3} were prepared, which were stained with DAPI (7µl/ml of a 100µg/ml stock solution) for 30min in the dark. One ml of stained extract was mixed with 9ml of filter-sterilized ASW. The mixture was filtered onto a black 0.2µm polycarbonate membrane (Millipore) that was stabilized with a 0.45µm cellulose nitrate filter. Two washing steps with sterile ASW and 70% EtOH followed by applying carefully a handpump. Finally, the polycarbonate filter was placed on a microscopic slide and mounted with Citifluor (Citifluor Ltd., London). The amount of sponge cell nuclei, bacteria as well as the extra- and intracellularly located cyanobacteria were counted in each tissue homogenate under the epifluorescence microscope using a 100x magnification with immersion oil. Cyanobacteria were easily detectable among the DAPI-stained bacteria and sponge cell nuclei due to the presence of numerous thylakoid membranes that are autofluorescing under the epifluorescence microscope. The counted results were extrapolated according to the initial volume (~1g) of sponge tissue.

8. Microbial cultivation

In general bacterial cultivation of Sponge Orange Band- as well as Sponge White Patch disease associated microbes was performed on different media (GPYNS, YPD and M1 after Mincer *et al.* (2002)) with a detailed description within the annex section. Homogenates of the selected sponge samples were fabricated of approximately $1cm^3$ cubes in size including pinacoderm as well as mesohyl. They were either prepared freshly and thus diluted in sterile artificial seawater or preserved with 20% glycerol for storage at -20°C. Subsequently, they were plated out in a dilution series ranging from 10^{-1} to 10^{-3} on the respective medium. Growth occurred for several days to weeks in an incubator at 30°C, which is the ambient seawater temperature, or during field work at room temperature which equated also 30°C. The newly grown or imported colonies were streaked out again on the respective growth medium. Grown isolates were preserved with 20% glycerol and stored at -20°C.

After sufficient growth the bacterial DNA of a single colony was either isolated by boiling it at 100°C for 10min in 100µl sterile H_2O_{dest} or via chromosomal DNA extraction. The latter method was performed also to obtain a positive control for the eubacterial PCR

reactions. Thus, 2ml of *E. coli* XL1 blue liquid culture in LB-medium (also valid for other bacterial species and their growth media), that have been shaken over night at 37°C, were extracted to obtain the chromosomal DNA. First of all, the overnight culture was centrifuged for 4min at 8000rpm at ambient temperature. Subsequently, the cell pellet was washed with 1ml TNE and was resuspended in 270µl TNEX and 25µl Lysozyme. The mixture was incubated for 30min at 37°C to destruct the bacterial cell walls. In the following, 100µl Proteinase K was added and the whole mixture was incubated for 2h at 60°C in a heat block until the solution was clear. This step served to destroy the proteins and the left-over enzymes such as lysozyme. At the end, 15µl of 5M NaCl and 500µl of ice-cold Ethanol (100%) were supplemented to precipitate the DNA. The mixture was centrifuged at 13 000rpm for 15min at room temperature and the obtained DNA-pellet was washed with 70% Ethanol followed by air-drying. The DNA was re-dissolved in 200µl sterile H_2O_{dest} and stored at 4°C until its application. If both extraction methods were insufficient for obtaining bacterial DNA, also the methodology of the FastDNA spin kit for soil (Q-biogene) was applied according to the manufacturer's instructions (see DNA extraction: page 29ff). Subsequently, a PCR-reaction for the amplification of the 16S rRNA gene (commonly referred to as "colony-PCR") has been performed on the isolated bacterial DNA using the following scheme for a 30µl approach: 3µl 10x PCR-Buffer, 0.6µl 10mM dNTPs, 0.6µl 27f (100pmol/µl), 0.6µl 1492r (100pmol/µl), 0.15µl Taq-Polymerase and 25.05µl H_2O_{dd}.

The primer pairs 27f and 1492r were used for PCR amplification of the eubacterial 16S rRNA gene. Each amplification included water as template for the negative control and no DNA. The polymerase chain reaction (PCR) was conducted using a T3 Thermocycler (Biometra, Germany) with the following conditions: initial denaturation at 95°C for 2min, 34 cycles of denaturation at 95°C for 1min, annealing of the primers at 56°C for 1min and elongation at 72°C for 90s. The final extension step was at 72°C for 10min. The size and the quality of the obtained PCR-products were examined on a 1% agarose gel stained with ethidium bromide. 10µl of the PCR-products were subsequently subject to RFLP-digestion to estimate the overall bacterial diversity (see RFLP: page 28f). The 16S rRNA products of interest were then PCR-purified with the Quiaquick PCR purification Kit (Quiagen) according to the manufacturer's instructions. Thus, one volume of PCR product was mixed with five volumes of buffer PB using a pipette. The mixture was transferred onto a QIAquick column and centrifuged at 13 000 rpm for 1min. The flow-through was removed and 750µl of buffer PE was applied to the column. After another centrifugation step at 13 000 rpm for 1min and the removal of the flow-through, the column has been set back into the tube and has been

centrifuged another time at 13 000 rpm for 1min. It was then transferred into a new 1.5ml tube and subsequently 30µl of buffer EB were applied. After settling of the column for 1min, it was centrifuged a last time at 13 000 rpm for 1min. The yielded flow through contained the purified PCR product and was stored at -20°C until its application. For direct sequencing the purified 16S rDNA PCR product was used as template according to the following pipetting scheme for a 10µl approach: 2µl BigDye Terminator v1.1 5x Sequencing Buffer, 2µl PreMix 1.1 ABI Prism, 1µl Primer (in this case: 27f or 1492r in 25pmol/µl), 4µl H_2O_{dd} and 1µl Template (purified PCR-product). The primer 27f or 1492r was used for amplification during the sequencing PCR. The polymerase chain reaction (PCR) was conducted using a T3 Thermocycler (Biometra, Germany) with the following conditions: initial denaturation at 94°C for 2min, 29 cycles of denaturation at 94°C for 30s, annealing of the primers at 58°C (always 3°C over T_m of the according primer) for 15s and elongation at 60°C for 4min. Subsequently, the PCR-products were brought to the sequencing team within the department of Virology and were further processed as described in the cloning and sequencing section (see page 31ff).

8.1 Sponge Orange Band disease and associated bacteria

Bacterial cultivation on Sponge Orange Band diseased samples was first performed in June 2007 during field work onboard the research vessel RV Seward Johnson throughout the Bahamas on fresh sponge samples ranging from healthy to Sponge Orange Band diseased *X. muta* individuals. Samples of ~1cm^3 in size containing pinacoderm as well as mesohyl were rinsed with sterile artificial seawater (ASW), homogenized and diluted in sterile ASW in a dilution series ranging from 10^{-1} to 10^{-8}. Subsequently, they were plated out on GPYNS-agar with/without cycloheximide (100µg/ml) against fungal growth and were grown for up to two weeks. Seawater was used as a negative control. Back home in the laboratory general procedures were conducted as for all cultivation trials mentioned above. In winter 2007 homogenates of the differently colored tissue parts of Sponge Orange Band diseased *X. muta* individuals (#3, #4 and #5) obtained from the Florida Keys National Marine Sanctuary were produced for cultivation back home in the laboratory. Later on, those were plated out in dilutions ranging from 10^{-1} to 10^{-3} on YPD- and M1 media. They were handled according to the methodology described above.

8.2 Sponge White Patch disease and associated bacteria

Bacterial cultivation on YPD- and M1 agar has been performed on the homogenates derived of one healthy (#12) and three Sponge White Patch diseased *A. compressa* individuals (#2, #13 and #29) obtained from the Florida Keys National Marine Sanctuary in winter 2007. The healthy sponge sample was just comprised of red tissue whereas the diseased sponge samples could be differentiated into either red or white tissue. Both parts were applied to the cultivation trials. In addition, for the potential isolation of spongin-boring bacteria I applied a marine collagen-containing agar, which consisted of 44.08g marine agar 2216 (Difco) and 0.8g Azocoll (Sigma) that has been autoclaved in 800ml H_2O_{dest}. It was first tested in the laboratory with the homogenates of one healthy *A. compressa* (#12) and one Sponge White Patch diseased individual (#29) from the cultivation trials of winter 2007. The latter sponge was differentiated into its red and white part. 100µl of the homogenates were plated out either pure or in dilutions of 1/10 and 1/100 in sterile artificial seawater. To obtain agarolytic colonies in pure culture, I streaked out visually agarolytic colonies one by one on azocoll-containing agar. As azocoll's dye is violet, it gives a distinctive color to the agar. Bacterial degradation of the azocoll-containing agar can thus be easily detected by pure eye via the degradative color change and the associated agar liquidation by bacterial growth. To elucidate the identity of these agar-degrading strains a eubacterial PCR (50µl approach) of their 16S rRNA genes has been performed following the subsequent methodology: 5µl 10x PCR-Buffer, 1µl 10mM dNTPs, 1µl 27f (100pmol/µl), 1µl 1492r (100pmol/µl), 0.5µl Taq-Polymerase, 40.5µl H_2O_{dd} and 1µl Template (bacterial DNA).

Bacterial cultivation on azocoll containing marine agar 2216 (Difco) was performed of one Sponge White Patch diseased *A. compressa* individual (#1, see annex: Tab. 7) obtained from the Florida Keys National Marine Sanctuary in May 2009 (Fig. 11a). The diseased sponge was differentiated into its red and white part, of which tissue homogenates have been produced (Fig. 11b). Those were applied either pure or in dilutions of 10^{-1} to 10^{-3} for bacterial cultivation. After field work, all 48 isolated bacterial colonies have been streaked out again on fresh azocoll containing agar plates. Ten bacterial isolates could not be revived anymore on fresh agar plates. Thus, the remaining 38 bacterial isolates were applied to further analysis after DNA extraction via polymerase chain reaction (PCR) of their 16S rRNA gene with the eubacterial primers 27f and 1492r as well as to restriction fragment length polymorphism (RFLP: see page 28f) of their individual gene products with the enzymes MspI and HaeIII. In addition, also the before by the same methodology isolated bacterial morphotypes, which

exhibited collagen and agar degrading characteristics, were subjected to RFLP. All of those bacterial isolates, including the collagen-degrading ones, were kept as backups in glycerol stocks at -80°C. Gel electrophoresis of the bacterial isolates after RFLP analysis exhibited 19 distinctive banding patterns that represented the morphological diversity among the bacterial isolates (see Fig. 46). One representative isolate of each RFLP banding pattern was subsequently selected for application by denaturing gradient gel electrophoresis (DGGE) (see Figs. 49-50).

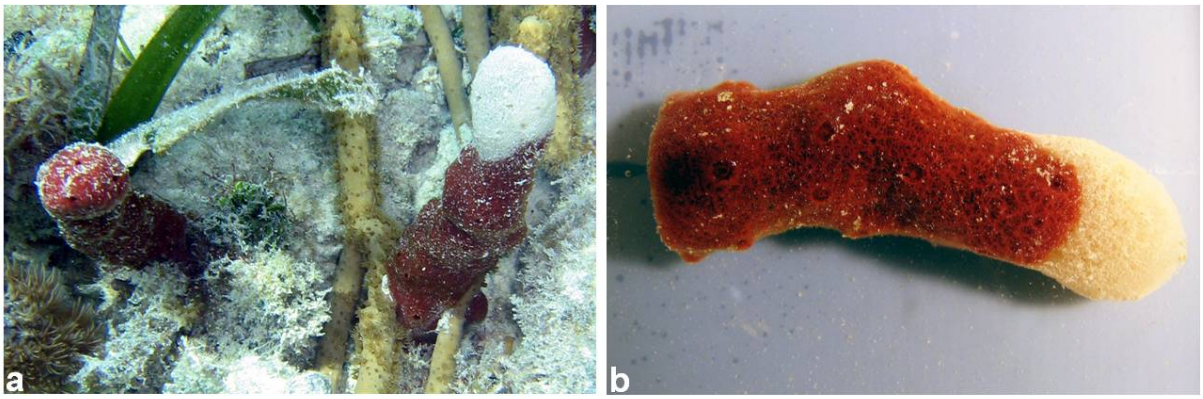

Fig. 11. Sponge White Patch diseased *A.compressa* (#1; see annex: Tab. 7) obtained from Conch Reef, Florida, in May 2009 that was applied to bacterial cultivation. Photographies by Volker Glöckner.

9. Restriction Fragment Length Polymorphism (RFLP)

After PCR-amplification with the primers 27f and 1492r restriction fragment length polymorphism (RFLP) was performed on the 16S rRNA gene products of bacterial isolates obtained from Sponge White Patch diseased *A. compressa* individuals. The RFLP method was applied to elucidate the bacterial diversity among the isolated colonies by digestion of their amplified PCR products via restriction enzymes, in this case by the enzymes HaeIII and MspI. The enzyme HaeIII has been derived from *Haemophilus influenzae,* the enzyme MspI from *Moraxella* species. The following pipetting scheme has been applied to obtain a 20µl digestion approach for one bacterial isolate: 10µl 16S rRNA gene product of the respective bacterial isolate, 2µl Buffer2, 1µl HaeIII, 0.5µl MspI and 6.5µl H_2O_{dd}. Due to digestion diverse fragments have been arising of the before ~1465bp long PCR product, as each bacterial strain shows its own species-specific RFLP-pattern. Similar sequences exhibit the same RFLP-pattern, whereas different sequences have varying banding profiles and thus reveal the present bacterial diversity. The digestion of the 16S rRNA gene products was

performed for 2h at 37°C in an incubator followed by gel electrophoresis on a 3% agarose gel at 100V and staining of the gel with ethidium-bromide for 30min.

10. DNA extraction and Denaturing Gradient Gel Electrophoresis

DNA was extracted either from bacterial colonies as described above (see microbial cultivation: page 24ff) or directly from sponge tissue. For the latter, about 0.5cm^3 pieces of 70% ethanol preserved sponge samples were air-dried and homogenized with mortar and pestle in liquid nitrogen. The DNA was extracted using the Fast DNA Spin Kit for soil (Q-Biogene, Heidelberg, Germany) in accordance with the manufacturer's instructions. Thus, ground sponge tissue was transferred to a lysing matrix tube and resuspended in 122µl MT buffer as well as 978µl sodium phosphate buffer. The tube was processed for 30s using a FastPrep® instrument (Q-Biogene) at a speed of 5.5 followed by a centrifugation step at 13 000 rpm for 30s. The supernatant was re-dissolved in 250µl PPS reagent within a new tube and subsequently shaken ten times. Centrifugation followed at 13 000 rpm for 5min and the obtained supernatant was transferred into a fresh 2ml micro-centrifuge tube. Binding of the DNA was performed by adding 1ml of binding matrix to the supernatant and mixing it for 2min. A three minutes rest of the tube within the rack was enabling the settling of the binding matrix. Subsequently, 500µl of supernatant was discarded while 700µl were transferred into a spin filter and centrifuged at 13 000 rpm for 1min. After emptying the catch tube, the procedure was repeated with the remaining supernatant. Washing of the DNA occurred by adding 500µl of SEWS-M to the spin filter followed by another centrifugation step at 13 000 rpm for 1min. The flow-through was removed and the spin filter was once more centrifuged at the same speed but this time for 2min. Subsequently, the spin filter was placed in a clean catch tube and exposed to air for 5min at room temperature to dry the binding matrix. 50µl of DES (DNase and pyrogen-free water) were carefully applied to the filter matrix by gently stirring the silica for a better elution of the DNA. A last centrifugation step occurred at 13 000 rpm for 1min to elute the DNA into the catch tube, which was subsequently stored at -20°C. The obtained DNA solutions (either sponge-derived or of pure bacterial origin) were applied as template in the PCR reactions. A general scheme for a DGGE-PCR is shown in the following 50µl approach: 5µl 10x PCR-Buffer, 10µl 5x Q-Solution, 1µl 10mM dNTPs, 1µl specific forward Primer+GC-clamp (100pmol/µl), 1µl specific reverse Primer (100pmol/µl), 0.5µl Taq-Polymerase, 1µl Template (or more) and 30.5µl H_2O_{dd} (or less depending on the amount of template).

During this thesis, several denaturing gradient gel electrophoreses (DGGE) were performed to obtain an insight into the unculturable bacterial communities within healthy or Sponge Orange Band- as well as Sponge White Patch diseased tissues. Thus, three different sets of primers were applied each specific to certain bacterial communities (see annex: page 153). For example the primer pair 106f+GC-clamp and 781r was frequently used during the study of Sponge Orange Band disease. It served the specific PCR amplification of the cyanobacterial 16S rRNA genes (Nübel *et al.*, 1997). Instead, the primer pair 341f+GC-clamp and 907r (Muyzer *et al.*, 1998) was frequently used within both studies (SOB- and SWP disease) to amplify the eubacterial 16S rRNA genes of preferentially all bacteria present within the sponge derived DNA mixture. It was also applied to amplify the 16S rDNA PCR products already obtained and digested via RFLP from the isolated *A. compressa* strains for their application within DGGE. Each amplification procedure by polymerase chain reaction (PCR) included positive as well as negative controls. The first were PCR reactions with bacterial DNA (e.g. *Escherichia coli*) as template and the latter PCR reactions without DNA but with sterile water as template. The polymerase chain reactions (PCR) for the DGGE runs were conducted according to the primer pairs but all using a T3 Thermocycler (Biometra, Germany). For the cyanobacterial DGGE-PCR, that revealed fragments of 675bp length, the initial denaturation step was at 94°C for 5min followed by 34 cycles of denaturation at 94°C for 1min, annealing of the primers at 60°C for 1min and elongation at 72°C for 1min. The final extension step was at 72°C for 10min. The eubacterial DGGE-PCR created PCR-products of 566bp length and had the following conditions: an initial denaturation step at 94°C for 2min followed by 29 or 34 cycles of denaturation at 94°C for 1min, annealing of the primers at 54°C (or up to 57°C if problematic) for 30s and elongation at 72°C for 40s. The final extension step was at 72°C for 5min. For each sponge sample independent PCR reactions were performed that have been applied within the same DGGE run. The size and quality of the obtained PCR-products were examined on 1-2% agarose gels (depending on the nucleotide length of the respective PCR-products) that were stained with ethidium bromide for 20min.

The DGGE runs were performed with the Bio-Rad DCode^{TM} Universal Mutation Detection System (Bio-Rad, Germany) on 8% or 10% (w/v) polyacrylamide gels in 1x Tris-acetate-EDTA (TAE) buffer using either 0-90% or 0-100% denaturing gradients, whereas 100% of the denaturants corresponded to 7M urea and 40% (vol/vol) formamide. All DGGE runs were conducted at 150V for 6h at 60°C. Staining occurred in two ways: either with SYBR-Gold in 1xTAE (Molecular Probes, Netherlands) for 30min followed by scanning with

the Typhoon 8600 photo imager system (Amersham Biosciences, Germany) or with ethidium bromide (Roth, Germany) and subsequent investigation with the Universalhood II gel documentation system (Biorad, München). DGGE-bands of interest were excised from the according DGGE gel under UV-light with an ethanol-sterilized scalpel and extracted overnight with 25µl H_2O_{dd} at 4°C. Cluster analysis of the DGGE banding pattern has been conducted for selected DGGE gels with the software program Quantity One (Bio-Rad, Munich, Germany) according to the manufacturer's instructions. Thus, dendrograms were constructed using the UPGAMA clustering method to compare the similarities in between the bacterial banding patterns of different sponge samples.

11. Cloning and sequencing

Cloning was performed in the majority of the cases for the bacterial phylotypes hiding within the DGGE bands. Thus, 4µl of eluted DNA from the excised DGGE band of interest were used as template for re-amplification of the 16S rDNA with the before applied DGGE-primers without GC-clamp. Either the cyanobacterial primers 106f and 781r (Nübel *et al.*, 1997) or the eubacterial primers 341f and 907r (Muyzer *et al.*, 1998) have been used depending on the DGGE gel. A 50µl approach contained: 5µl 10x PCR-Buffer, 1µl 10mM dNTPs, 1µl specific forward Primer+GC-clamp (100pmol/µl), 1µl specific reverse Primer (100pmol/µl), 0.5µl Taq-Polymerase, 4µl Template and 37.5µl H_2O_{dd}. The following PCR conditions were applied for re-amplification of the cyanobacterial DNA with the primer pair 106f and 781r (Nübel *et al.*, 1997): An initial denaturation step at 94°C for 5min followed by 34 cycles of denaturation at 94°C for 1min, annealing of the primers at 60°C for 1min and elongation at 72°C for 1min. The final extension step was at 72°C for 10min. The eubacterial DNA re-amplification with the primer pair 341f and 907r (Muyzer *et al.*, 1998) had the following conditions: initial denaturation at 94°C for 2min followed by 29 cycles of denaturation at 94°C for 1min, annealing of the primers at 60°C for 30s and elongation at 72°C for 40s. The final extension step was at 72°C for 5min. However, cloning has also been performed on the purified 16S rDNA products of the bacterial *A. compressa* isolates that have been applied to DGGE in respect of the infection trials. This was achieved by ligation of the obtained PCR-products after PCR-purification with the QuiaQuick gel extraction kit (Quiagen, Germany) into the pGEM-T-Easy vector system (Promega, USA). The ligation assay comprised 10µl and consisted out of: 1µl vector pGEM-T easy (Promega: 50ng/µl), 5µl 2xT4 DNA ligase buffer, 1µl T4 DNA ligase (3U/µl) and 3µl PCR product as template. As a final step the

ligation was incubated overnight at 4°C. For its transformation two methods were applied: either 'transformation via electroporation' or 'transformation via heat shock'. For the first the apathogenic bacterial strain *E. coli* XL1 blue was applied. Therefore, the electroporation cuvettes were sterilized for 90s with UV-light. Three µl of the according ligation were mixed with one aliquot of 100µl competent cells that were stored at -80°C and defrosted right before usage. This mixture was pipetted into the gap of the cooled eletroporation cuvette and subsequently exposed to the electroporation impulse of 2500V. Then 1ml LB-medium was added and the whole mixture was transferred into a 1.5ml reaction tube. The latter was shaken for 2h at 37°C in an incubator for recovery and growth of the transformed cells. For the heat-shock transformation in contrast, one aliquot of *Escherichia coli* Novablue cells was defrosted on ice and mixed with 5µl ligation product. Afterwards it was incubated first on ice for 30min and then in a heater for 90s at 42°C. After another cooling step on ice for 5min, 1ml of LB-medium was added to the transformation product and the whole mixture was shaken in an incubator at 37°C for 2h.

After the 2 hour incubation of both transformation methods, 70% of the cells were plated out on Ampicillin, IPTG and X-gal containing LB-agar plates (commonly called AIX-plates). Those were incubated overnight at 37°C. The next day white transformants containing the insert were detected by pure eye via the blue-white screen. They were picked and streaked out on another AIX-plate before their inoculation of 3ml LB/Ampicillin broth each. The latter was incubated overnight at 37°C in a shaker. One ml of the liquid, bacterial culture was diluted with 86% glycerol to obtain a concentration of 20%. It was subsequently frozen away as a cryo-culture. The other 2ml were used for the isolation of the plasmid DNA by standard miniprep procedures (Sambrook *et al.*, 1989). Therefore, they were filled in a 2ml tube and centrifuged at 13 000 rpm for 5min each followed by discard of the supernatant. The pellet was then resuspended in 150µl of buffer P1 and subsequently in 150µl of buffer P2. The tube was placed for 5min in a rack at room temperature. Subsequently, the pellet was mixed with 150µl of buffer P3 and stored on ice for 30min. Thereafter, a centrifugation step was conducted with 13 000 rpm for 10min. The supernatant was transferred to a new tube and centrifuged one more time under the same conditions. It was transferred again into a clean 1.5ml tube and mixed with 350µl of isopropanol (0.7% vol/vol). Another centrifugation step followed at 13 000 rpm for 15min. The resulting pellet contained the plasmid DNA. It was washed with 70% ethanol and dried by air. Finally, it was resuspended in 50µl of sterile water and stored until its usage at -20°C. The correct insert size was verified via restriction digestion by using the following 20µl approach: 2µl 20x EcoRI buffer (New England Biolabs), 1µl

EcoRI (New England Biolabs, 20.000 U/ml), 12µl sterile H_2O_{dest} and 5µl plasmid DNA. Afterwards, the reaction was incubated at 37°C for 2h and its restriction patterns were analyzed via gel electrophoresis on a 3% agarose gel. Sequencing was conducted using the ABI Prism sequencing protocol and an ABI 377XL automated sequencer (Applied Biosystems) with one of the plasmid-specific primers SP6 or T7 (25pmol/µl). The ContigExpress tool in Vector NTI suite 6.0 (InforMax, Inc.) was used for editing the obtained sequences. Chimeras and other sequencing artefacts were identified with the program Pintail (Ashelford *et al.*, 2005). The chimeras were removed from the dataset. The sequences were compared with the present database entries in the NCBI (National Center for Biotechnology Information) Genbank using the basic local alignment search tool (BLAST) algorithm (http://www.ncbi.nlm.nih.gov) for sequence identification (Altschul *et al*. 1990).

12. Phylogenetic analysis

The ARB program package (Ludwig *et al.*, 2004a) was used for sequence alignment and phylogenetic tree construction of the *X. muta* derived cyanobacterial sequences. The latter and their closest basic local alignment search tool (BLAST) hits were imported into the SILVA 16S rRNA database (version 93) (Pruesse *et al.*, 2007b) for automatic alignment and manual refinement using the integrated alignment tool by ARB. Only sequences ≥1200bp were used for the calculation of neighbour joining, maximum likelihood and maximum parsimony trees. Shorter sequences were added using the parsimony interactive tool in ARB without changing the tree topology. All trees were constructed using conservation filters for *Cyanobacteria* and bootstrap analysis (1000 resamplings). They were compared and the maximum likelihood tree was chosen for publication within this thesis. The highlighted group was supported by all three treeing methods.

13. GenBank accession numbers of nucleotide sequences

All 16S rRNA gene sequences received during the study of Sponge Orange Band disease affecting *Xestospongia muta* have been deposited in the GenBank database under the accession numbers GU590802-GU590859. In addition, the 16S rRNA gene sequences obtained during the study of Sponge White Patch disease affecting *Amphimedon compressa* have been deposited in GenBank under the accession numbers HQ659567-HQ659575.

14. Chlorophyll *a* analysis via spectrophotometry

As the abundance of cyanobacteria correlates with the concentration of chlorophyll *a* (Wilkinson, 1983; Rai, 1990), its content within the selected sponge *X. muta* tissues was measured via spectrophotometry (Parsons *et al.*, 1984). Three 0.5g cubes containing sponge surface tissue and associated mesohyl were sampled per sponge individual for chlorophyll *a* analysis. The samples were kept dark inside a cooler during transport to the laboratory and were extracted with a 90% acetone:water mixture at 4°C until analysis. After centrifugation the absorbance of 1ml supernatant was measured against the reference, 1ml of 90% acetone, in a cuvette at 750, 664, 647 and 630nm using an optic spectrophotometer. The content of chlorophyll *a* within the sponge sample of interest was calculated via the equations of Parsons *et al.* (1984) and standardized to the volume of sponge tissue.

15. High-performance liquid chromatography

Lyophilized sponge samples were ground with mortar and pestle and extracted overnight by stirring at room temperature with twice the volume of 100% methanol. After vacuum filtration, the supernatants were dried on a rotary evaporator at 40°C. For each extract, 5mg were dissolved in 1ml of methanol, from which 5µl was analyzed via analytical HPLC using a Jasco system (pump PU1580, gradient unit LG-980-025, degasser DG-2080-53 and UV detector MD-2010Plus) on a Chromolith RP-18e column (4.6 x 100mm; Merck). The separation was achieved with a solvent mixture of acetonitrile and water complemented with 0.05% trifluoroacetic acid, starting with 10% acetonitrile:H_2O to 100% acetonitrile over a time span of 15min and at a flow rate of 3ml/min. Preparative isolation was carried out using a HPLC Jasco system (pump PU1580, gradient unit LG-980-025, degasser DG-2080-53 and UV detector MD-2010Plus) on a Chromolith SemiPrep RP-18e column (10x100mm; Merck). A solvent gradient of 10% acetonitrile:H_2O to 100% acetonitrile supplemented with 0.05% trifluoroacetic acid was used over a time span of 15min at a flow rate of 10ml/min. HPLC-ESI-MS/MS analysis was performed on 5µl of healthy sponge extract utilizing a triple-stage quadrupole 7000 tandem mass spectrometer system equipped with an ESI interface (Finnigan MAT, Bremen, Germany). Data acquisition and evaluation were conducted on DEC 5000/33 digital equipment (Unterföhring, Germany) with ICIS 8.1 software (Finnigan MAT, Bremen, Germany). Positive ions were detected by scanning from 170-900u with a 1s scan duration for a single spectrum.

16. Pathogenicity trials

16.1 Infection experiments on Sponge Orange Band disease

Underwater infection experiments on Sponge Orange Band disease were conducted at a depth of ~20m on Conch Reef within the Florida Keys. For the tissue transplantation study one healthy (n=1) and three diseased (n=3) *Xestospongia muta* individuals were chosen as donor sponges and twelve healthy *X. muta* individuals (n=12) were randomly chosen as recipient sponges according to optical characteristics (see annex: Tab. 6). The tissue of each donor sponge was sampled nine times with the help of a cork-borer that served to stance out holes the size of 1.5cm width x 5cm depth (Figs. 12-13). In addition, three cores per recipient sponge had been removed so that an immediate transplantation of three donor cores into a single recipient sponge could be performed. Altogether three recipient sponges (n=3) were applied per donor sponge resulting in nine transplanted donor cores (n=3 per recipient). The same procedure was conducted for the healthy control sponge and its three corresponding recipient sponges. The entire transplantation experiment was carried out under in situ conditions for a time period of up to 11 days. It served to prove the Koch's postulates for disease transmission via direct tissue contact. After completion of the trial a visual documentation of the transplanted cores via underwater photography has been performed to record the recipient sponges' overall state of health.

Fig. 12. Sampling of *X. muta* donor tissue with a cork borer during the underwater infection trials. Underwater photography by Volker Glöckner.

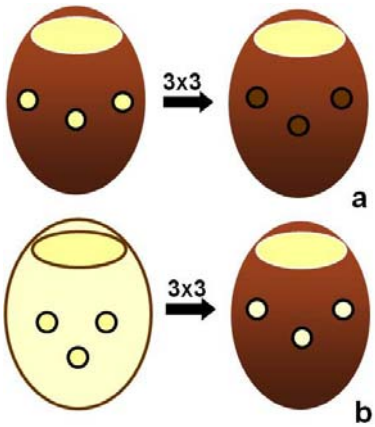

Fig. 13. Scheme of the transplantation trial: Three cores of one donor sponge, which was either the healthy control (a) or a SOB-diseased *X. muta* individual (b), were fit into one healthy recipient sponge. This procedure was repeated three times, as nine cores were obtained per donor sponge. Those were put into the sponge's respective recipient sponges (n=3 per donor).

16.2 Infection experiments on Sponge White Patch disease

The *Amphimedon compressa* underwater infection experiments were conducted as well at Conch Reef within the Florida Keys National Marine Sanctuary at Key Largo on a 20m transect in September 2009 (see respective video on supplementary CD). First of all, three randomly selected Sponge White Patch diseased individuals, that were showing characteristic signs of disease, were visually observed and their disease progressions were documented via underwater photography for up to seven days. Furthermore, twenty healthy *A. compressa* individuals were chosen randomly as recipient sponges for the infection trials. To them either red tissue of a healthy donor sponge (n=10 as a control) or white tissue of a diseased donor sponge (n=10) was attached via cable ties (Fig. 14). The sponges were monitored daily by SCUBA diving for up to nine days.

Fig. 14. The experimental set-up of the tissue transplantation trial: donor sponge tissue was attached in situ via three cable ties to a slightly injured recipient sponge.

In addition, infection trials on Sponge White Patch disease were performed by the injection of bacterial strains into healthy *A. compressa* sponges (Fig. 15; see respective video on supplementary CD). The isolates were selected from a collection of 38 bacterial strains that had previously been isolated from Sponge White Patch diseased *A. compressa* tissues on azocoll-containing marine agar 2216 (see microbial cultivation: page 27f). An analysis via restriction fragment length polymorphism (RFLP: see page 28f) was performed on their 16S rRNA genes, obtained with the primer pair 27f and 1492r, to get an insight into their overall bacterial diversity. Thus, 18 different RFLP patterns were revealed that were compared via denaturing gradient gel electrophoresis (see DGGE: page 30f). Strains with similar DGGE banding patterns as the diseased tissue itself were chosen for the infection experiments and their sequences were analyzed afterwards (see page 92: Tab. 5). Thus, 30 healthy individuals (n=30) were randomly chosen as recipient sponges along the 20m transect at Conch Reef within the Florida Keys National Marine Sanctuary. The sponges were divided into five groups á six individuals each (n=6) for injection with one of the bacterial strains #14, #16 and #K3 as well as the positive and negative control. The negative control consisted out of Zobell-medium only without any inoculated strain. At the onset of the experiment, for each strain 100ml Zobell-medium were inoculated either with one of the respective bacterial isolates

(#14, #16 or #K3) or with homogenized and pooled white tissue of ten Sponge White Patch diseased *A. compressa* individuals (positive control). The inoculations were incubated at 30°C for 48h. The injection of one strain was performed for six sponges each, but in two different dilutions: either 10ml of pure inoculation (n=3) or 10ml of a 1/10 dilution with sterile seawater (n=3). This dilution series was also performed for the negative and positive controls.

Into each sponge 10ml of that inoculation was injected repeatedly, once on day 1 and twice on day 5. The sponges were monitored for a total time period of nine days. The infection experiment was repeated again in July 2010 with the two bacterial strains #4 and #29 that had been isolated from the white tissue of diseased *A. compressa* #1 during microbial cultivation in May 2009. This time the experiment was monitored for 29 days thanks to Steve McMurray and Tse-Lynn Loh from the laboratory of Prof. Pawlik (UNCW, USA).

Fig. 15. Representative injection of a healthy *A. compressa* individual during the inoculation trials at Conch Reef, Florida, in September 2009. Underwater photography by Volker Glöckner.

IV. Results

1. Sponge Orange Band disease of *Xestospongia muta*

1.1 Underwater observations

Healthy specimens of *Xestospongia muta* are barrel-shaped and have a brown, robust and irregular surface, often with protrusions (Fig. 16a). Diseased individuals instead show a gradual color change of the surface from brown to bleached white (Figs. 16b-l). The process typically starts at isolated patches and affects the entire sponge body over time. This color transition, also termed bleaching, can be accompanied by an orange band giving rise to the name 'Sponge Orange Band' of this disease (Cowart *et al.*, 2006). Diseased *X. muta* individual #4 (Fig. 16e) is a prime example, as it exhibits clearly the color gradient from brown over an orange transition zone to bleached white. Additionally the sponge body seems to be slightly overgrown. An orange band could only be documented in about half of the cases of diseased *X. muta* sponges (Figs. 16b-f). In addition to loss of the surface coloration, massive tissue destruction and erosion have been observed (Figs. 16f-h, j-k), which usually result in collapse of the entire sponge within up to six weeks. As optical variations were present among the diseased sponge specimens, the individuals were grouped into either early- (low degree of bleaching without erosion: Figs. 16b-c, i, l) or advanced stages of disease (high degree of bleaching with erosion: Figs. 16d-h, j-k). Interestingly, only sponges in the early stages of disease (Figs. 16l, 17c) have been observed to be still actively pumping as visually judged by the application of fluorescent dye, whilst the water flow had ceased in sponges undergoing already advanced stages of disease (Figs. 16j-k, 17b, e). Chris Finelli (UNCW) proved the latter observation additionally via in situ flow measurements (Figs. 17d-e) (unpublished data).

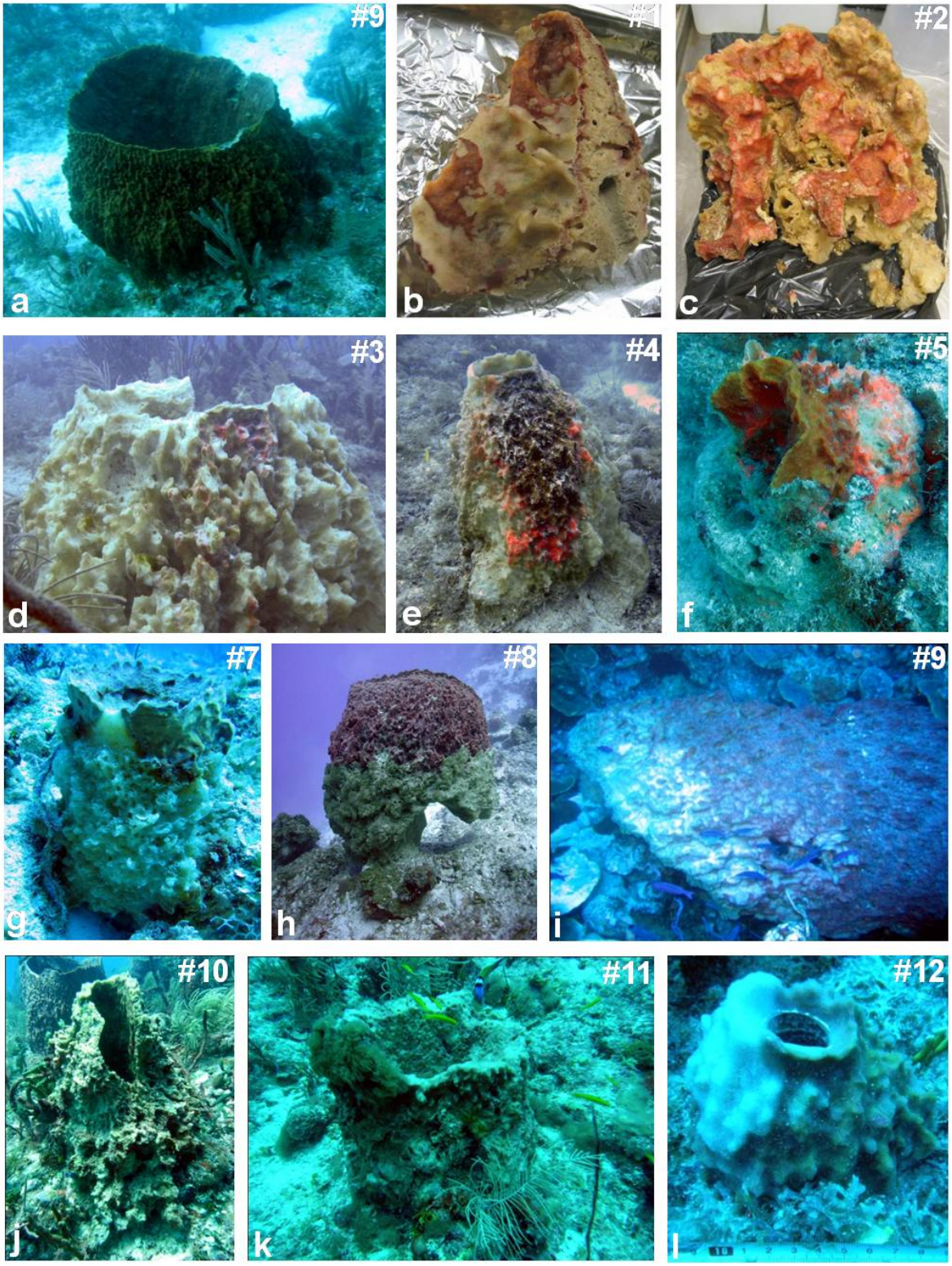

Fig. 16. Underwater photographs of healthy *X. muta* #9 (a) and the diseased individuals #1 (b), #2 (c), #3 (d), #4 (e), #5 (f), #7 (g), #8 (h), #9 (i), #10 (j), #11 (k) and #12 (l) undergoing early (b, c, i, l) or advanced (d, e, f, g, h, j, k) stages of Sponge Orange Band disease.

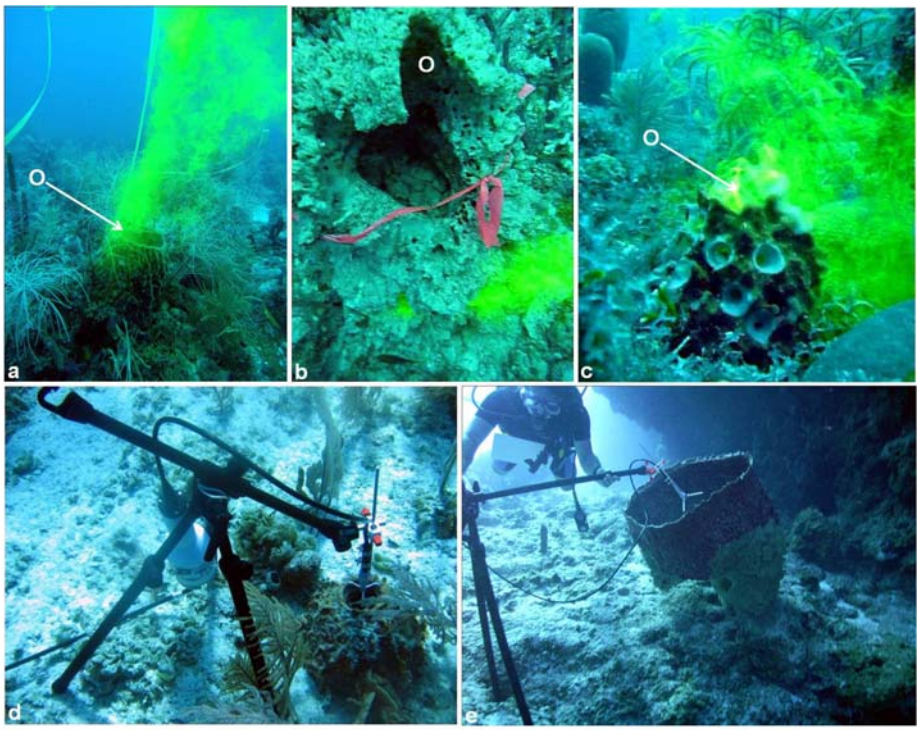

Fig. 17. Pumping activity of *X. muta* individuals: application of fluorescent dye (yellow) reveals the pumping activity of a healthy sponge (a) versus no activity within an advanced stage diseased sponge (b) and activity within an early stage diseased individual (c). In situ flow measurements by C. Finelli (UNCW) documented the pumping activity of a healthy sponge (d) versus no activity of an advanced stage diseased individual (e). All diseased sponges were applied to this study. Abbreviation: O, osculum.

1.2 Marine invertebrates associated with *X. muta*

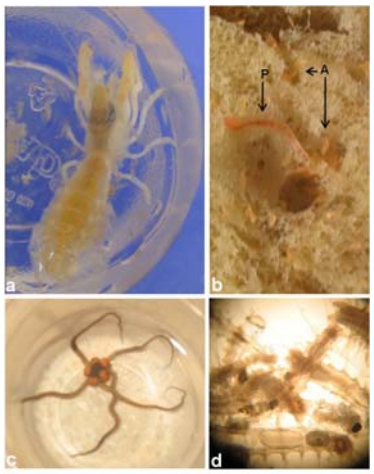

Sillid polychaetes (Fig. 18d) as well as brittlestars (Fig. 18c) were found to be present within the aquiferous canals of healthy *X. muta* individuals. Sponge Orange Band diseased individuals instead were often infected by marine amphipods (Fig. 18b) in addition presumably belonging to the family Anamixidae (personal comment J.D. Thomas, Smithonian Institution, 2008). A shrimp (Fig. 18a) has also been detected within Sponge Orange Band diseased individual #3 (Fig. 16a).

Fig. 18. Marine invertebrates associated with healthy (c, d) or diseased (a, b) *X. muta* individuals: a shrimp (a), marine amphipods (b), sillid polychaetes (b, d) and a brittlestar (c). Abbreviations: A, amphipods; P, polychaetes.

1.3 Histological investigations of Sponge Orange Band disease

Cross sectioning healthy sponges revealed the before described consistency of two diverse tissue layers (see page 18) comprising an outer brown pinacodermal surface layer of approximately 2mm and an inner reddish surface layer of approximately 3-5mm. The latter seems to belong to the mesohyl and separates the pinacoderm visually from the normal tan mesohyl (Fig. 19a). Diseased *X. muta* individuals undergoing early stages of disease seem to suffer from bleaching just within the outer surface layer. The inner surface layer still exhibits the reddish coloration (Fig. 19b). Instead, individuals in advanced stages of Sponge Orange Band disease show bleaching within the overall sponge surface tissue including the outer and the inner surface layers (Fig. 19c).

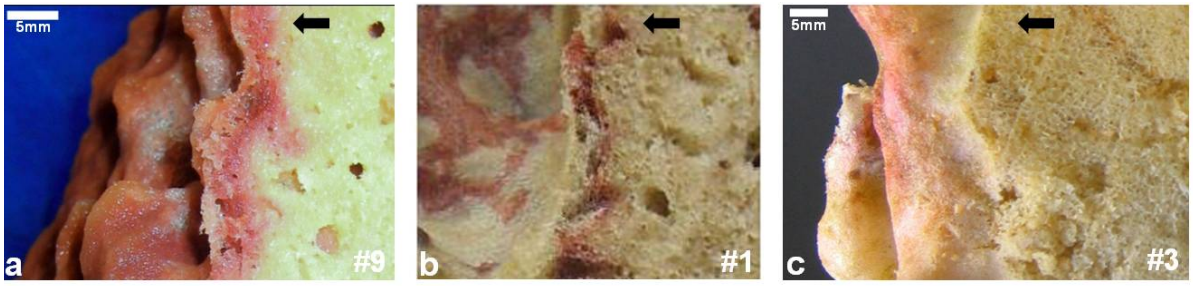

Fig. 19. Cross sections of a healthy (a) *X. muta* individual (#9, Fig. 16a), an early-stage diseased (b) individual (#1, Fig. 16b) and an advanced-stage diseased (c) individual (#3, Fig. 16d) demonstrating the variable consistency of the surface tissue during progression of disease. The arrows point towards the total sponge surface tissue of approximately 8mm.

Binocular microscopy on formaldehyde preserved samples of healthy *X. muta* sponges exhibited a reddish coloration of their surface tissues. This deviation from the normal brown has been arising from fixation (Fig. 20a). Yet, during bleaching the surface tissue of SOB-diseased individuals gradually lost its coloration and resulted in orange (Fig. 20b) or white (Fig. 20c). This process has been demonstrated in detail for diseased *X. muta* #3 (Figs. 16d, 19c).

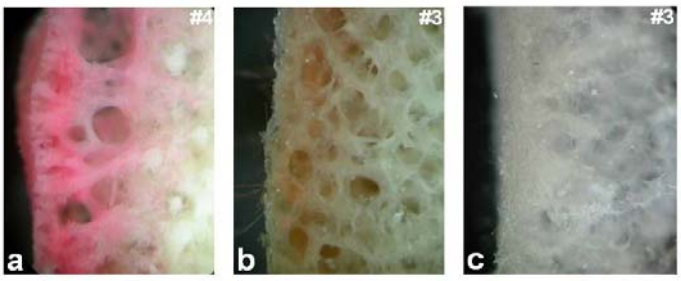

Fig. 20. Binocular microscopy on the surface of a healthy (a) *X. muta* individual (#4) and on the orange (b) and white surface (c) of an advanced stage diseased individual (#3, Fig. 16d).

1.4 Electron microscopical observations

Scanning electron microscopy

Tissues from five healthy and five diseased *X. muta* individuals were inspected by scanning electron microscopy (SEM). It revealed characteristic features for healthy *X. muta* surfaces such as ostia leading into aquiferous canals (Fig. 21a). The tissue itself is stabilized by a meshwork of spicules, which are readily identified as spines embedded within the extracellular matrix (Figs. 21a-c). Flattened pinacocyte cells form an incoherent layer on top of the tissue covering large areas of the mesohyl (Figs. 21b-e). Cyanobacteria are incorporated into a meshwork of collagenous fibers (Figs. 21c-e). The brown surface tissue of advanced stage diseased individuals resembles the one of healthy sponges with the exemption that the pinacocytes are already vastly absent and that cellular detritus is recognizable instead on the sponge surface. The spicule and collagen meshwork, that is embedding sponge cells and cyanobacteria, is getting more and more exposed to the marine environment (Figs. 21f-j) resulting in an increased destruction and dissolution of sponge cells over time (Fig. 21j). The degradation is even more advanced within the orange surface tissues (Figs. 21k-o) laying bare the spicule skeleton (Fig. 21l), the sponge cells and the cyanobacteria within the collagen fibers (Figs. 21m-o). Again cellular detritus (Fig. 21l) is revealed by the dissolution of sponge cells (Fig. 21o). In contrast, the white surface tissue of diseased sponges is made up of the spicule skeleton only and just very little biomass is left besides the basic bauplan (Fig. 21p). The sponge cells and cyanobacteria are absent, but numerous filaments, presumably of bacterial origin, are replacing them beleaguering the spicules next to the detritus (Figs. 21q-t).

Particular care has been taken to visualize the cellular processes in the orange band transition zone. For this purpose, orange surface tissues have been compared from early and advanced stages of Sponge Orange Band diseased individuals. Interestingly, among the five examined sponges all Bahamian samples were undergoing early stages of disease, whereas the Florida samples were undergoing advanced stages showing more severe symptoms of disease. Within early stages flattened pinacocytes can still be recognized on the surface of the orange transition zone (Fig. 22a). Abundant cyanobacteria are embedded close to the surface within the collagen matrix (Fig. 22b). Phagocytotic archaeocytes, surrounded by cyanobacteria, bacteria and variant sponge cells, are present within the inner surface layer which normally possesses a reddish coloration (Fig. 22c). In contrast, the orange surface tissue of sponges undergoing advanced stages of disease is devoid of pinacocytes, but therefore dominated by cellular detritus and microbial filaments (Figs. 22d-e). Phagocytosis

by sponge cells and their degradation is visible on a cellular level within the inner surface layer of the orange band transition zone (Fig. 22f).

As already described for Sponge Orange Band diseased individual #5 (Fig. 21p-t) the white surface tissue of all diseased individuals consists out of a spicule skeleton only that is intervened by cellular detritus and diverse microbial filaments (Figs. 23b-f, i). Those belong even partly to spore-producing (Figs. 23c-d, f) and colony-forming (Figs. 23g-h) types. In addition, a marine mite has been detected within the white surface tissue of Sponge Orange Band diseased *X. muta* #3 (Fig. 23a).

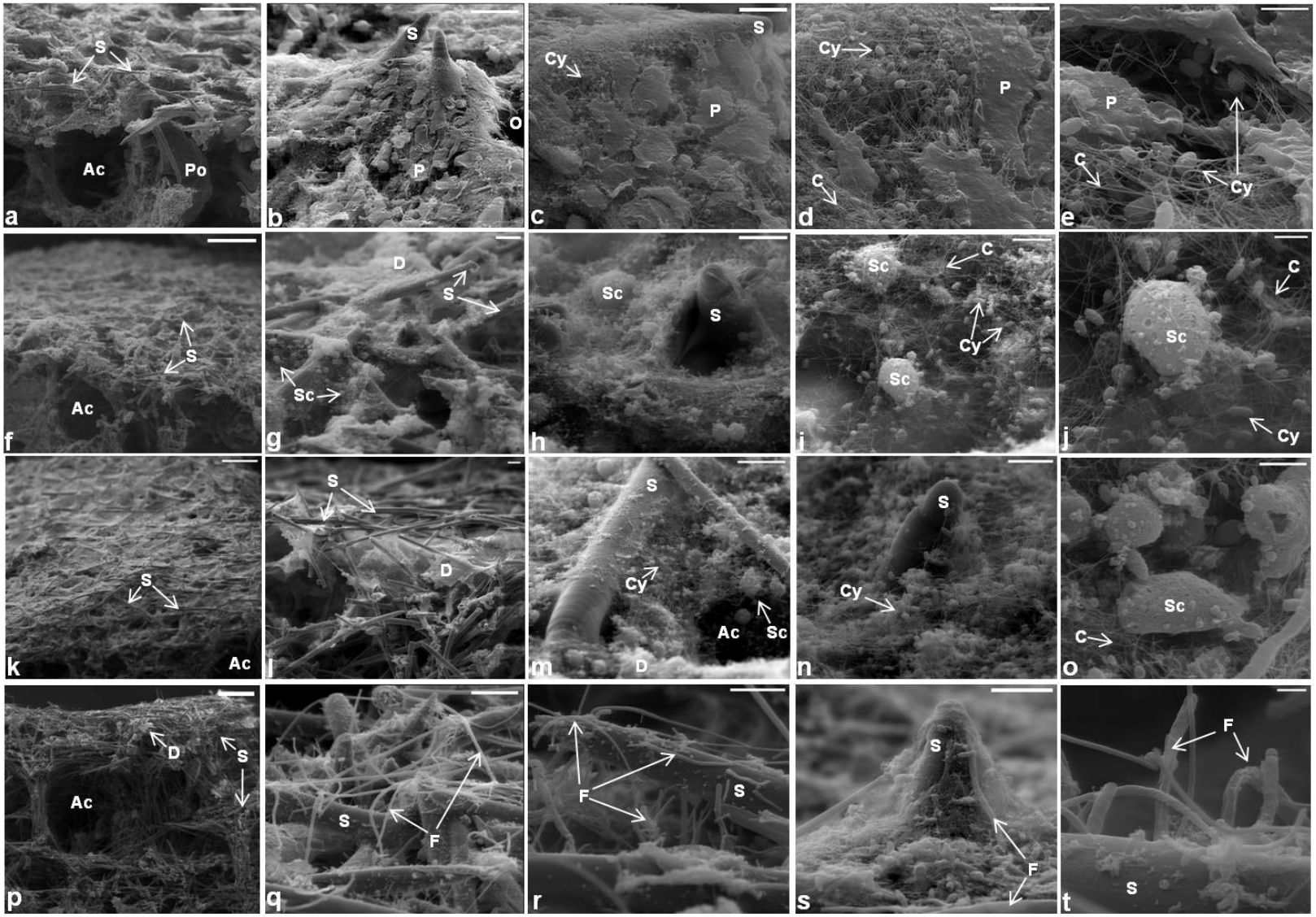
a
S
Ac
Po
b
S
O
P
c
S
Cy
P
d
Cy
P
C
e
P
C
Cy
f
S
Ac
g
D
S
Sc
h
Sc
S
i
Sc
C
Cy
Sc
j
C
Sc
Cy
k
S
Ac
l
S
D
m
S
Cy
Ac
Sc
D
n
S
Cy
o
Sc
C
p
D
S
Ac
q
S
F
r
F
S
s
S
F
t
F
S

Fig. 21. Scanning electron micrographs on the surface tissue of a healthy (a-e) *X. muta* individual (#4) in comparison to the brown (f-j), orange (k-o) and white (p-t) surface tissue of Sponge Orange Band diseased individual #5 (Fig. 16f). The scale bars represent 200µm (a, f, k, p), 20µm (b, g, l, q), 10µm (c, h, m, r), 5µm (d, i, n, s) and 2µm (e, j, o, t), respectively. Abbreviations: S, spicule; Ac, aquiferous canal; Po, polychaete; O, osculum; P, pinacocyte; Cy, cyanobacterium; C, collagen; Sc, sponge cell; D, detritus; F, filament.

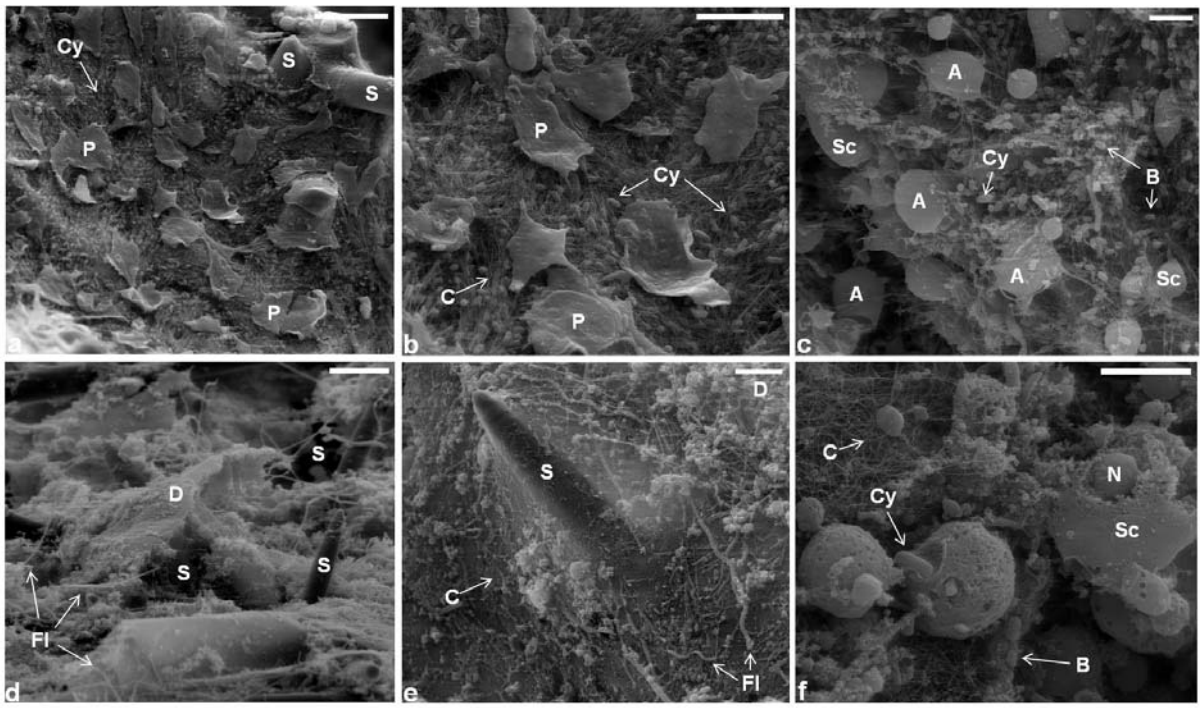

Fig. 22. Scanning electron micrographs on the orange transition zone of *X. muta* individuals undergoing an early (a-c; individual #2) versus an advanced stage (d-f; individual #3) of Sponge Orange Band disease. The scale bars represent 20µm (a, d), 10µm (b, e) or 5µm (c, d), respectively. Abbreviations: Cy, cyanobacterium; P, pinacocyte; S, spicule; C, collagen; A, archaeocyte; Sc, sponge cell; B, bacterium; Fl, filament; D, detritus; N, nucleus.

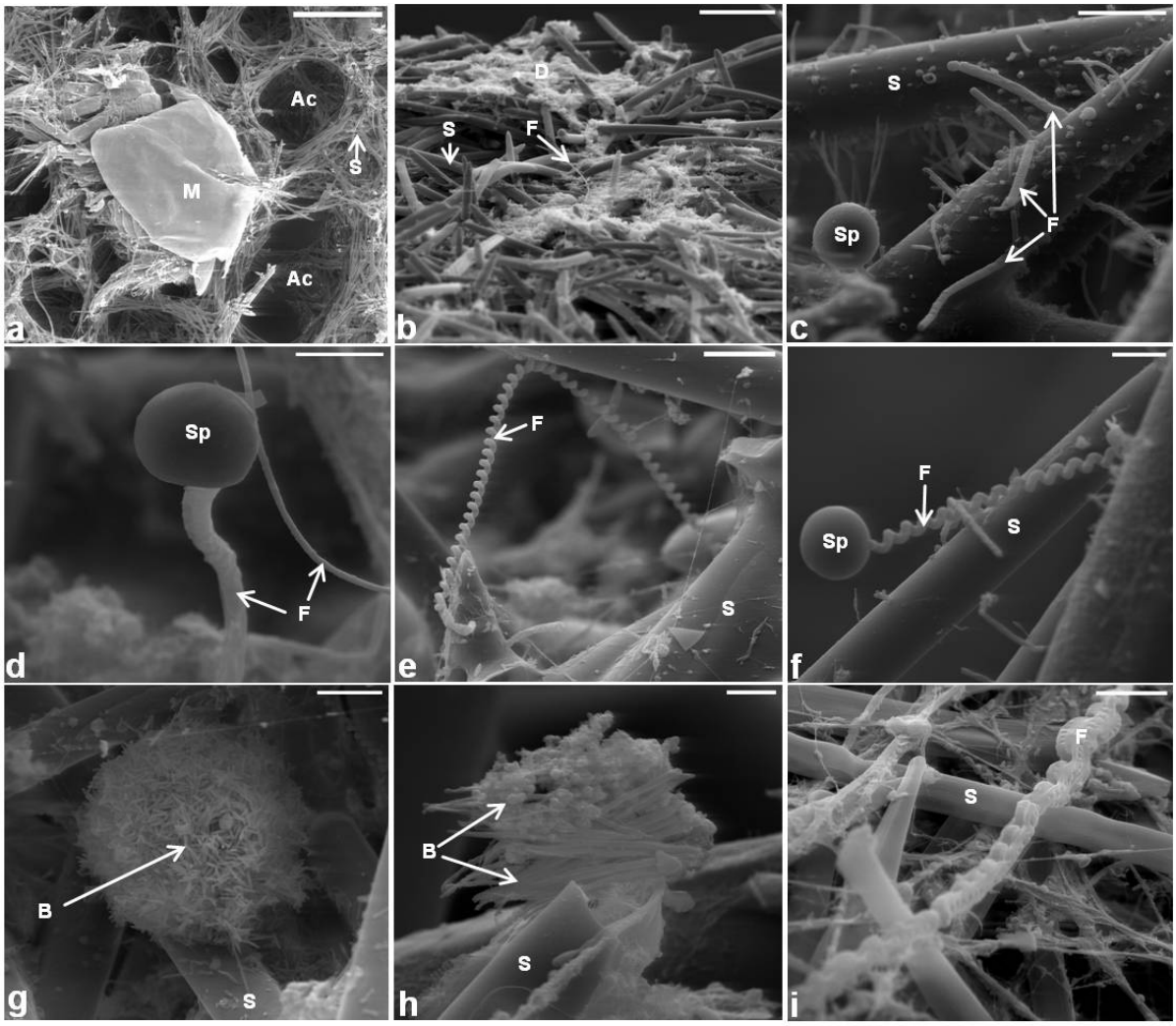

Fig. 23. Scanning electron micrographs on the white surface tissue of Sponge Orange Band diseased individuals #2 (i), #3 (a-b), #4 (e-h) and #5 (c-d) depicting a mite (a) in an overall destroyed tissue environment (b) as well as various filaments (c-f, i), spores (c-d, f) and colonies (g-h) of presumably bacterial origin. M, mite; Ac, aquiferous canal; S, spicule; D, detritus; F, filament; Sp, spore; B, bacterium.

Transmission electron microscopy

Tissues from three healthy and five diseased *X. muta* individuals were inspected by transmission electron microscopy (TEM). Representative images of one healthy individual (#9, Fig. 16a) are shown in comparison to the brown, orange and white surface tissues of one diseased individual (#5, Fig. 16f). Transmission electron microscopy revealed destruction that has been gradually increasing during bleaching from the brown over the orange to the white surface tissues of diseased individuals. Those were undergoing advanced stages of disease. In general, healthy sponge cells can be clearly distinguished by their cellular shape and size of about 10µm x 5µm with a nucleus of approximately 5µm in diameter. They are often extracellularly surrounded by diverse bacterial morphotypes (Fig. 24a). In contrast, the sponge cells within the brown tissue of advanced stage diseased individuals exhibit already signs of cellular destruction by the formation of apoptotic bodies. Even the bacteria seem to be affected by this phenomenon (Fig. 24b). During bleaching the overall health state of sponge cells deteriorates visibly. Within the orange surface tissue the sponge cells are dissolving completely conceiling the cell shape and leaving just the nucleus to be recognized (Fig. 24c). Mostly spicules (data not shown) comprise the white surface tissue. The little biomass that is left behind consists exclusively out of dispersed bacterial morphotypes and cellular debris such as apoptotic bodies. No clear cellular organisation, neither sponge cells or their nuclei nor the symbiotic cyanobacteria are recognizable anymore (Fig. 24d).

By comparing the tissue of healthy sponge surfaces to the orange transition zone of diseased sponges a different grade of affection has been revealed depending on the sponge's stage of disease (early versus advanced). Healthy sponge surfaces consist of integer sponge cells with differentiated cell nuclei (N), few bacteria-filled vesicles and clear cell membranes (Fig. 25a). Within the orange tissue of early stage diseased individuals (Figs. 25b-c) instead, phagocytotic sponge cells (presumably archaeocytes) have been observed engulfing and containing high numbers of intravesicular cyanobacteria (Cy). Those are apparently subject to digestion and can be identified by their thylakoid membranes. The overall state of the sponge cells seems unaffected. However, for the orange surface tissue of the advanced stage diseased sponges (Figs. 25d-f) TEM revealed cellular destruction of nearly all cells inspected. The sponge cells disintegrated entirely into numerous vesicles that resemble apoptotic bodies leaving solely nuclei (N) and partly destructed cyanobacteria (Cy) as well as bacterial morphotypes (B) behind.

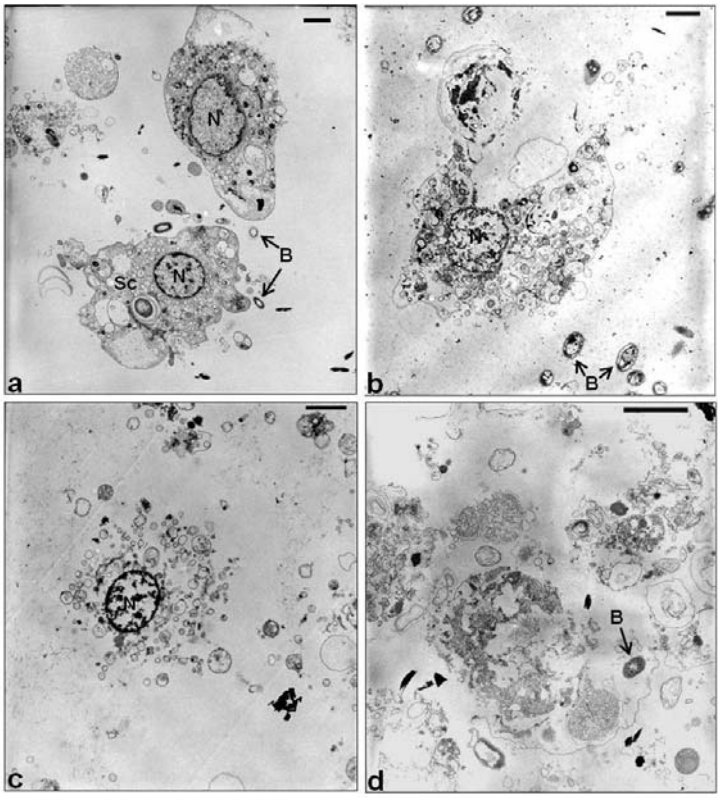

Fig. 24. Transmission electron micrographs of healthy (a) *Xestospongia muta* surface tissue (#9, Fig. 16a) versus the brown (b), orange (c) and white (d) surface tissue of an advanced stage diseased individual (#5, Fig. 16f). The scale bars represent 1µm each. Abbreviations: N, nucleus; Sc, sponge cell; B, bacterium.

A magnification of cyanobacteria present within healthy sponges revealed a cyanobacterium of approximately 1.5µm x 2µm in diameter, whose cytoplasm is densely filled with thylakoid membranes and whose cell is surrounded by an undulating capsule giving rise to few pilis (Fig. 26a). Looking at the cyanobacteria within the orange surface tissue of early stage diseased sponges indicates the same cell type, but also a potential swelling of its cyanobacterial capsule (Figs. 26b) followed by cellular damage. However, within the orange surface tissue of sponges undergoing an advanced stage of disease the protecting cyanobacterial capsule seems to be lacking. This has been underlined by the emergence of holes in the nucleoid-containing centre of the cyanobacteria and the cellular dissolution into numerous vesicles (Fig. 26c) as well as by the appearance of dark blotches within the cytoplasm (data not shown). The latter is presumably due to degradation of the thylakoid membranes.

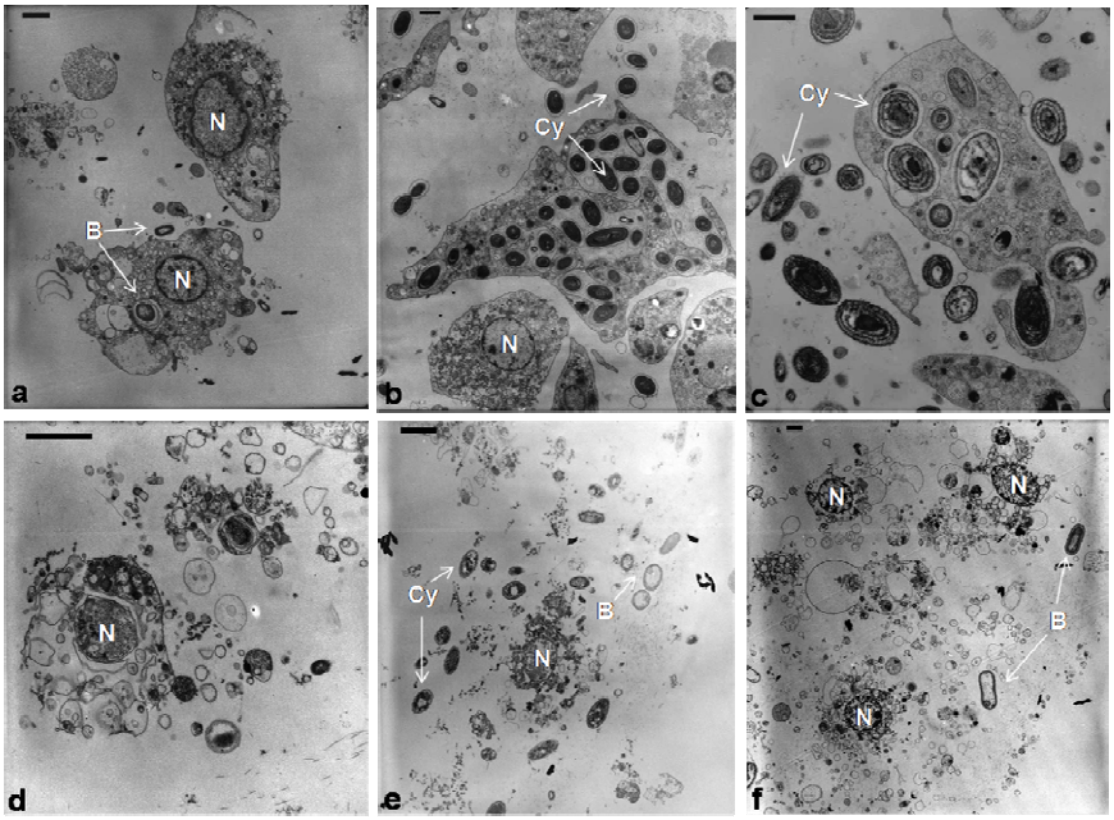

Fig. 25. Transmission electron micrographs of a healthy *X. muta* individual (a; #9) versus the orange transition zones of early stage Sponge Orange Band diseased individuals (b: #1; c: #2) and advanced stage diseased individuals (d: #3; e: #4 and f: #5). The scale bars depict 1µm each. Abbreviations: B, bacterium; N, nucleus; Cy, cyanobacterium.

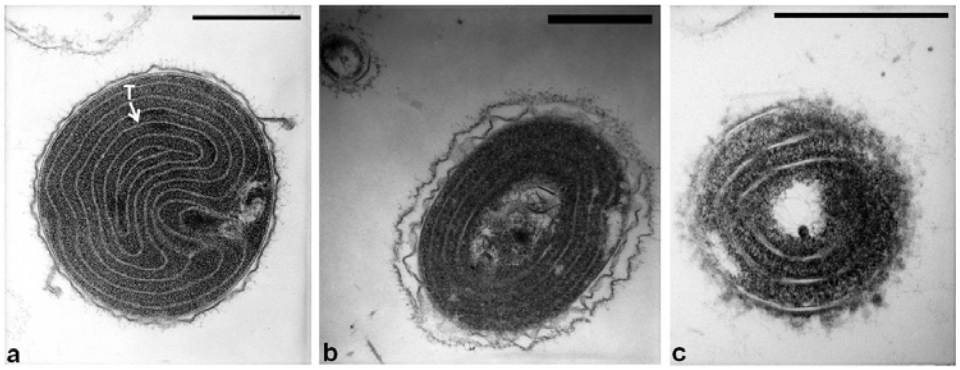

Fig. 26. Transmission electron micrographs of the *X. muta* associated cyanobacteria within a healthy (a) sponge (#9) and within the orange transition zones of Sponge Orange Band diseased individuals (b: #2 and c: #3). A special focus was put on early (b) versus advanced stages (c) of Sponge Orange Band disease. The scale bars depict 1µm each. Abbreviations: T, thylakoid membranes.

The role of X. muta's cyanobacterial symbionts

When *X. muta* individuals are injured mechanically, they lose the site-specific coloration of their surface tissues into the surrounding seawater. I will refer to this phenomenon as 'sponge bleeding' in the further context. It has been observed underwater after sponge injury as well as after sample transfer to the sea surface within zipbloc bags. The seawater within the sponge containing bags turned pinkish-red and the overall sponge sample looked paler than before the collection. Investigating the pellet of the centrifuged seawater sample via fluorescence-microscopy revealed bright orange signals (Fig. 27a). Transmission electron microscopy on it demonstrated the ubiquitous presence of cyanobacteria, which were easily identified by the abundance of their thylakoid membranes. They were interspersed by other bacterial morphotypes and sponge cells with the latter being recognized by their nucleus and their cellular size of approximately 3 x 5µm (Fig. 27b). This has been additionally confirmed via scanning electron microscopy, where the surface composition and size of the sponge associated cyanobacteria (~2 x 5µm), bacteria and sponge cells were revealed (Fig. 27c). Thus, the elucidation of the seawater-staining *X. muta* constituents via 'sponge bleeding' was helpful to visually identify the color-giving cyanobacteria during the electron microscopical studies.

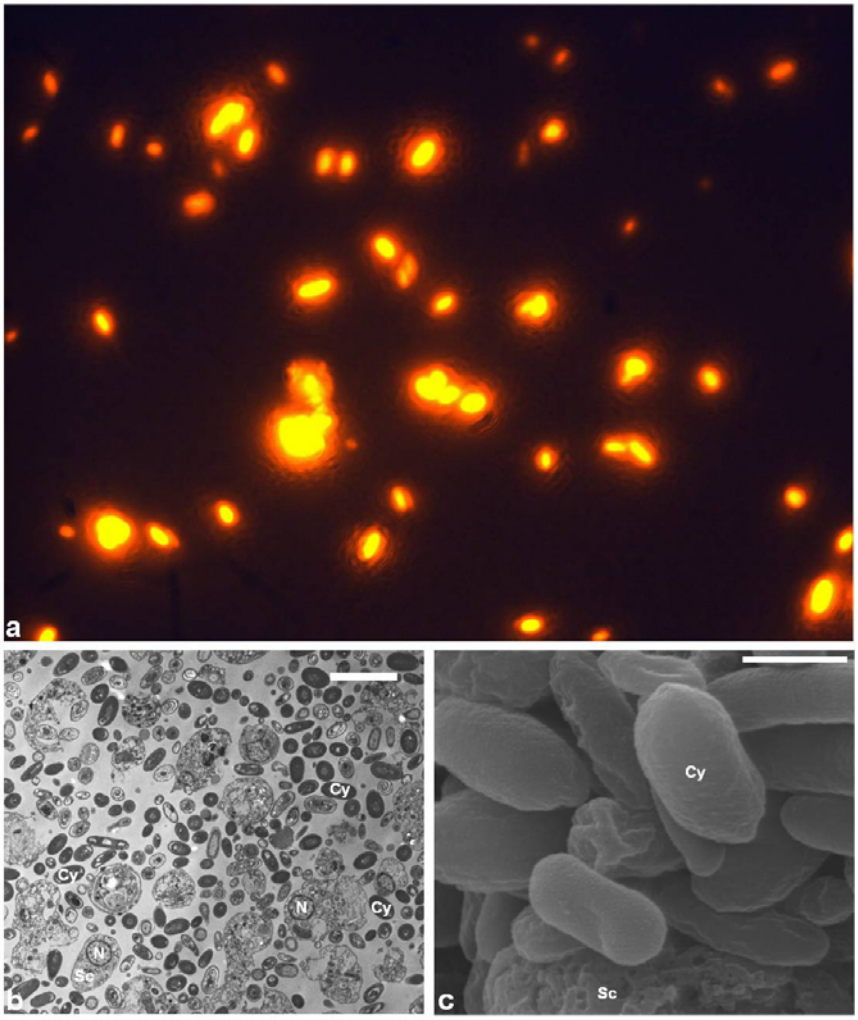

Fig. 27. Investigating the reddish-brown pellet obtained from seawater after mechanical injury of *X. muta* exhibited the presence of autofluorescent cyanobacteria via fluorescence microscopy (a) and of diverse cyanobacterial morphotypes and sponge cells via TEM (b; scale bar=5µm). Scanning electron microscopy revealed the surface morphology of the cyanobacteria, few bacteria and sponge cells (c; scale bar=1µm). Abbreviations: N, nucleus; Sc, sponge cell; Cy, cyanobacterium.

1.5 Cell counts on *X. muta* tissues

As described in Tab. 1 the amount of DAPI-stained bacteria, cyanobacteria and sponge cell nuclei per gram sponge tissue were enumerated via fluorescence microscopy for healthy sponges (n=3) and Sponge Orange Band diseased individuals undergoing early stages of disease (n=2). Interestingly, the healthy *X. muta* individuals possessed on average a lower amount of bacteria per gram sponge than the diseased representatives, which showed the highest value within their white tissues followed by the brown and orange ones. The orange tissues of diseased *X. muta* exhibited the highest amount of cyanobacteria per gram sponge tightly followed by the healthy sponges. The least cyanobacteria were present within the white tissues of diseased individuals. However, also the highest amount of sponge cell nuclei was revealed for the orange tissues of diseased sponges followed by the healthy *X. muta* individuals (Tab. 1).

The amount of sponge cell nuclei, extra- and intracellular cyanobacteria as well as their ratio have been evaluated per gram sponge for dilutions of 10^{-3} derived from healthy *X. muta* individuals as well as from brown, orange and white surface tissues of a Sponge Orange Band diseased individual (Fig. 28, see annex Tab. 2). The amount of sponge cell nuclei was higher in healthy sponges (6.3 ± 1.6) than in the brown (3.9 ± 0.5), orange (4.4 ± 0.5) and white parts (3.6 ± 0.3) of the diseased sponge. Most cyanobacteria were present within healthy *X. muta* sponges (32.3 ± 10.6) followed by the orange (25.5 ± 3.5) and then brown (13.8 ± 1.1) tissue of the diseased sponge. Its white tissue revealed the least cyanobacteria (1.9 ± 0.5). The amount of extracellular cyanobacteria was by far the highest in healthy *X. muta* surface tissues (29.9 ± 10.0) in comparison to the orange (12.4 ± 0.7) and brown ones (7.8 ± 0.8) of the diseased sponge with neglectable values for its white counterpart (0.9 ± 0.1). In contrast, during SOB-disease an astonishing increase in intracellular cyanobacteria has been observed for early stage diseased sponges starting already within the brown surface tissues (6.0 ±0.7) and reaching its maximum in the orange transition zone (13.2 ± 3.1) of the diseased sponge (n=1), where also the highest amount of cyanobacteria had been measured before. Healthy sponges in contrast had a fairly low value (2.8 ± 1.0). Even the few cyanobacteria within the white tissue (1.1 ± 0.6) of the diseased sponge showed a higher percentage of intracellular than extracellular cyanobacteria. This has been additionally highlighted by their ratio, which was the lowest in the white tissue (0.8) followed by the orange (0.9) and brown parts (1.3) of the diseased sponge in comparison to the very high ratio of healthy individuals (10.7) (Fig. 28).

Due to the presence of numerous thylakoid membranes, it was possible to distinguish the cyanobacteria from the ambient heterotrophic bacteria by their autofluorescent properties. Intracellular cyanobacteria were located within single sponge cells of the diseased *X. muta* individual (#1; Fig. 16b) via the overlay of pictures showing autofluorescent cyanobacteria and DAPI-stained sponge cells at the same time by using epifluorescence microscopy (Fig. 29).

X. muta sample	Bacteria per g/sponge	Cyanobacteria per g/sponge	Sponge cell nuclei per g/sponge
Healthy sponge (n=3)	$3.2x10^8 \pm 4.5x10^7$	$1.1x10^7 \pm 2.3x10^6$	$2.4x10^6 \pm 5.9x10^5$
Diseased sponge: brown (n=2)	$2.3x10^9 \pm 7.2x10^8$	$6.6x10^6 \pm 2.3x10^6$	$1.4x10^6 \pm 6.8x10^5$
Diseased sponge: orange (n=2)	$5.1x10^8 \pm 2.5x10^8$	$4.8x10^7 \pm 3.9x10^7$	$1.6x10^7 \pm 1.4x10^7$
Diseased sponge: white (n=2)	$1.9x10^9 \pm 1.5x10^9$	$2.4x10^6 \pm 2.4x10^6$	$1.7x10^6 \pm 1.7x10^6$

Tab. 1. Amount of bacteria, cyanobacteria and sponge cell nuclei per gram sponge within healthy *X. muta* surface tissues and the brown, orange and white surface tissues of early stage diseased individuals (#1 and #2; Figs. 16b-c).

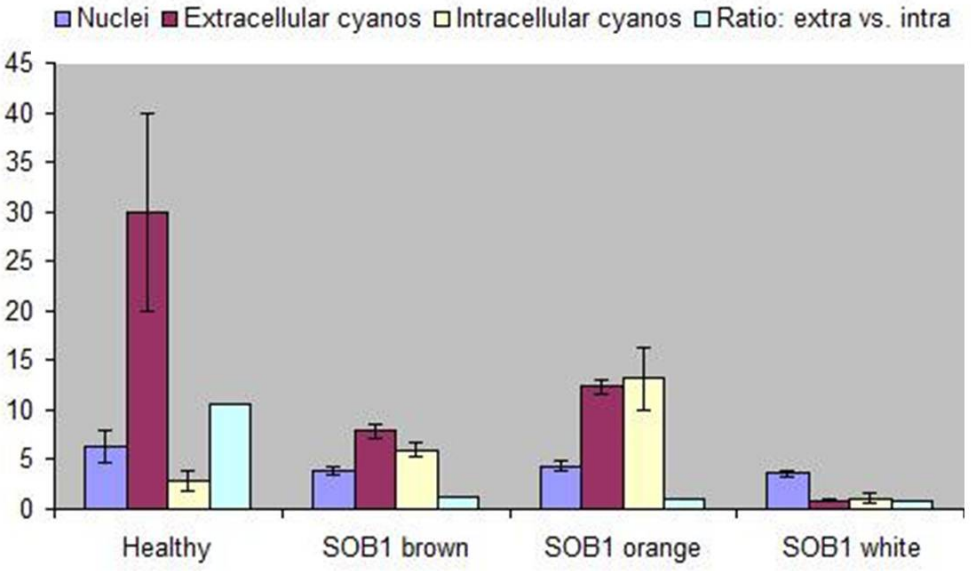

Fig. 28. Sponge cell nuclei, extracellular and intracellular cyanobacteria as well as their ratio per gram sponge within dilutions of 10^{-3} derived from healthy surface tissues (n=4) as well as brown, orange and white surface tissues of Sponge Orange Band diseased *X. muta* #1 (n=1).

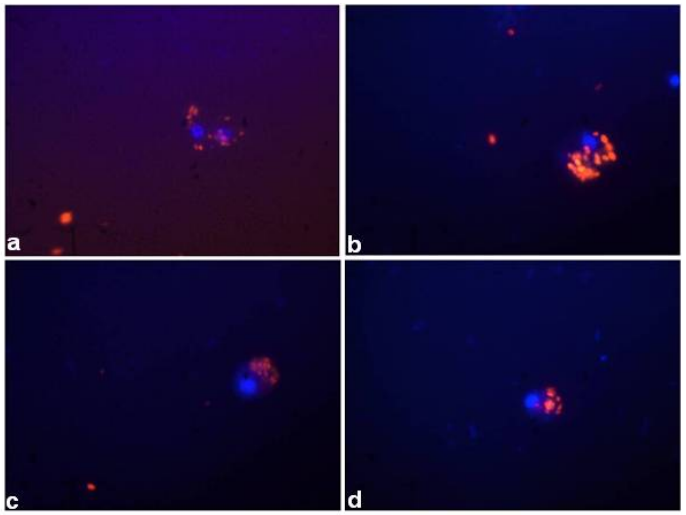

Fig. 29. Epifluorescence micrographs of intracellular cyanobacteria of sponge cells obtained from Sponge Orange Band diseased individual #1 (a-d). The magnification is 100-fold.

1.6 Microbial cultivation

Bacterial diversity of Bahamian sponges

During the Bahamas expedition 2007 bacteria were cultivated on GPYNS-agar from homogenates of healthy *X. muta* individuals and of the orange surface tissue of an early stage diseased individual (#1; Fig. 16b). As a result, a white colony has been isolated from the healthy sponge, which was to 97% similar to the antimicrobial and cytotoxic *Bacillus* sp. 094802. The orange tissue revealed also representatives of the *Firmicutes*: two yellow colonies with highest similarity to the amoebic gill disease associated *Staphylococcus* sp. AC9 (91% and 98%, respectively) as well as one yellow colony belonging to 99% to the deep water sponge associated *Staphylococcus* sp. J688 and another one resembling to 98% the surface colonizing *Bacillus* sp. SUB8. Additionally, representatives of the *Gammaproteobacteria* were identified, which encompassed two white colonies resembling either to 98% the uncultured *Acinetobacter* sp. clone 3 or to 97% the clone BB1H16S-19, which had been isolated from the healthy mucus of a Black Band diseased coral before. Thus, the bacterial diversity obtained on GPYNS-agar from healthy and diseased Bahamian sponges yielded representatives of the *Firmicutes* and *Gammaproteobacteria* only.

Bacterial diversity of sponges from the Florida Keys

Bacterial cultivation on YPD- and M1-agar has been performed in winter 2007 on the brown, orange and white surface tissues of the advanced stage diseased individuals #3, #4 and #5 obtained from the Florida Keys National Marine Sanctuary. The overall bacterial diversity was highest within the orange tissues of diseased sponges, followed by their brown and white tissues. The healthy *X. muta* individuals were the least diverse regarding the yield of bacterial colonies. Cultivation on M1-agar proved to be better suited than on YPD-agar yielding a higher bacterial diversity. Thus, altogether 101 colonies have been isolated: 9 from healthy *X. muta* individuals (n=2), 46 from the orange (n=3), 27 from the white (n=3) and 19 from the brown surface tissues (n=2) of diseased sponges (n=3). Ten isolates were of special interest. The identification of their 16S rRNA genes revealed the following results (see Tab. 2): The brown surface tissue yielded two white colonies that were both to 98% *Alphaproteobacteria*. They were most closely related either to *Pseudovibrio* sp. PaH3.35a1, isolated from the mucopolysaccharide layer of healthy *Pseudopterogorgia americana*, or to Rhodobacteraceae bacterium 1tc10, obtained from healthy *Montastrea annularis* tissue. The orange tissue revealed one yellow colony belonging to the *Actinomycetales*, that resembled to 97% the

freshwater sediment associated *Micrococcus* sp. HB-1. In addition another representative of the *Pseudopterogorgia americana* associated *Pseudovibrio* sp. PaH3.35a1 (similarity 95%) was identified as well as two ocher colonies. Those belonged either to the *Firmicutes* and were with 99% most similar to *Bacillus pumilus* strain B20 or to the *Actinomycetales* and were with 98% highly related to *Rhodococcus* sp. SCSIO 00026 derived from marine gray sands. The white surface tissue exhibited two yellow colonies representing the *Firmicutes* with *Bacillus pumilus* strain JS-45 (96% similarity) and the skin-associated clone nbw1097d02c1 (94% similarity). It exhibited also a strain clustering among the *Ruegeria* (*Alphaproteobacteria*) and belonging with 98% to *Silicibacter* sp. PaD1.36a derived from the surface mucopolysaccharide layer of diseased *Pseudopterogorgia americana*. The white-rose colored colony showed with 98% highest similarity to the cave coral *Oculina patagonica* associated bacterium c1cb24. Thus, I conclude that the bacterial diversity within the advanced stage diseased sponges obtained from the Florida Keys consisted mostly of *Alphaproteobacteria*, the *Actinomycetales* (*Actinobacteria*) and the *Firmicutes*.

X. muta sample	Colony: color	Closest sequence match in GenBank	Similarity (%)	Length (bp)	Taxonomic affiliation
Diseased: brown tissue	32: white	Mucopolysaccharide layer of healthy *Pseudopterogorgia americana* associated *Pseudovibrio* sp. PaH3.35a1 (GQ406798)	98	642/651	*Alphaproteobacteria*
	94: white	Healthy tissue of *Montastrea annularis* associated Rhodobacteraceae bacterium 1tc10 (FJ952794)	98	589/595	*Alphaproteobacteria*
Diseased: orange tissue	28: yellow	Freshwater sediment associated *Micrococcus* sp. HB-1(GU073283)	97	666/680	*Actinobacteria; Actinomycetales*
	29: white	Mucopolysaccharide layer of healthy *Pseudopterogorgia americana* associated *Pseudovibrio* sp. PaH3.35a1 (GQ406798)	95	741/779	*Alphaproteobacteria*
	12: ocher	*Bacillus pumilus* strain B20 (GQ167199)	99	557/562	*Firmicutes*
	77: ocher	Marine gray sands sediment associated *Rhodococcus* sp. SCSIO 00026 (GQ871747)	98	661/673	*Actinobacteria; Actinomycetales*
Diseased: white tissue	47: yellow	*Bacillus pumilus* strain JS-45 (GQ280115)	96	591/613	*Firmicutes*
	62: yellow	Skin-associated clone nbw1097d02c1 (GQ054000)	94	505/534	*Bacteria*
	15: white	Surface mucopolysaccharide layer of diseased *Pseudopterogorgia americana* associated *Silicibacter* sp. PaD1.36a (GQ391987)	98	628/636	*Alphaproteobacteria; Ruegeria*
	17: white-rose	Cave coral *Oculina patagonica* associated Bacterium c1cb24 (EF207119)	98	620/632	*Bacteria*

Tab. 2. 16S rRNA gene sequence analysis of selected bacterial colonies from the brown, orange and white surface tissues of Sponge Orange Band diseased *X. muta* individuals (#3, #4 and #5; see annex: Tab. 1) obtained from the Florida Keys in winter 2007.

1.7 Profiling microbial community changes by DGGE

The bacterial community during Sponge Orange Band disease

The eubacteria-specific DGGE gel (Fig. 30a) displays the bacterial community present within the surface tissues of two healthy *X. muta* individuals and their replicates in comparison to the differently colored surface tissues (brown, orange, white) of five Sponge Orange Band diseased individuals (Figs. 16b-f: #1, #2, #3, #4 and #5) undergoing early (#1 and #2) and advanced stages of disease (#3, #4 and #5). According to visual observations the molecular fingerprints of the healthy sponge surface tissues are nearly identical to each other enumerating at least 12-13 bands per lane. The bacterial communities of the diseased sponge surface tissues in contrast are highly diverse among each other in position, amount and intensity of bands. The microbial banding patterns of all diseased sponge surface tissues, no matter obtained from which surface coloration, differ to a great extend from the ones of the healthy sponges. They lack some GC-rich bacterial phylotypes that are present in healthy sponges and come up with additional bands of lower GC-content, which are located higher in the gel. Except for the brown and orange surface tissues of the early stage diseased sponges #1 and #2, both derived from the Bahamas, no overall color-bound or individual-specific disease pattern seems to be present.

The molecular fingerprint of the eubacterial DGGE gel was additionally analyzed with the software program Quantity One by dendrogram construction using the clustering method UPGAMA (Fig. 30b). Thus, the percentage similarities in between the banding patterns derived from the diverse sponge samples within one gel were elucidated. The bands obtained from the healthy surface tissue were with up to 96% nearly identical to each other. In contrast, the brown surface tissues of the diseased sponges #4, #5 and #2 were the least related to the healthy sponges with a 23% similarity only. Interestingly, they were with 47% and 57% most similar among each other and clustering together. Additionally, the orange surface tissues of the diseased sponges #1 and #2, which were identical in coloration and sample origin as well as their early stage of disease, clustered as well together with 75%. Despite that, there was no pattern of color- or individual specificity among the other sponge surface tissues. Thus, the software analysis confirmed the visual interpretation on the molecular fingerprint of Sponge Orange Band disease that no clear pattern of disease is recognizable. This negates the finding of an omnipresent eubacterial phylotype as an infectious agent of SOB-disease.

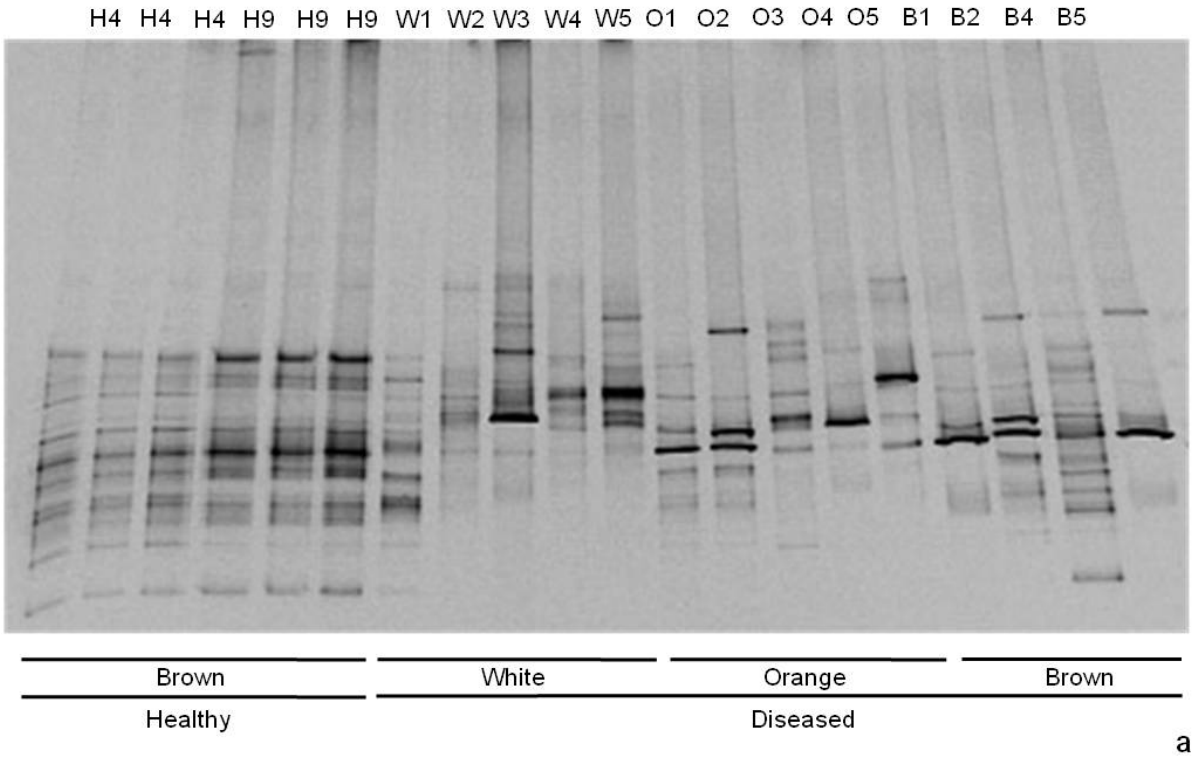

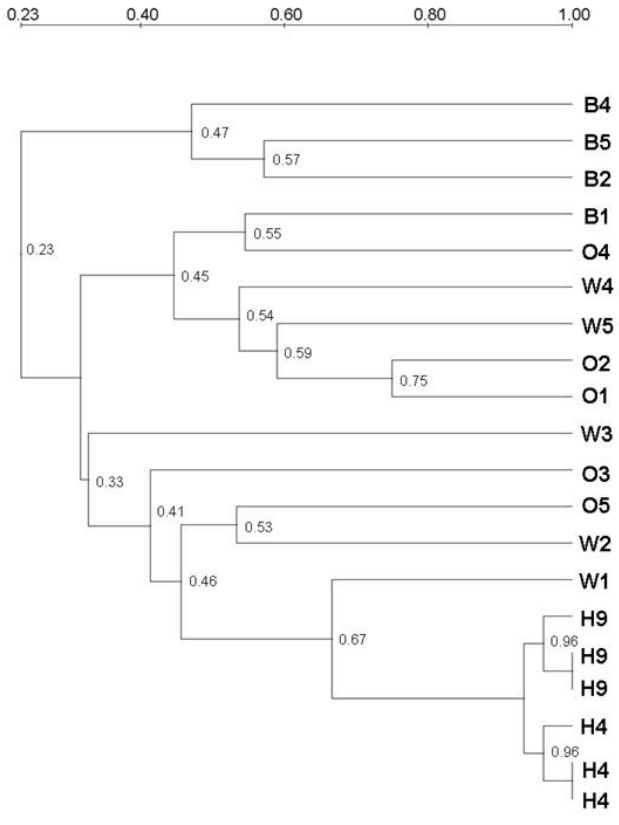

Fig. 30a: Denaturing gradient gel electrophoresis (DGGE) of eubacterial 16S rRNA genes in two healthy and five diseased *X. muta* individuals (Fig. 16; see annex: Tab. 1). 30b: UPGAMA cluster analysis of the banding pattern within the eubacteria-specific DGGE gel in Fig. 30a.

The cyanobacterial community during Sponge Orange Band disease

The same sponge specimens as in the eubacteria-specific DGGE gel (Fig. 30a) were applied to the cyanobacteria-specific DGGE gels (Figs. 31a, 32a). Thirty-one bands have been excised and cloned from the first cyanobacterial DGGE gel (Fig. 31a) and their 16S rRNA-gene sequences were checked for chimeras before analysis via NCBI Blast. Up to three clones per DGGE band were sequenced. Altogether 36 clones were obtained with 7 sequences derived from healthy *X. muta* individuals (n=2), 7 from the brown, 5 from the orange and 17 sequences from the white surface tissues of diseased sponges (n=3). Three clones belonging to the phylum *Verrucomicrobia* and two chimeric sequences were removed from the dataset. Additionally, sixty-one bands have been excised from the second cyanobacterial DGGE gel (Fig. 32a). Seven bands could not be re-amplified with the primer pair 106f and 781r and were discarded. Up to four clones per DGGE band were sequenced. In addition, four clones belonging to the phylum *Verrucomicrobia* as well as two chimeric sequences were removed from the dataset. Thus, 58 bacterial 16S rRNA gene sequences were obtained from the second cyanobacterial DGGE gel with one sequence derived from healthy *X. muta,* whilst 17 sequences were derived from the brown, 19 from the orange and 21 from the white surface tissue of diseased individuals (n=5).

Inspection of both cyanobacterial DGGE gels (Figs. 31a, 32a) revealed consistently two to three major bands obtained from the healthy sponge surface tissue and from the brown and orange surface tissue of diseased *X. muta* individuals (Fig. 16; see annex: Tab. 1). The DGGE banding patterns of the corresponding white surface tissue of diseased sponges were much more heterogeneous. While the conspicuous DGGE bands from the healthy sponge tissues were largely missing within the white surface tissues of diseased individuals, a large number of new bands appeared that formed no consistent pattern. Thus, the banding patterns of both DGGE-gels were subsequently analyzed independently from each other with the software program Quantity One and dendrograms were constructed using the clustering method UPGAMA (Figs. 31b, 32b). It revealed the percentage similarities in between all lanes of one gel. Interestingly, within the first cyanobacterial gel a cluster built up out of the white surface tissues only with a similarity ranging from 42-57% (Fig. 31b). This cluster was to only 35% similar to the one containing the lanes derived from healthy, brown and orange surface tissues. The lanes of the healthy surface tissues clustered with a minimum similarity of 54% together with the brown and orange surface tissues of diseased sponge #4. The banding patterns of all other lanes containing brown and orange surface tissues built up

another cluster with a minimum similarity of 64%. Those two clusters resembled each other only to 48%. Within the dendrogram of the second cyanobacterial DGGE gel (Fig. 32b) one coherent cluster was striking with similarities of 36-56%, which contained solely the white surface tissue of all diseased sponges. It resembled only to 19% the other DGGE lanes obtained from the healthy sponge or the brown as well as orange surface tissues of diseased sponges, which formed another similarity cluster of at least 56%. Therefore the banding pattern analysis confirmed the visual interpretation of both DGGE gels, in that the cyanobacterial phylotypes within the white surface tissues distinguish themselves remarkably from the ones within the healthy as well as the brown and orange surface tissues of diseased *X. muta* individuals.

The molecular analysis via 16S rRNA gene sequencing of the 36 bacterial phylotypes derived from the first (see annex: Tab. 3) and the 58 bacterial phylotypes obtained from the second cyanobacterial DGGE gel (see annex: Tab. 4) revealed with the exemption of band 26 (marine sediment clone Ct-5-36; see annex: Tab. 3) exclusively cyanobacteria of the *Synechococcus/Prochlorococcus* clade of sponge symbionts described by Schmitt *et al.* (2008). Those were obtained from healthy as well as the brown and orange surface tissues of diseased *X. muta*. In contrast, within the white surface tissues of the diseased sponges only few cyanobacteria were detected belonging to the symbiotic clade (see annex Tab 3: bands 5 and 8; see annex Tab. 4: bands 28, 34, 51 and 61), whereas the majority of their bacterial phylotypes affiliated with various unspecific cyanobacterial genera.

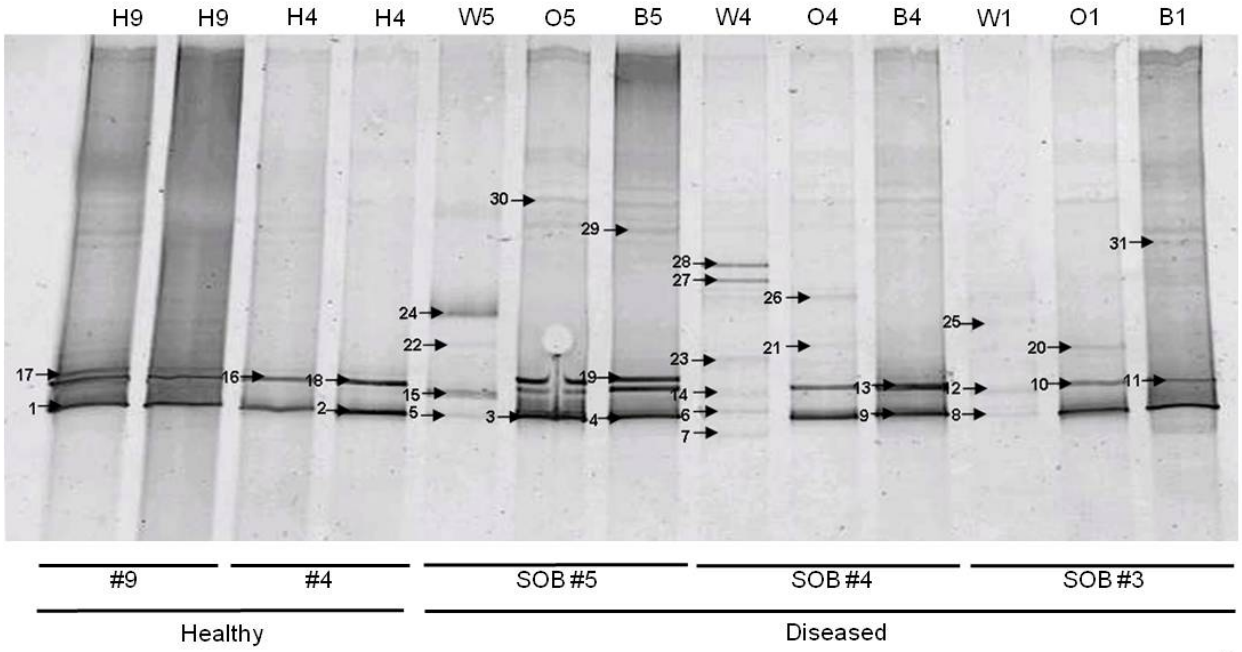

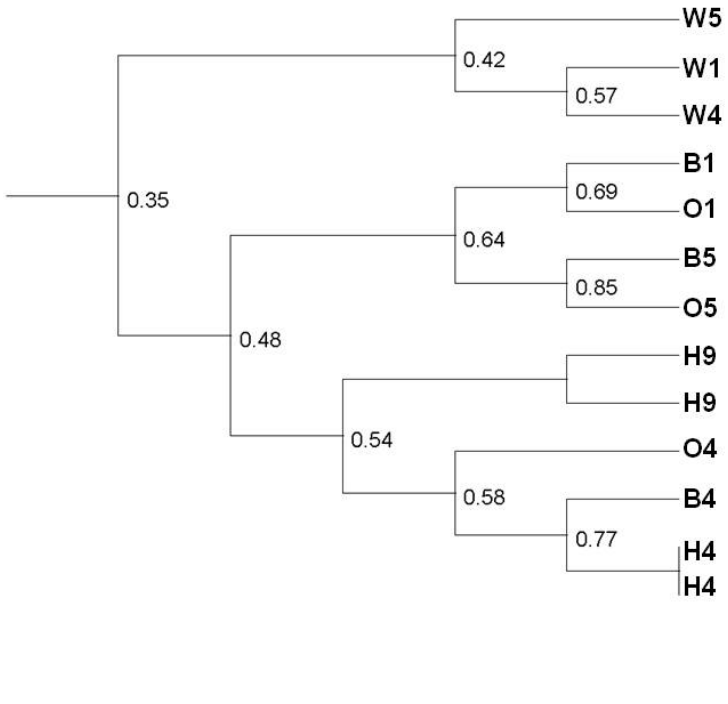

Fig. 31a: Denaturing gradient gel electrophoresis (DGGE) of cyanobacterial 16S rRNA genes in two healthy and three diseased *X. muta* individuals listed per individual (Fig. 16; see annex: Tab. 1). Arrows point towards the 31 excised bands. 31b: UPGAMA cluster analysis of the banding pattern within the cyanobacteria-specific DGGE gel in Fig. 31a.

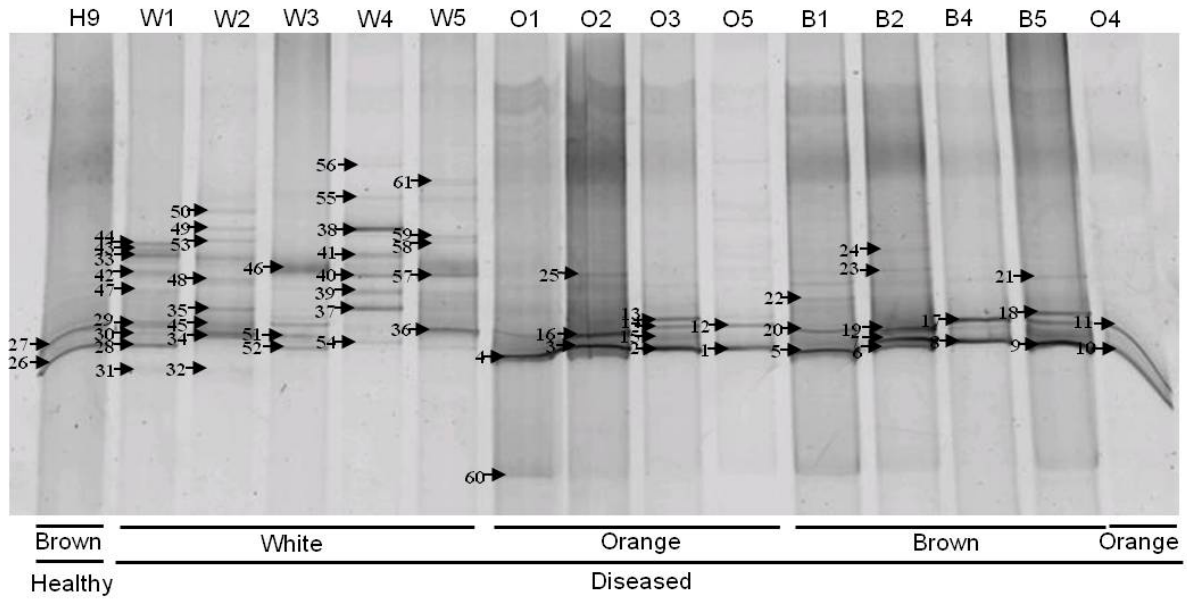

a

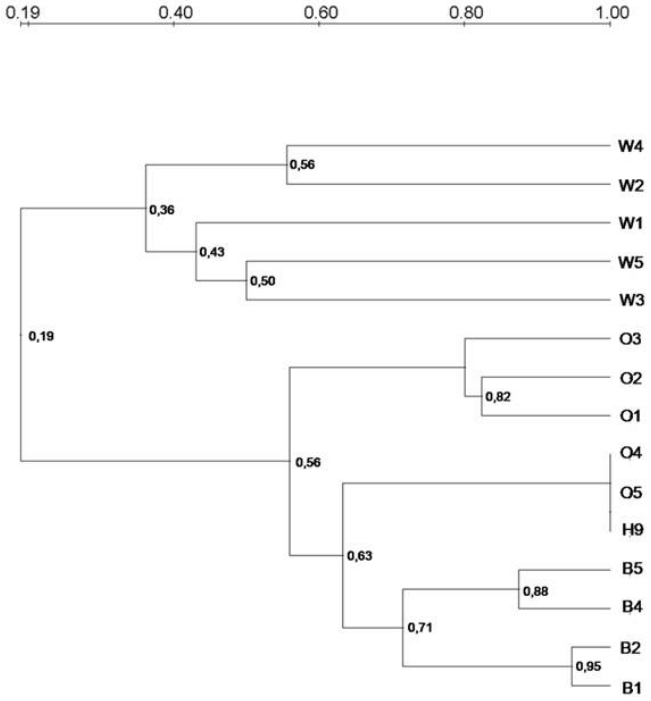

b

Fig. 32a: Denaturing gradient gel electrophoresis (DGGE) of cyanobacterial 16S rRNA genes in one healthy and five diseased *X. muta* individuals listed per surface tissue coloration (Fig. 16; see annex: Tab. 1). Arrows point towards the 61 excised bands. 32b: UPGAMA cluster analysis of the banding pattern within the cyanobacteria-specific DGGE gel in Fig. 32a.

1.8 Phylogenetic analysis

Phylogenetic tree construction (Fig. 33) was conducted for the 58 bacterial phylotypes obtained from the second cyanobacterial DGGE gel (Fig. 32a, see annex: Tab. 4). All 37 cyanobacterial sequences, which were derived from the healthy sponge as well as from the brown and orange surface tissues of diseased sponges, were revealed to form one coherent, monophyletic sequence cluster together with the well-described *Synechococcus/Prochlorococcus* clade of sponge symbionts (see annex: Tabs. 3-4). This cluster contains representatives of clade B and L *Synechococcus spongiarum* (Erwin and Thacker, 2008) as well as of the vertically transmitted phylotypes described by Schmitt *et al.* (2008). Only four cyanobacterial DGGE sequences obtained from the white surface tissues fell into the cyanobacterial symbiont cluster (DGGE 28, DGGE 34, DGGE 51 and DGGE 61). The remaining 17 sequences from white tissues of diseased sponges affiliated with diverse cyanobacterial genera such as *Limnothrix*, *Plectonema*, *Acaryochloris*, *Leptolyngbya* and *Myxosarcina*. Their closest reference sequences were obtained from freshwater (DGGE 30), seawater (DGGE 57), hypolithic slime (DGGE 43), microbial mat (DGGE 36), rock oyster (DGGE 31), coral reef (DGGE 48) as well as its sediment (DGGE 29, 33-3, 40), healthy corals (DGGE 33-1, 38, 44, 41), mucus of Black Band diseased corals (DGGE 37) and Black Band diseased corals themselves (DGGE 39) as well as from White Syndrome affected dead coral skeleton (DGGE 33-2, 42).

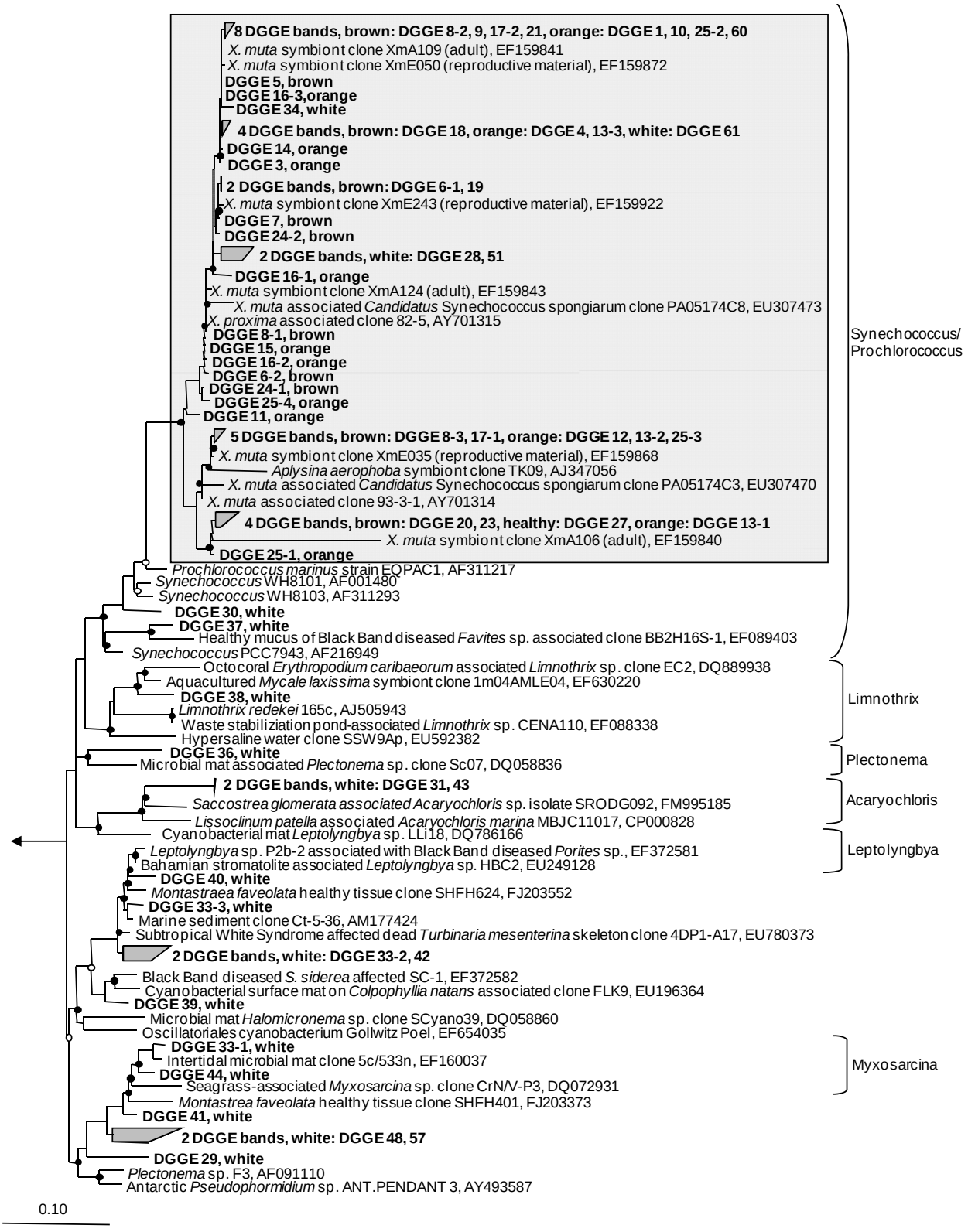

Fig. 33. Phylogenetic maximum likelihood tree with cyanobacterial 16S rRNA gene sequences obtained from the second cyanobacterial DGGE gel (Fig. 32a) and its closest reference sequences. Sequences from this study are shown in bold. Full circles indicate bootstrap support ≥90% and open circles bootstrap support ≥75%. The arrow points towards the outgroup *Rhodothermus marinus* (AF217494). The scale bar indicates a 10% sequence divergence. The grey box depicts the monophyletic, sponge-specific, cyanobacterial symbiont cluster.

1.9 Chemical Ecology

Profiling of secondary metabolites via HPLC

HPLC analysis was performed on the isolated extracts of two healthy and five diseased *X. muta* individuals. Representative chromatograms of one healthy and the differently colored surface tissues (brown, orange and white) of one diseased sponge are shown (Fig. 34). The HPLC analysis of the healthy specimen (#9; Fig. 16a), that had a typical reddish-brown coloration, revealed 5 major peaks (A-E) (Fig. 34a). Five partially pure compounds were identified from these peaks based on UV/MS data and comparison to published *X. muta* metabolites. Peak A represented Mutasterol (Rt 6.3min) (Li *et al.*, 1981), peak B Mutafuran A, B, E or F (all of which have equal molecular masses) (Rt 6.9) (Morinaka *et al.*, 2007), peak C Mutafuran G (Rt 7.0) (Morinaka *et al.*, 2007), peak D 18-bromo-octadecadiene-diyonic acid (Rt 7.3min) (Patil *et al.*, 1992) and peak E 5,28-Stigmastadien-3β,24-diol (Rt 7.9) (Duque *et al.*, 1985). The HPLC chromatogram of the brown surface tissue of the diseased sponge showed that the major peaks, including peaks A-E, were still present albeit at lower concentrations (Fig. 34b). The secondary metabolite profile was significantly reduced within the orange surface tissue of the diseased sponge unveiling only a single peak, which presumably belonged to B (Fig. 34c). Those peaks were entirely absent in the white surface tissue of the diseased sponge (Fig. 34d). This observed pattern was valid for all diseased sponges investigated (n=5).

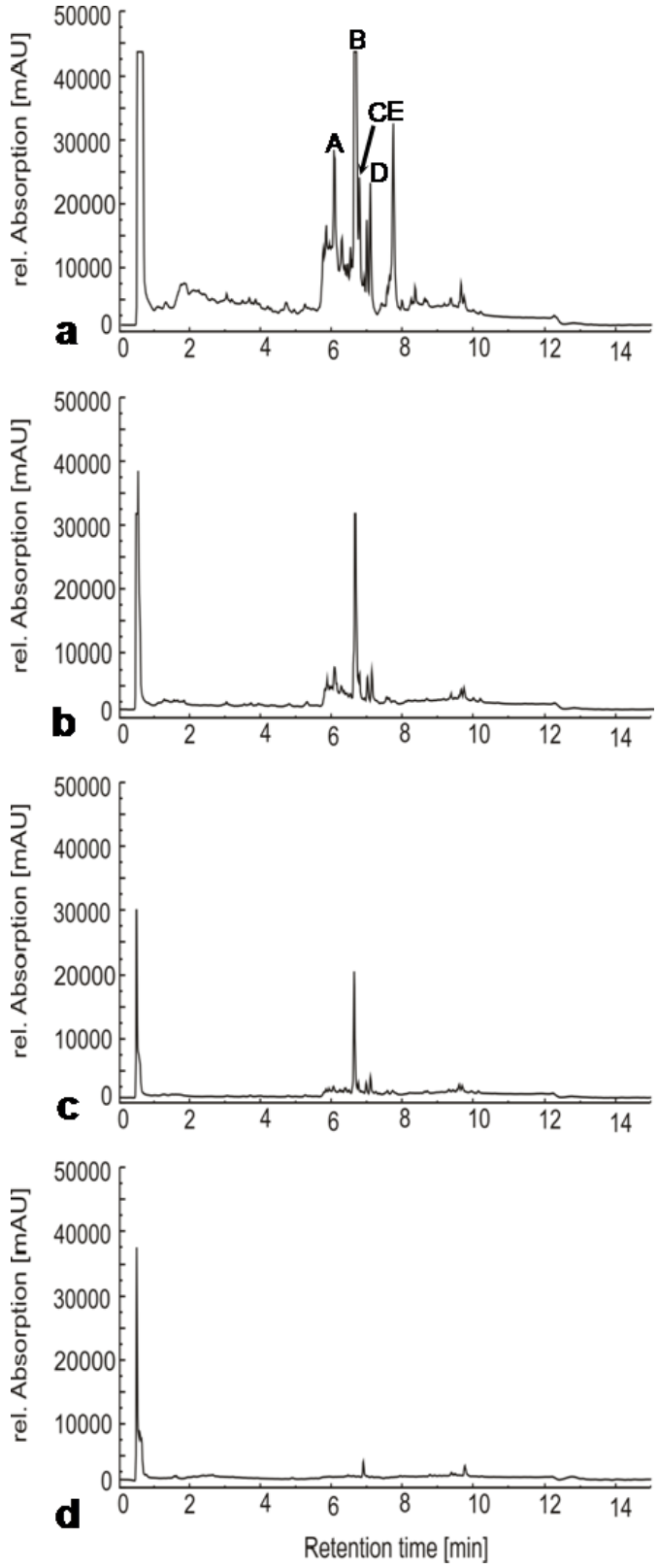

Fig. 34. HPLC chromatograms of methanolic extracts measured at 220nm that were obtained from a healthy (a) *X. muta* individual (#9, Fig. 16a) as well as from the brown (b), orange (c), and white (d) surface tissues of a SOB-diseased individual (#5, Fig. 16f). The letters A-E depict the identified secondary metabolite compounds from the healthy sponge.

Profiling of chlorophyll a via spectrophotometry

The chlorophyll *a* content within the brown surface tissues of healthy sponges and the brown, orange and white surface tissues of diseased sponges was compared to elucidate the variation in coloration during SOB-disease. The average chlorophyll *a* value obtained from the brown surface tissues of healthy *X. muta* individuals was measured at 32.1µg/g ± 4 (n = 9). The amount of chlorophyll *a* within the brown surface tissues of diseased sponges equaled those values with 32.9µg/g ± 11.2 (n = 2). However, the amount of chlorophyll *a* per gram sponge has been directly correlated with the degree of bleaching that is affecting the surface tissue. Therefore a decrease in chlorophyll *a* content appeared gradually during the course of disease for the surface colorations from brown (32.9µg/g ± 11.2, n = 2) over orange (29.9 µg/g ± 10, n = 3) to white (7.5 ± 4.2 µg/g, n = 3) (Fig. 35). Remarkably, decreases in chlorophyll *a* content were especially striking in between the differently colored surface tissues of one and the same individual (see annex: Tab. 5) than compared to the obtained average values (Fig. 35). The high standard error of the mean among the average values arose due to the small sample sizes of diseased tissue (n=3: orange and white surface tissues, n=2: brown surface tissues) in comparison to the sample size of healthy individuals (n=9). Additionally, it can be attributed to general variations in chlorophyll *a* content, which existed even among healthy *X. muta* individuals and which might depend upon the habitat depth. The sponges applied to this study were all undergoing advanced stages of disease (Figs. 16d-f). However, this observation has been additionally confirmed by field measurements via pulse amplitude modulation within the Florida Keys National Marine Sanctuary in winter 2007 for the same specimens. Moreover, also measurements with a transportable fluorometer during the Bahamas field trip in summer 2008 stated the same trend for additional *X. muta* individuals (Figs. 16h-i), that have been undergoing both, early or advanced, stages of disease (data not shown).

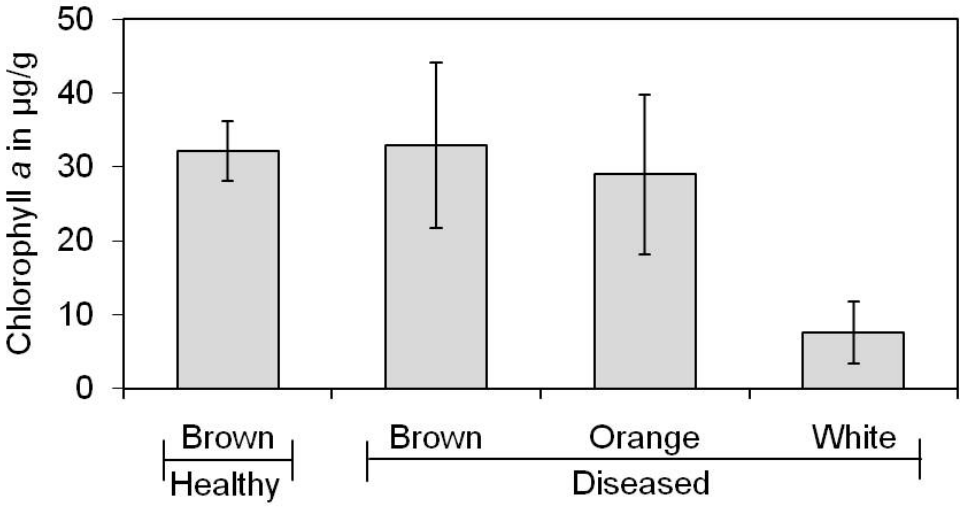

Fig. 35. Average chlorophyll *a* concentration within surface tissues of healthy (n=9 ± S.E.) and Sponge Orange Band diseased (n=3 ± S.E.) *X. muta* individuals as listed by tissue coloration.

1.10 Infection experiments

Underwater infection experiments were conducted on healthy *X. muta* individuals to survey a possible transmittance of disease by the transfer of diseased tissue cores, containing surface as well as mesohyl tissue, from so called donor sponges into healthy recipient sponges. Additionally as a control also healthy sponge tissue was transplanted from healthy donor sponges into healthy recipient sponges (see annex: Tab. 6). All of the healthy *X. muta* recipients, into which cores of diseased sponges were transplanted, responded in the same manner: Within a time period of up to 11 days the surface tissues around the implanted cores appeared to heal up. A rejection of the foreign sponge material was not observed. Donor material was taken from sponges in early (#12; Fig. 36d) and advanced stages of disease (#10 and #11; Figs. 36b-c) as well as from the healthy control sponge (Fig. 36a), but no difference in recipient sponge response has been observed, neither to diseased nor to healthy cores (Fig. 36). Thus, in vivo underwater infection experiments provide no evidence for an infectious process during Sponge Orange Band disease.

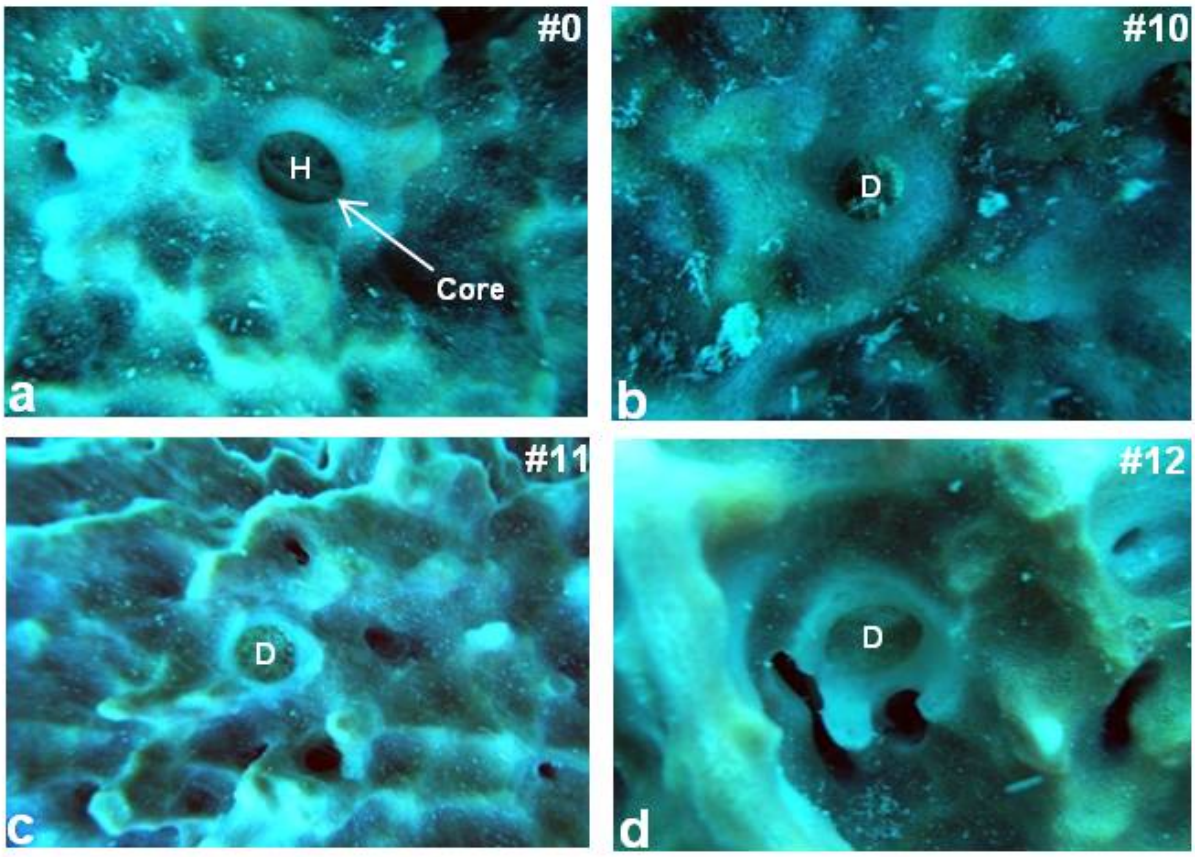

Fig. 36. Underwater photographs of representative recipient sponges that harbour transplanted cores from either the healthy control sponge (a) or the SOB-diseased individuals (b: #10, c: #11 and d: #12) undergoing either an advanced (b-c) or an early stage (d) of disease. The transplantation was observed for up to 11 days (see annex: Tab. 6). Abbreviations: H, core from healthy donor; D, core from diseased donor.

2. Sponge White Patch disease of *Amphimedon compressa*

2.1 Visual documentation of Sponge White Patch disease

Healthy *Amphimedon compressa* individuals are normally red in color and possess a rope-like or massive shape of about 0.6-1m length (Fig. 37a). During Sponge White Patch disease small patches (Fig. 37b) up to even whole branches (Figs. 37c-d) of sponge tissue turn white and can thus be easily differentiated from the overall red sponge body. There is no gradual color change from the pinacoderm to the mesohyl with the red parts being completely red and the white parts being entirely white. Remarkably, diseased sponges seem to recover and regenerate their affected body over time by repelling the diseased, white parts. This occurs presumably by strong environmental impacts like currents in nature, which cause the white tissue to dispatch revealing integer sponge tissue below the lesion (Fig. 37b). In few cases, the impression was conveyed that a border exists in between red and white tissue areas of a diseased sponge, but this phenomenon deserves further observation. Additionally, sillid polychaetes were observed in the laboratory to burrow predominantly through the diseased white parts of freshly collected and diseased *A. compressa* individuals.

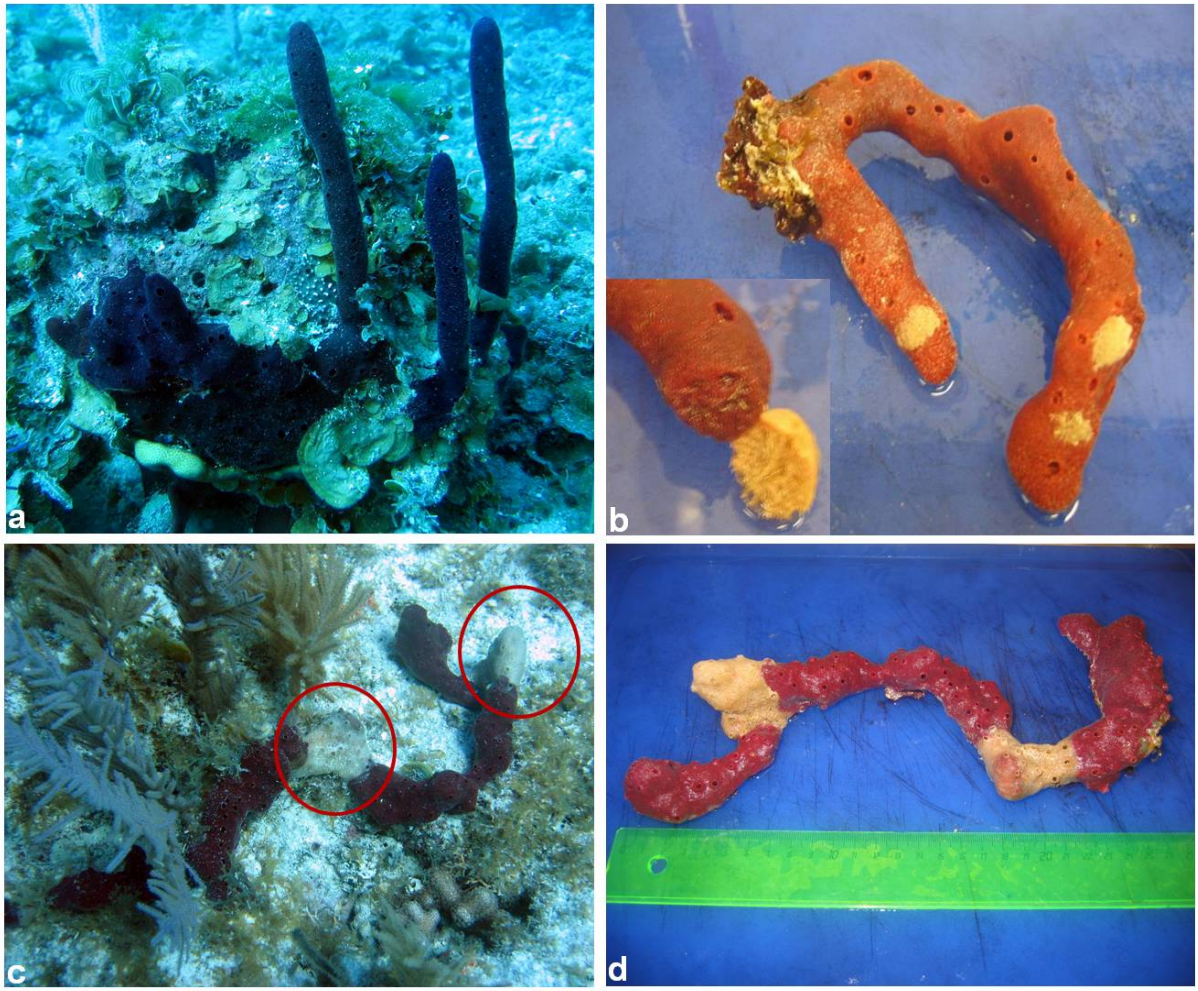

Fig. 37. Underwater photography of a healthy (a) versus a Sponge White Patch (SWP) diseased *A. compressa* individual (c) and its measurement back in the laboratory (d; the ruler represents 30cm in length). The two additional SWP diseased individuals demonstrate the often patchy appearance of disease followed by the rejection of white tissue (b).

2.2 Disease ecology

By randomly selecting 80 squares of $1m^2$ size 7.6 (SD=5.03, SE=0.56) *A. compressa* individuals were documented per m^2 (Fig. 38a). Also the amount of healthy versus diseased *A. compressa* individuals has been counted. Thus, altogether 610 sponge specimens were surveyed within these 80 squares. 82% of the *A. compressa* population (n=503) was showing no signs of disease and was therefore considered as healthy, whereas 18% (n=107) was showing lesions of Sponge White Patch disease in variable sizes and were thus considered as diseased (Fig. 38b). In average 6.3 (SD=4.86, SE=0.54) representatives of *A. compressa* per m^2 were counted to be healthy at Dry Rocks Reef, Florida, whereas 1.3 individuals (SD=0, SE=0) were counted to be diseased.

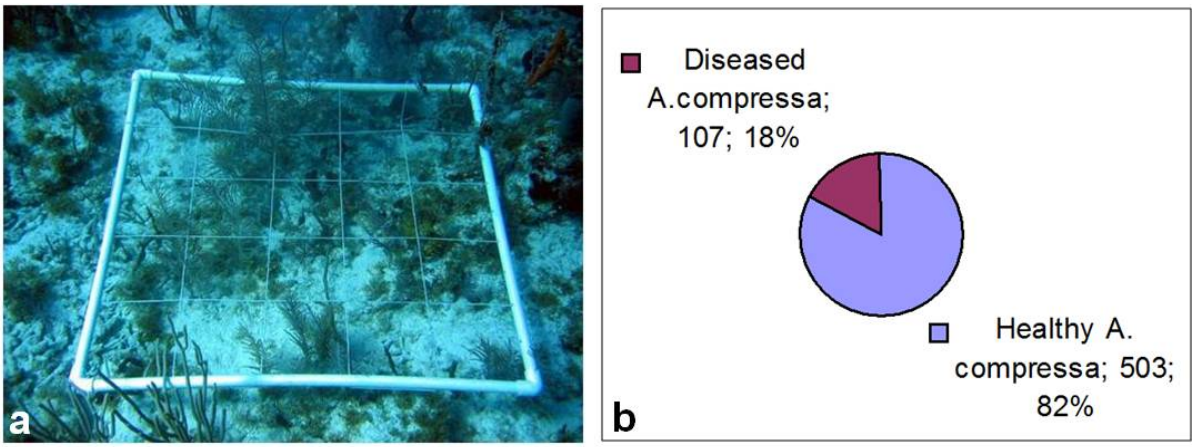

Fig. 38. This random square ($1m^2$) has been applied to survey the prevalence of Sponge White Patch disease within the *Amphimedon compressa* population at Dry Rocks Reef, Florida, in winter 2007 (a). Roughly one fifth of its population (18%) was shown to exhibit symptoms of disease (b).

In addition, the average amount of red versus white tissue was documented for 40 Sponge White Patch diseased *A. compressa* individuals (n=40) from Dry Rocks Reef, Florida, via volume displacement studies. The measured *A. compressa* representatives had a mean sponge volume of 59.0 ml (SD=46.95, SE=7.42, n=40). In average 78.8% (SD=0.25, SE=0.04) of the sponge volume were derived from red tissue, whereas 21.2% (SD=0.25, SE=0.04) belonged to white tissue. The high standard deviations and standard errors originate from the highly variable amount of sponge volume and SWP-affected tissue within the 40 *A. compressa* individuals investigated in this experiment (Fig. 39).

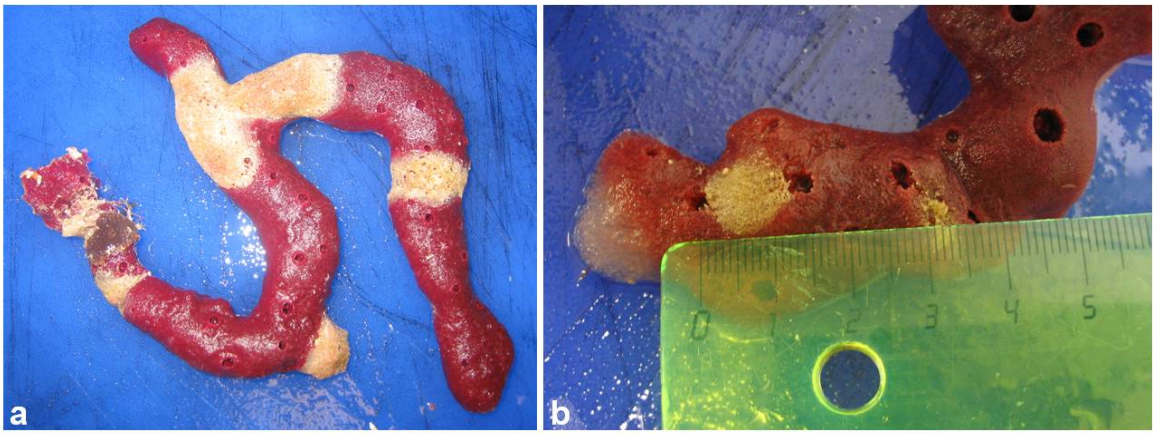

Fig. 39. Representative *A. compressa* individuals investigated within the volume displacement studies. Some sponges exhibited large (a) and some only small (b) patches of white, diseased tissue distorting the result.

2.3 Histological investigations

Binocular microscopy

Binocular microscopy of healthy *A. compressa* sponges (Fig. 40a) as well as the intact looking parts (Fig. 40b) of Sponge White Patch diseased individuals revealed the for *A. compressa* characteristic red tissue coloration. In contrast, the optically SWP-diseased tissue areas (Fig. 40c) were all completely bleached, white in color. Thus, an abrupt color change seems to take place during disease progression, as no gradual transition zone has been observed. Neither in healthy, nor in diseased sponges a differentiation in color or tissue consistency inbetween the pinacoderm and the mesohyl has been found. Additionally, the binocular microscope demonstrated the presence of marine sillid polychaetes that manifested themselves mainly within the diseased *A. compressa* individuals.

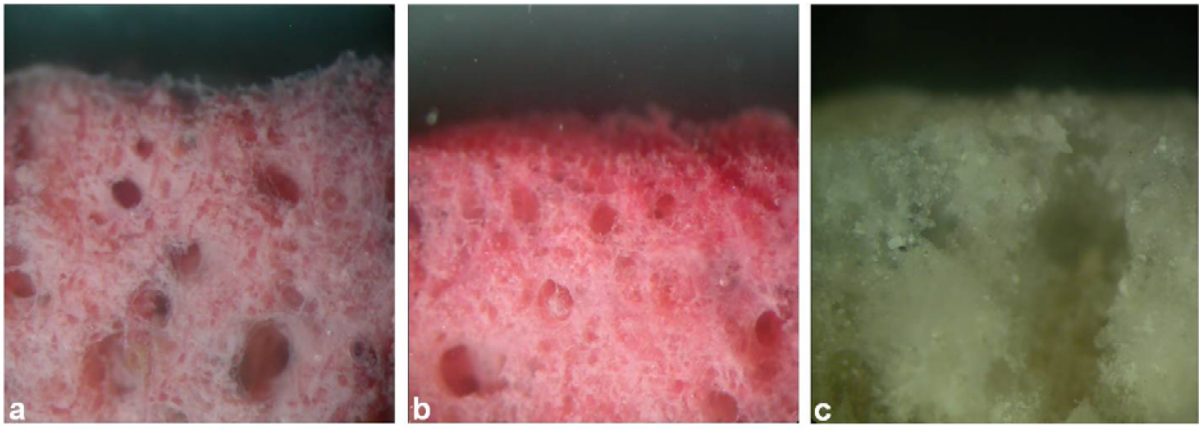

Fig. 40. Representative binocular micrographs of healthy *A. compressa* tissue (a) versus the red (b) and white (c) tissue of a Sponge White Patch diseased individual.

Light microscopy

Semi-thin sections, which were fabricated during the processing of samples for electron microscopy, were inspected via light microscopy. Healthy individuals (n=2) were revealed to consist out of scattered sponge cells (SP) and spongin, a sponge-specific collagen (C) type, that was interspersed by insular spicules (SP) (Figs. 41a-b). The same characteristics were documented for the red parts of Sponge White Patch diseased individuals (n=2), which were also constituted out of intact sponge cells that were loosely surrounding the spicule-containing collagen patches (Figs. 41c-d). Within the white parts of diseased sponges in contrast, hardly any sponge cells were recognizable anymore. Instead, cellular debris was loosely scattered around the spongin, which has been observed to be degraded by collagen-boring bacteria (B). Those have been creating numerous channels and were beleaguering them inside the collagen (Figs. 41e-f).

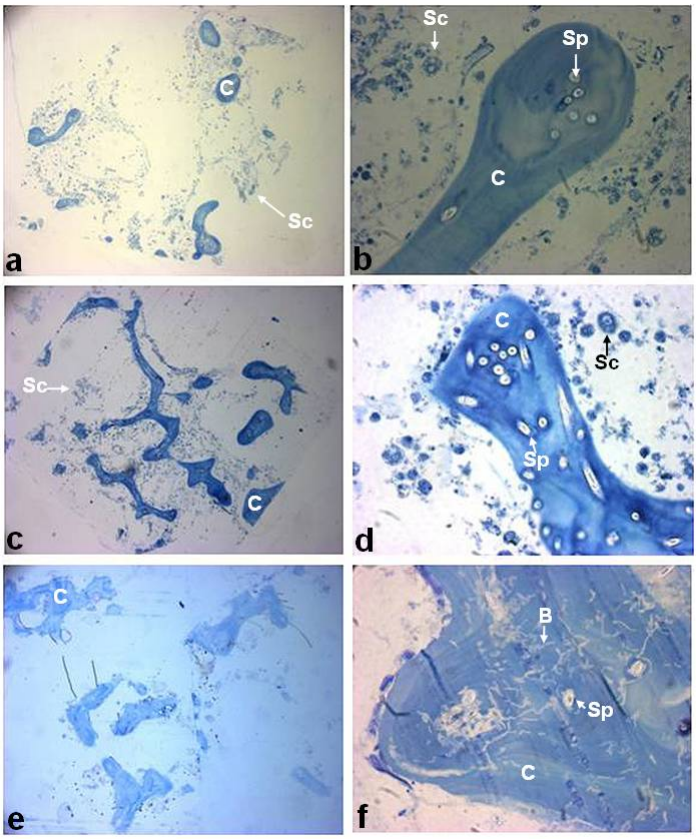

Fig. 41. Representative light micrographs of healthy and Sponge White Patch diseased *A. compressa* individuals investigated in this study (see annex Tab. 7: #12 and #13). Healthy sponge tissue (a-b) as well as the red (c-d) and white part (e-f) of SWP diseased individual #13 are magnified either 10x (a, c, e) or 100x (b, d, f). Abbreviations: Sc, sponge cell; C, collagen; Sp, spicule; B, bacterium.

2.4 Electron microscopical observations

Scanning electron microscopy

Tissues from two healthy and three diseased *A. compressa* individuals were inspected by scanning electron microscopy. Representative images of one healthy sponge (#12) and of the two different tissue colorations of a Sponge White Patch diseased individual (#2) are shown (see annex: Tab. 7). Characteristic features were revealed for healthy sponges as well as for the red tissue of SWP-diseased individuals: In both cases abundant sponge cells created a tissue-like structure that had been interweaved by spicules (Figs. 42a-e) and aquiferous canals were visible within the tissues (Figs. 42d-e, h). Collagenous fibers seemed to be involved in the fixation of the sponge cells (Fig. 42c). In addition, pinacocytes comprised the pinacoderm of the sponge. Their presence differentiated the surface tissue from the mesohyl (Figs. 42e-g).

In contrast, the white parts of Sponge White Patch diseased *A. compressa* individuals showed vast signs of destruction within their surface tissues and mesohyls: spicules and collagen were clearly exposed. They were interspersed by cellular detritus as well as single sponge cells (Figs. 42i-l). Only few intact sponge cells were still present among the highly destroyed tissue remnants (Fig. 42i). Remarkably, only via SEM bacteria were visually described within the bleached white sponge tissues. They were located to their majority on damaged spicules (Fig. 42k). These kinds of degradative processes have been documented for all white parts of SWP-diseased *A. compressa* individuals investigated (n=3).

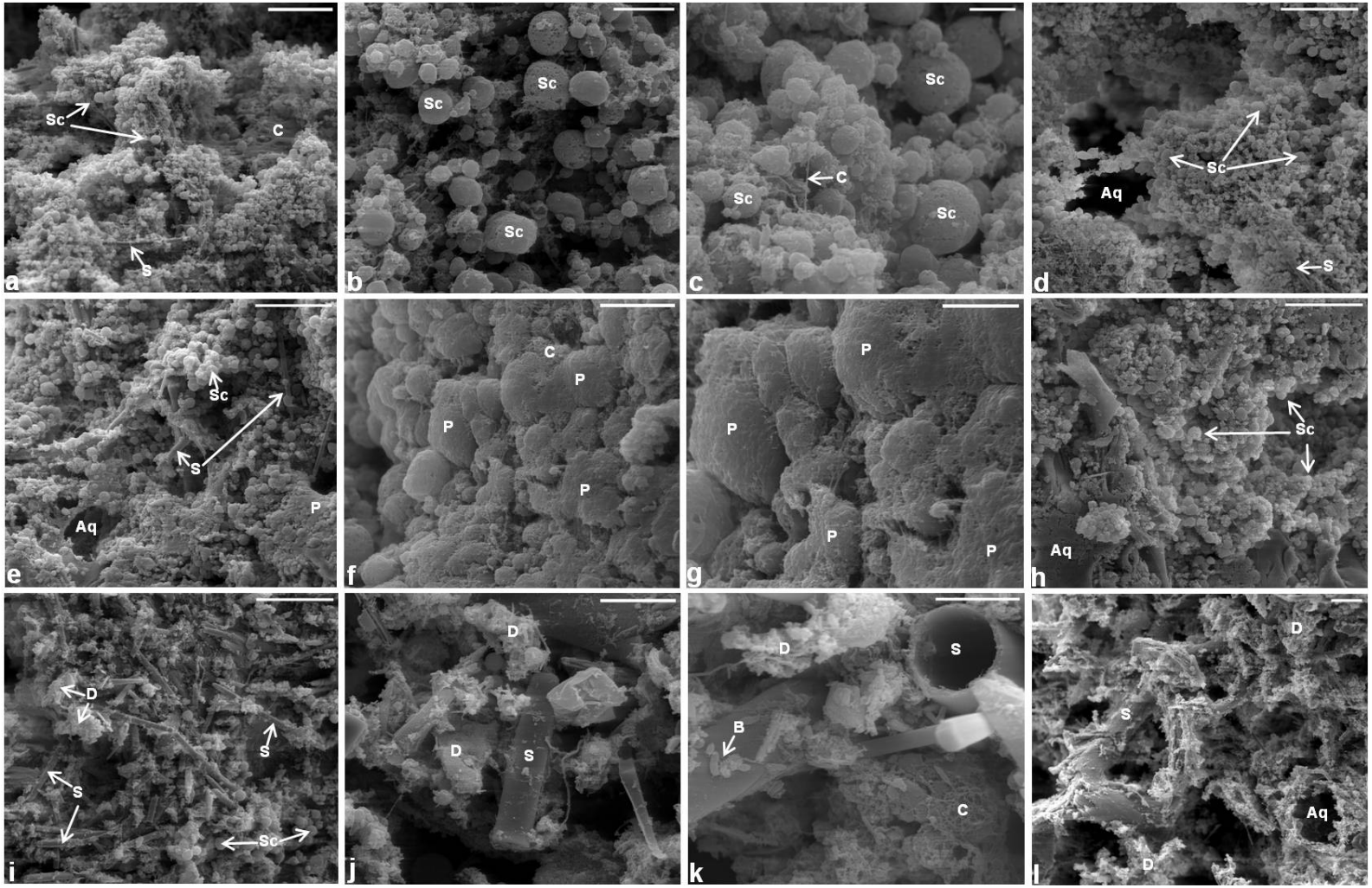

Fig. 42. Representative scanning electron micrographs on the surface tissue (a-c, e-g, i-k) and mesohyl (d, h, l) of a healthy (a-d) *A. compressa* individual and of a Sponge White Patch diseased individual, that has been differentiated into its red (e-h) and white (i-l) areas. The scale bars represent 50µm (a, e, i, d, h, l), 10µm (b, f, j) and 5µm (c, g, k), respectively. Abbreviations: Sc, sponge cell; C, collagen; S, spicule; Aq, aquiferous canal; P, pinacocyte; D, detritus; B, bacterium.

Transmission electron microscopy

Extensive electron microscopic studies were conducted on five healthy (n=5) and nine Sponge White Patch diseased (n=9) *A. compressa* individuals, out of which all but one individual (#6; see annex: Tab. 7) showed characteristic signs of disease as described in the following paragraph.

Healthy *A. compressa* individuals consisted out of sponge specific collagen (C), that is termed spongin within the phylum *Porifera*, and scattered sponge cells (Sc) lining it. Spicules (sp) were dispersed within the collagen. Those built up the overall body skeleton of *A. compressa* resulting in the extensive flexibility of this species (Figs. 43a-b). Sponge White Patch diseased *A. compressa* individuals instead were comprised out of red as well as white body parts. All red tissue areas of the diseased sponges investigated in this study possessed integer collagen interspersed with spicules. Intact sponge cells were encompassing the sponge skeleton (Figs. 43c, 44a). The white tissue areas of diseased *A. compressa* sponges in contrast were of particular interest. In all but one case the destruction of the present collagen was observed to be accompanied by channel-burrowing bacteria, which were localized within channels boring through the spongin (Figs. 43d, 44b-f). Remarkably, the spongin destruction seemed to be caused by bacterial activity that has been even diffusing the collagen into small particles at some sites. A magnification revealed elongated or rod-shaped bacteria of approximately 0.5 x 2.5µm or 0.5 x 1µm in size (data not shown) as well as spherical bacteria of approximately 0.5 x 1µm in size (Figs. 44b-f). However, just one kind of bacterial morphotype has been detected within the diseased, white tissue areas. In addition to the collagen degrading bacteria, the absence of intact sponge cells was striking within the white tissues. Those are normally clearly differentiable by their nucleus and cell membrane. Cellular debris has been replacing them instead, lining the collagen at sites where sponge cells might have been located before and indicating degradative processes (Figs. 43d, 44b).

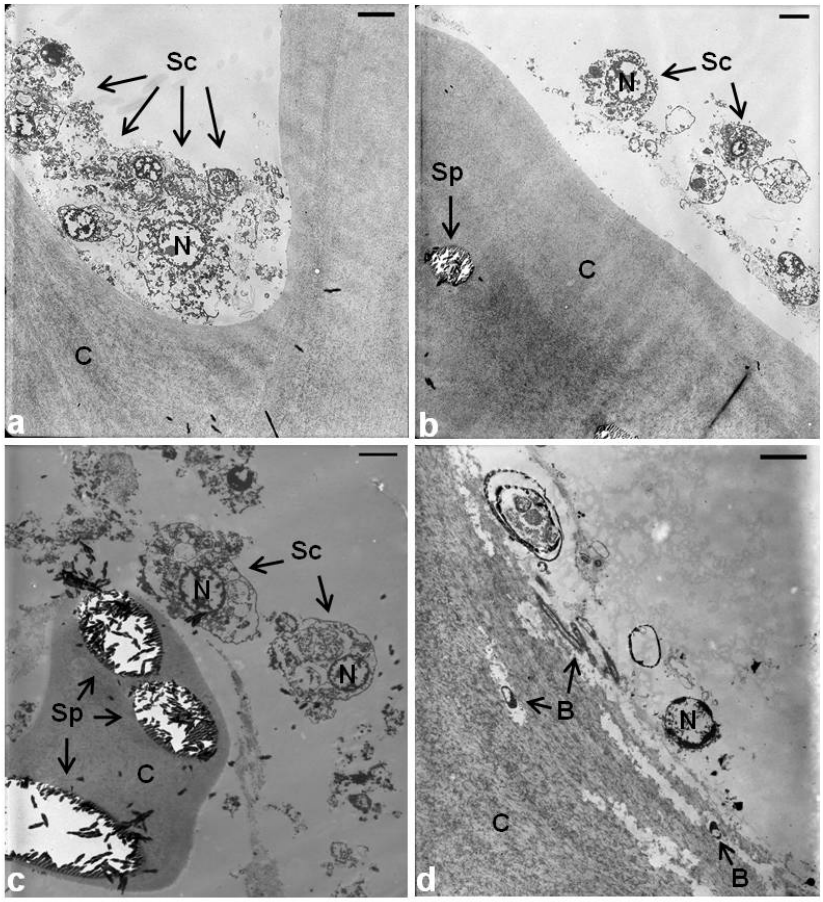

Fig. 43. Representative transmission electron micrographs of a healthy (a-b) and a Sponge White Patch diseased *A. compressa* individual (c-d). The latter is differentiated into its red (c) and white (d) tissue area. The scale bars represent 2μm each. Abbreviations: N, nucleus; Sc, sponge cell; Sp, spicule; B, bacterium; C, collagen.

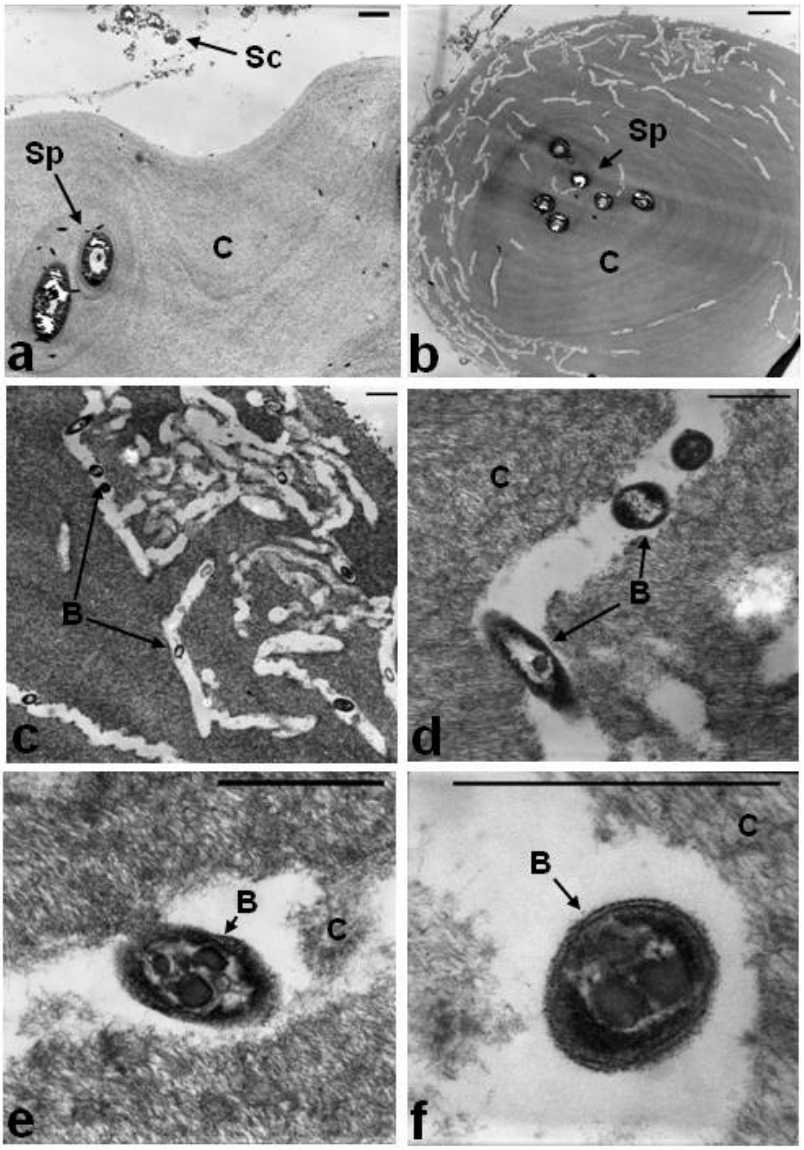

Fig. 44. Representative transmission electron micrographs of a Sponge White Patch diseased *A. compressa* individual (#29). The red (a) and white (b-f) area of the sponge are shown. The scale bars represent 5µm (b), 2µm (a), 1µm (c) and 0.5µm (d,e,f), respectively. Abbreviations: Sc, sponge cell; C, collagen; Sp, spicule; B, bacterium.

2.5 Microbial cultivation

Bacterial diversity of Sponge White Patch disease in winter 2007

Bacterial cultivation on YPD- and M1-agar has been performed of one healthy (#12) and of three Sponge White Patch diseased *A. compressa* individuals (#2, #13 and #29), that have been obtained from the Florida Keys in winter 2007 (see annex: Tab. 7). Interestingly, the overall bacterial diversity was highest within the white tissues of diseased sponges, as the isolation of bacteria from the red tissues of diseased *A. compressa* and from the healthy individual turned out to be difficult. Also cultivation on M1 agar proofed to be better suited than on YPD agar yielding a higher bacterial diversity. Altogether 28 bacterial colonies have been isolated: six from healthy *A. compressa* (n=1), six from the red tissues (n=3) and 16 from the white tissues (n=3) of diseased sponges (n=3). Thirteen colonies were of special interest due to divergent colony morphologies that frequently go along with different taxonomic affiliations. Thus, for eight of them their 16S rRNA genes have been identified (Tab. 3). From the tissue of healthy *A. compressa* #12 three colonies were derived: a white bacterial colony which was to 96% similar to *Bacillus acidicola* strain TSAS-1 belonging to the *Firmicutes* and two likely contaminations. They consisted out of a white colony with 95% similarity to a human-pouch biopsy derived clone and a brown colony of 82% similarity to a bacterial dust-isolate. From the red tissue of diseased individual #2 only one yellow colony was obtained, which was to 96% similar to *Micrococcus* sp. 100H42-1 belonging to the *Actinomycetales*. In contrast, the bacterial colonies obtained from the white tissue of SWP-diseased *A. compressa* #29 had several attributes in common. They were all ocher or brown in coloration and mostly belonging to the *Proteobacteria*. One ocher colony showed a similarity of 94% to the antibiotic-resistant *Gammaproteobacterium* RA3 clustering among the *Alteromonadaceae*. Another ocher colony was to 96% related to the sponge *Pseudoceratina clavata* associated *Alphaproteobacterium* D29. The brown colony had a similarity of 93% to the *Pseudoceratina clavata* associated *Gammaproteobacterium* DE07. Remarkably, one ocher colony was to 96% related to the clone OTU036 of uncertain bacterial affiliation that was originally derived from a heat-stressed juvenile coral of the species *Acropora tenuis* (Tab. 3). To conclude, the bacterial diversity within diseased *A. compressa* individuals from the Florida Keys in winter 2007 was much higher within their white than within their red parts or within healthy sponges. The majority of isolates from the white parts were representing *Proteobacteria* belonging to the classes *Alpha-* or *Gammaproteobacteria*.

Color	Sample	Colony: color	Closest sequence match in GenBank	Similarity (%)	Length (bp)	Taxonomic affiliation
Red tissue	Healthy #12	1: white	*Bacillus acidicola* strain TSAS-1 (GQ389780)	96	565/588	*Firmicutes*
		2: brown	Dust-associated isolate BF0002D021 (AM697510)	82	529/643	*Bacteria*
		107: white	Human mucosal pouch biopsy associated clone 16slp101-2d10.w2k (GQ157150)	95	568/594	*Bacteria*
Red tissue	Diseased #2	4: yellow	*Micrococcus* sp. 100H42-1 (EU181230)	96	542/563	*Actinobacteria; Actinomycetales*
White tissue	Diseased #29	41: ocher	Antibiotic-resistant bacterium RA3 (AB194570)	94	488/518	*Gammaproteobacteria; Alteromonadales; Alteromonadaceae*
		43: ocher	*Pseudoceratina clavata* associated *Alphaproteobacterium* D29 (DQ227659)	96	682/707	*Alphaproteobacteria*
		46: brown	*Pseudoceratina clavata* associated *Gammaproteobacterium* DE07 (DQ399735)	93	523/561	*Gammaproteobacteria*
		103: ocher	heat-stressed juvenile *Acropora tenuis* associated coral clone OTU036 (GU174682)	96	480/498	*Bacteria*

Tab. 3. 16S rRNA gene sequence analysis showing the diversity of bacterial isolates from healthy *A. compressa* individual #12 as well as from the red tissue of diseased individual #2 and the white tissue of diseased individual #29 obtained from the Florida Keys National Marine Sanctuary in winter 2007.

Isolation of collagen degrading bacteria

First sequencing results of the collagen-degrading bacterial isolates K1 and K3, obtained from the white tissue of *A. compressa* #29, yielded highest similarities to the gammaproteobacterial strain *Microbulbifer agarilyticus* JAMB A3 with 97% and 95%. This strain belongs to the *Alteromonadaceae* (Fig. 45), is known to degrade agar and thus likely also collagen. Full-sequencing of its 16S rRNA gene revealed later, on after the infection trials, its identity as *Bacillus pumilus* strain Tbl with a maximal similarity of 99% (see Tab. 5).

Fig. 45. Degradation of azocoll-containing marine agar 2216 by one of the bacterial isolates obtained from the white tissue of Sponge White Patch diseased *A. compressa* #29.

Bacterial diversity of Sponge White Patch disease in spring 2009

However, bacterial cultivation on the same agar from Sponge White Patch diseased *A. compressa* individual #1 in spring 2009 revealed not a single bacterial colony exhibiting collagen- or agar-degrading properties. The overall bacterial diversity was with 41 isolated colonies highest within the white part of the diseased sponge and not within its red part, which revealed only seven isolates. Ten bacterial isolates could not be revived anymore on fresh agar plates. Thus, the remaining 38 bacterial isolates and additionally the collagen-degrading strains K1 and K3, as mentioned above, were applied for further analysis. Gel electrophoresis of the bacterial isolates after restriction fragment length polymorphism (RFLP) analysis exhibited 19 distinctive banding patterns that represented the morphological diversity among the bacterial isolates (Fig. 46). One representative isolate of each RFLP banding pattern was selected for application by denaturing gradient gel electrophoresis (see page 91f: Figs. 49-50 and Tab. 5) in terms of the inoculation trials (see page 93).

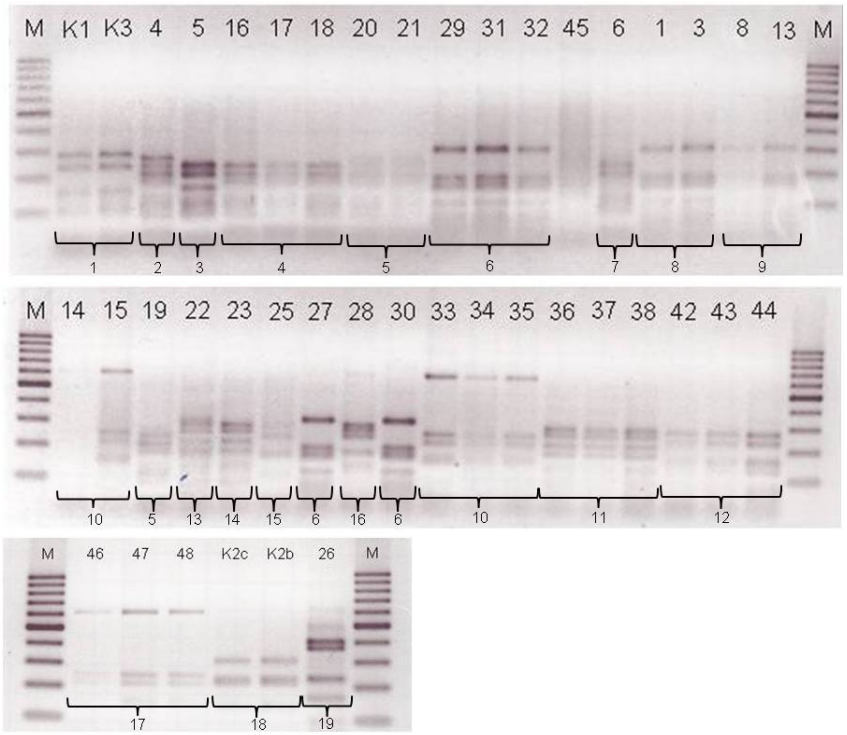

Fig. 46. Gel electrophoresis representing the 19 distinct RFLP-patterns derived of the 16S rRNA genes obtained from the 38 bacterial isolates of *A. compressa* #1 (labeled in numbers) and the agarolytic isolates (#K1-3) of *A. compressa* #29. M=100bp DNA marker.

2.6 Profiling microbial community changes by DGGE

The bacterial community of healthy A. compressa

DGGE of healthy *A. compressa* individuals revealed a common microbial profile. Up to eleven bands were recognizable within healthy *A. compressa* individuals, here at the example of sponge #8. The presence or absence of bands was likely dependent upon DNA content as well as PCR amplification. This is why within healthy sponge #12 only one band was visible, that was in contrast present within all other sponges investigated. It was located at approximately 44% of the denaturing agents. In addition, seven bands were common to the healthy sponges #8, #9 and #14 and ten bands to the sponges #8 and #14. Thus, healthy *Amphimedon compressa* individuals exhibit a partly conserved and omnipresent microbial pattern that is roughly ranging along the denaturing gradient from 40 to 54% (Fig. 47).

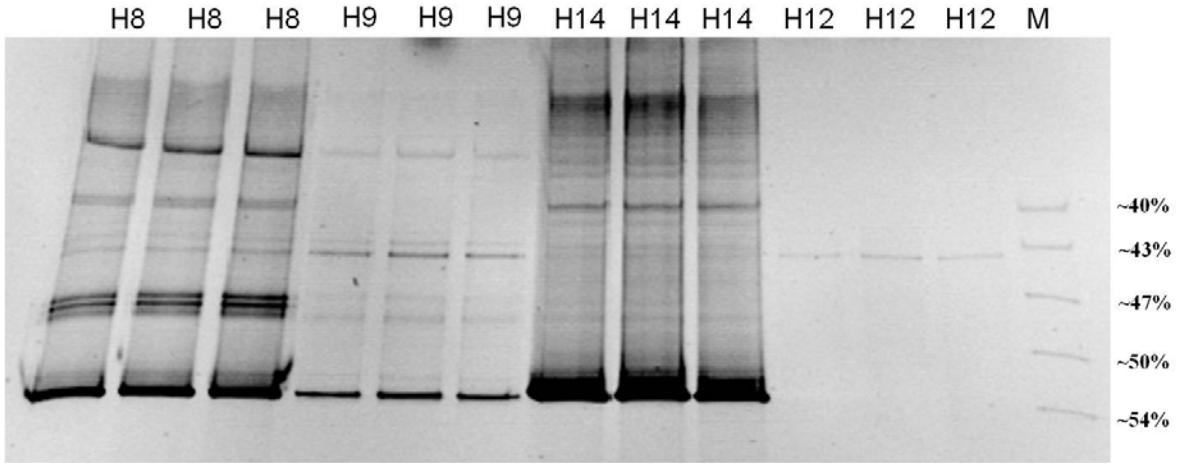

Fig. 47. Eubacterial DGGE profile of the 16S rRNA genes of four healthy (H) *A. compressa* individuals (#8, #9, #14 and #12; see annex: Tab. 7) collected within the Florida Keys National Marine Sanctuary in winter 2007.

The bacterial community of Sponge White Patch disease

To compare the characteristic profiles of healthy and Sponge White Patch diseased *A. compressa* individuals within one gel, a eubacterial DGGE has been performed (Fig. 48). It revealed a common bacterial profile to healthy *A. compressa* (#8) and the red parts of all Sponge White Patch diseased individuals (#1, #2 and #29, see annex: Tab. 7). On the contrary, the white counterparts of the respective specimens (#1, #2 and #29) possessed a completely divergent microbial fingerprint. This characteristic microbial profile has been revealed for all diseased sponges investigated. In addition, the pattern was consistent in all conducted DGGE gels varying just slightly according to independent DGGE runs. The healthy appearing red parts of all diseased sponges exhibited more bands with different intensity patterns than their bleached white counterparts. In maximum, up to eight bands (#29) were recognized within the red tissues of SWP-diseased individuals, which had their strongest intensities at a high denaturing gradient. In contrast, the white tissues of the respective sponges had a very divergent microbial profile. They were characterized by maximal 12 bands of intermediate GC-content with only one intense band in common to all of them. Those bands were absent within the red sponge parts, but remarkably also the characteristic GC-rich phylotypes of the red parts were lacking within the white parts. The bands in common to all bleached sponge parts were of particular interest, as they were absent within healthy sponges and their red counterparts. Therefore ten DGGE bands have been excised and were applied for further analysis (Fig. 48, Tab. 4).

Sequence identification revealed only one sponge specific and thus presumably symbiotic clone that was obtained from the red, diseased sponge tissue (DGGE band #10). It had its highest similarity to the sponge *Crambe crambe* associated clone transformant 10 of uncertain bacterial affiliation. The other nine DGGE bands have been isolated from the white parts of diseased sponges. DGGE band #7 yielded the *Thiotrix* sp. FBR0112 clustering among the *Gammaproteobacteria* and DGGE band #8 the coral *Montastrea faveolata* associated *Clostridiaceae* bacterium clone MD3.13. All other seven DGGE bands were either most similar to clones obtained from microbial flocs (DGGE band #6) as the *Alphaproteobacterium* clone Bac1_Flocs, to clones from hydrocarbon and oil spill polluted sand resembling the *Flavobacteriacea* isolate DGGE band S12 (DGGE band #3), to the aquarium-kept coral *Montastraea faveolata*-associated clone SGUS1003 (DGGE band #1), to 33°C exposed and thus temperature stressed *Rhopaloeides odorabile* associated clone 33aA1 (DGGE band #2) or to clones from three different coral species undergoing disease. Those had their highest

similarities to the *Alphaproteobacterium* clone 4-7-2 associated with White Plague-like syndrome affected coral *Montastraea annularis* (DGGE #4), to the *Alphaproteobacterium* clone RB_18f associated with the Black Band diseased Bahamian coral *Siderastrea siderea* (DGGE #5) and to the cyanobacterial clone BBD-Dec07-1BB-2 associated with the Black Band Disease consortium of the coral *Favia* sp. (DGGE #9) (Tab. 4).

To conclude, not a single sponge-specific symbiont clone was present within the white tissues of Sponge White Patch diseased *A. compressa* individuals. Therefore, diverse bacterial clones have been obtained that were associated with environmental stress such as rising seawater temperature, marine pollution, aquarium transferal or coral disease.

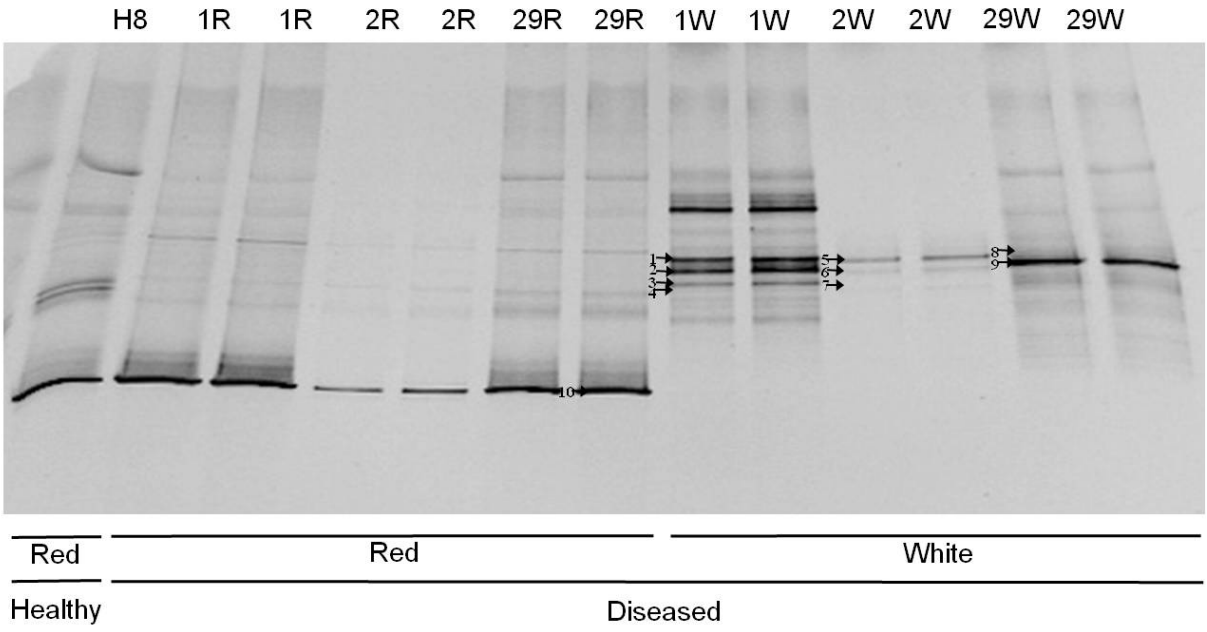

Fig. 48. Eubacterial fingerprinting of a healthy (H) *A. compressa* individual (#8) in comparison to the red (R) and white (W) parts of three Sponge White Patch diseased *A. compressa* individuals (#1, #2 and #29) via denaturing gradient gel electrophoresis (DGGE). The arrows point towards the 10 excised bands.

Sample	Tissue	Band	Accession number	Closest sequence match in GenBank	Similarity (%)	Length (bp)	Taxonomic affiliation
1W	diseased: white	1	HQ659567	Aquarium kept *Montastraea faveolata* associated clone SGUS1003 (FJ202771)	99	583/586	*Bacteria*
1W		2	HQ659568	33°C kept *Rhopaloeides odorabile* associated clone 33aA1 (EU183945)	99	439/441	*Bacteria*
1W		3	HQ659569	Hydrocarbon and oil spill polluted sand associated *Flavobacteriaceae* isolate DGGE gel band S12 (EU375150)	89	474/531	*Flavobacteriaceae*
1W		4	HQ659570	White plague-like syndrome affected *Montastraea annularis* associated *Alphaproteobacterium* clone 4-7-2 (AF544940)	97	424/433	*Alphaproteobacteria*
2W		5	HQ659571	Bahamian black band diseased *Siderastrea siderea* associated *Alphaproteobacterium* clone RB_18f (EF123421)	98	553/560	*Alphaproteobacteria*
2W		6	-	Microbial flocs associated *Alphaproteobacterium* clone: Bac1_Flocs (AB491817)	92	489/529	*Alphaproteobacteria*
2W		7	HQ659572	*Thiothrix* sp. FBR0112 (DQ067608)	96	542/562	*Gammaproteobacteria: Thiothrix*
29W		8	HQ659573	*Montastrea faveolata* associated *Clostridiaceae* bacterium clone MD3.13 (FJ425601)	96	540/559	*Clostridiaceae*
29W		9	HQ659574	Black Band Disease consortium in *Favia* sp. associated clone BBD-Dec07-1BB-2 (GQ215183)	99	561/564	*Cyanobacteria*
29R	diseased: red	10	HQ659575	*Crambe crambe* associated clone transformant10 (GU799622)	91	538/589	*Bacteria*

Tab. 4. 16S rRNA gene sequence analysis of the ten excised eubacterial DGGE bands from Fig. 48.

Comparative DGGE of Sponge White Patch disease and its associated isolates

The bacterial strains, that have been isolated from the SWP-diseased *A. compressa* individuals and that were representing the 19 unique RFLP patterns (Fig. 46) each, were applied within denaturing gradient gel electrophoresis to obtain a direct visual comparison of their banding patterns to the characteristic microbial profile of bleached SWP-tissue (Figs. 49-50). The idea was to identify with this method the responsible bacterial strains for the characteristic banding pattern within bleached, white *A. compressa*. The arrows on the left hand side of both DGGE gels point towards the DGGE banding position of interest. Due to their banding pattern I decided to apply the bacterial strains #K3, which was shown to possess agarolytic activity, as well as the strains #14 and #16 (Fig. 50: encircled in red) to the first trial of the underwater inoculation experiments in September 2009 (see page 93). The 16S rRNA genes of all bacterial isolates that had been applied to DGGE have been identified after the first underwater infection trial (Tab. 5). Their sequence analysis revealed exclusively representatives of the *Firmicutes* as well as the *Alpha*- and *Gammaproteobacteria*. Strain #14 exhibited its highest similarity to strain 741 of *Staphylococcus xylosus* and strain #K3 finally to strain Tbl of *Bacillus pumilus*. Four strains (#1, #8, #22 and #29) were belonging to the *Alphaproteobacteria*: strain #8 had the highest similarity to the coral *Montastrea faveolata* associated *Rhodobacteraceae* clone MD2.32 and strain #1 to clone WA_06f isolated from the Black Band diseased coral species *Siderastrea siderea*. Strain 22 was maximally related to clone 3.11 and had been obtained from the body wall lesions of the sea urchin *Tripneustes gratilla.* Last but not least strain 29 showed highest homology to clone NW4327 that had been isolated from the diseased sponge *Rhopaloeides odorabile* by Webster *et al.* (2002). Seven strains (#4, #5, #6, #16, #19, #20 and #28) affiliated with the *Gammaproteobacteria*. Two of them, strains #19 and #20, were most similar to a seaweed associated *Vibrio* sp. S4053. Also strain #6 was highly related to *Vibrio* sp. clone BWDY-57 and strain #5 to *Vibrio* sp. clone K882 that had been obtained from the marine sponge *Erylus* species. However, also pathogenic *Gammaproteobacteria* have been isolated: strain #4 was identified to be highly related to the *Vibrio coralliilyticus* strain LMG 10953. However, also strain #16 was most similar to the clone WA_08f derived from the Black Band diseased coral species *Siderastrea siderea*. In addition, strain #28 resembled maximally clone 3.4 that was also obtained from the body wall lesions of the sea urchin *Tripneustes gratilla* (Tab. 5). The isolated bacterial strains were all predominantly representatives of the classes *Alpha- and Gammaproteobacteria*. It was striking, that a major extent of them resembled clones that had been isolated from diseased marine invertebrates before (Tab. 5). Therefore, strains #4 and

#29 (Figs. 49-50: encircled in red) have been of extraordinarily high interest for the second underwater inoculations trials. They were re-cultivated and applied within the underwater injection experiments on healthy *A. compressa* individuals in July 2010 (see page 93).

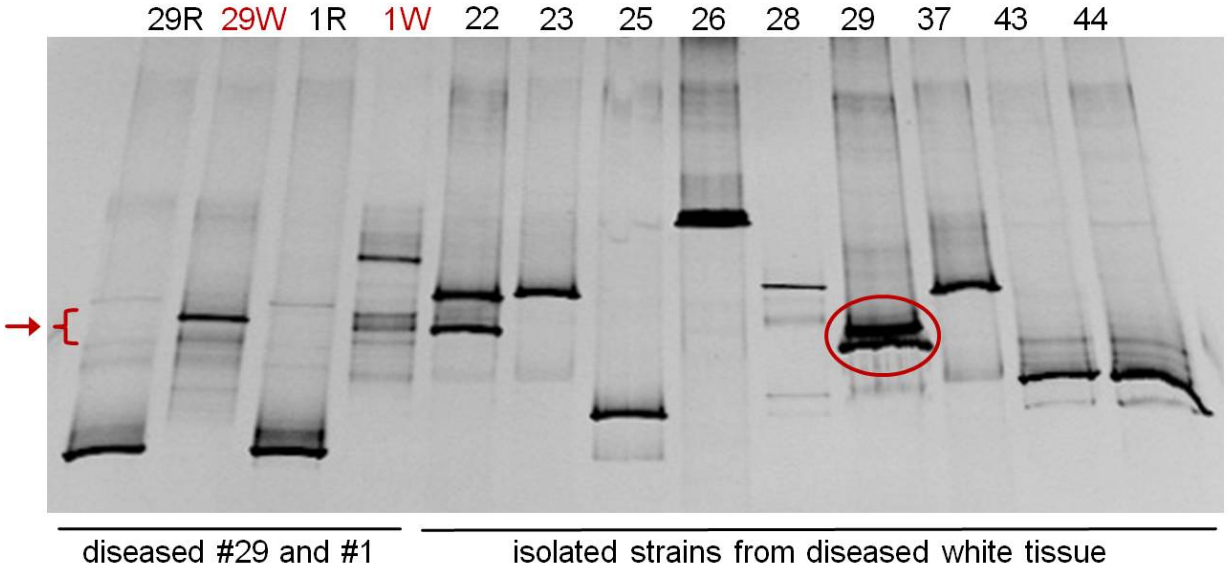

Fig. 49. Microbial fingerprinting of Sponge White Patch diseased *A. compressa* individuals (#1 and #29) and their bacterial isolates. The arrow indicates interesting banding positions. The red circle highlights the in July 2010 injected bacterial strain #29.

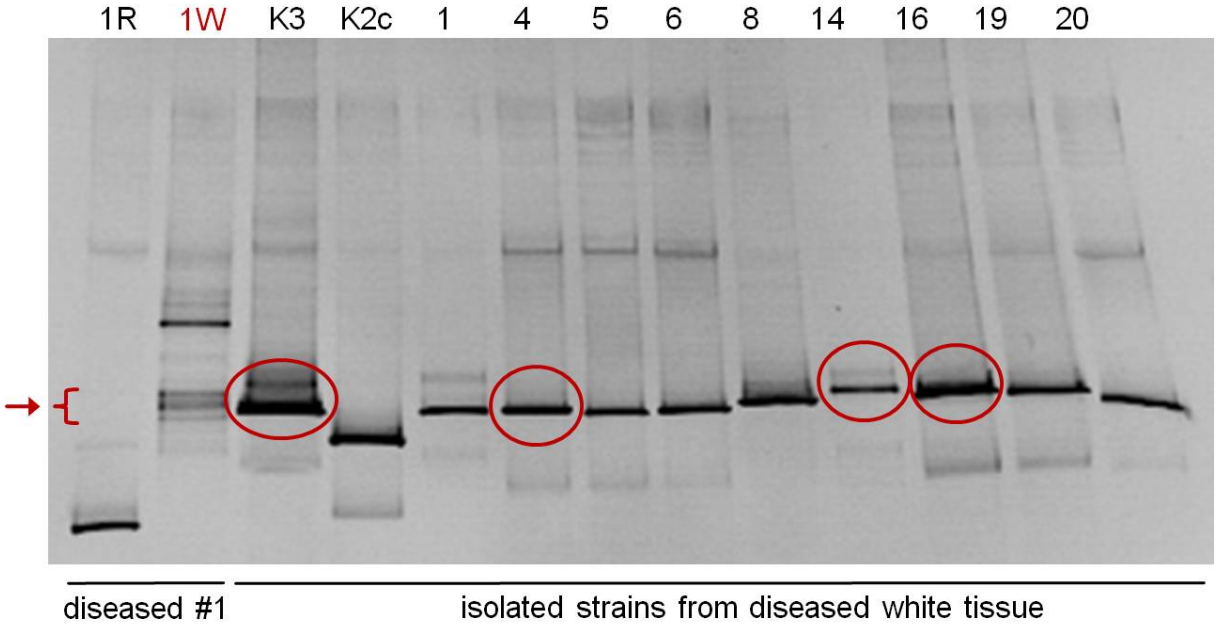

Fig. 50. Microbial fingerprinting of SWP-diseased *A. compressa* individual #1 and of bacterial isolates from white tissue. The arrow indicates interesting banding positions. The red circles highlight the in September 2009 (#K3, #14 and #16) and in July 2010 (#4) injected bacterial strains.

Sample	Tissue	Strain	Closest sequence match in GenBank	Similarity (%)	Length (bp)	Taxonomic affiliation
1W	diseased: white	1	Black Band diseased *Siderastrea siderea* associated *Alphaproteobacterium* clone WA_06f (EF123405)	98%	1407/1428	*Alphaproteobacteria*
		4	*Vibrio coralliilyticus* strain LMG 10953 (AJ316167)	99%	1461/1470	*Gammaproteobacteria: Vibrio*
		5	*Erylus* sp. associated *Vibrio* sp. K882 (GU223587)	99%	1454/1463	*Gammaproteobacteria: Vibrio*
		6	*Vibrio* sp. BWDY-57 (DQ328956)	99%	1502/1517	*Gammaproteobacteria: Vibrio*
		8	*Montastrea faveolata* associated *Rhodobacteraceae* clone MD2.32 (FJ403081)	96%	1158/1196	*Alphaproteobacteria: Rhodobacteraceae*
		14	*Staphylococcus xylosus* strain 741 (GQ222240)	99%	1503/1518	*Firmicutes: Staphylococcus*
		16	Black Band diseased *Siderastrea siderea* associated *Gammaproteobacterium* clone WA_08f (EF123487)	98%	1503/1523	*Gammaproteobacteria*
		19	Seaweed associated *Vibrio* sp. S4053 (FJ457584)	98%	1479/1495	*Gammaproteobacteria: Vibrio*
		20	Seaweed associated *Vibrio* sp. S4053 (FJ457584)	98%	1467/1496	*Gammaproteobacteria: Vibrio*
		22	Body wall lesions of *Tripneustes gratilla* associated *Alphaproteobacterium* 16S rRNA gene, clone 3.11 (AM930444)	99%	1381/1392	*Alphaproteobacteria*
		28	Body wall lesions of *Tripneustes gratilla* associated *Gammaproteobacterium* 16S rRNA gene, clone 3.4. (AM930466)	98%	1443/1469	*Gammaproteobacteria*
		29	Diseased *Rhopaloeides odorabile* associated *Alphaproteobacterium* NW4327 (AF384141)	99%	1366/1375	*Alphaproteobacteria*
29W		K3	*Bacillus pumilus* strain Tbl (AB195283)	99%	1503/1513	*Firmicutes: Bacillus*

Tab. 5. 16S rRNA gene sequence analysis of the isolated bacterial strains from the white parts of Sponge White Patch diseased *A. compressa* #1 and #29.

2.7 Infection experiments on Sponge White Patch disease

The progression of Sponge White Patch disease was visually observed underwater for up to seven days on three randomly selected *Amphimedon compressa* individuals that were exhibiting characteristic signs of disease. No deterioration of the health states in terms of lesion extension was reported for all sponges investigated within the documented time interval. For example, the lesion of individual #7 was L-shaped and stayed around 2x7cm in size from day 1 over day 5 to day 7.

Underwater transplantation experiments were conducted along a 20m transect at Conch Reef, Florida, in September 2009 to prove the contagiousness of Sponge White Patch disease. They revealed the following results for the twenty randomly chosen healthy *Amphimedon compressa* individuals (n=20), to which either tissue from healthy donor sponges (n=10) or from the white parts of diseased donor sponges (n=10) was attached. Both, healthy donor tissue used as a control as well as diseased donor tissue led in most cases to bleaching of the formerly red and underlying recipient sponge tissue. This phenomenon has been observed to different extents for all twenty sponges investigated in this study and was attributed to mechanical injury caused by sectioning and cable-tying of the recipient sponge only.

The in situ inoculation experiments with the five selected bacterial isolates (Tab 5: #K3, #14, #16, #4 and #29 standing for *Bacillus pumilus* Tbl, *Staphylococcus xylosus* 741, *Gammaproteobacterium* WA_08f, *Vibrio coralliilyticus* strain LMG and *Alphaproteobacterium* NW4327) have been conducted to prove each strain's capability to evoke Sponge White Patch disease on healthy *A. compressa* individuals. As a result, the incubation of healthy *A. compressa* individuals (n=41 for both infection trials combined) with any of the selected bacterial strains did not evoke symptoms of Sponge White Patch disease, not even among a single healthy sponge individual. The same was validated for injection with SWP-disease incubated Zobell medium that served as positive control. The total time span of inoculation, which lasted either 9 or 29 days depending on the specific trial, did not seem to be of relevance for disease transmittance by direct contact.

Consequently, I conclude that neither the progression of Sponge White Patch disease nor the tissue transplantation trials or the injection of before isolated, potential infectious agents revealed any evidence for the aggressiveness and transmittance of Sponge White Patch disease, speaking against its direct contagiousness.

2.8 The presence of accessory sponge diseases

Remarkably, I did not only encounter Sponge Orange Band and Sponge White Patch disease, affecting *Xestospongia muta* or *Amphimedon compressa* respectively, during my missions on Caribbean reefs. Especially within the Florida Keys National Marine Sanctuary, I was also running across various other Poriferan species showing diverse symptoms of disease: *Ectyoplasia ferox* (Fig. 51a), *Ircinia felix* (Fig. 51b) and *Agelas* sp. (Fig. 51c) exhibiting bleached surface patches as well as *Agelas cerebrum* (Fig. 51d), *Aplysina lacunosa* (Fig. 51e) and *Callyspongia* sp. (Fig. 51f) containing bleached rings. Those whitened areas comprised presumably necrotic sponge tissue and were built up by spicules only. Some sponge individuals belonging to the species *Callyspongia* (Fig. 51f) and *Niphates digitalis* (Fig. 51g) showed algal overgrowth, as additional colorations appeared on the sponge surfaces. Representatives of the species *Callyspongia plicifera* (Fig. 51h) and *Cliona* sp. (Fig. 51i) exhibited vast areas of destructed sponge tissue that might have been due to mechanical destruction by turtle bites. Obviously, the phenomenon of sponge disease has been vastly neglected within molecular research until the start of my PhD thesis. Though few publications arose within the last years, it still exhibits a great working surface for upcoming research projects, as many more sponge diseases and especially their underlying mechanisms are yet awaiting to be explored (Fig. 51).

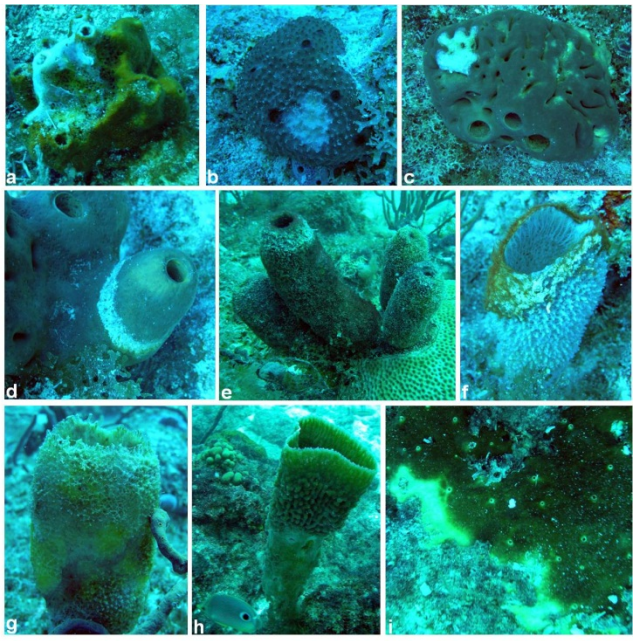

Fig. 51. Accessory Caribbean sponge species documented within the Florida Keys National Marine Sanctuary, that are showing still vastly unexplored symptoms of sponge disease: *Ectyoplasia ferox* (a), *Ircinia felix* (b), *Agelas* sp. (c), *Agelas cerebrum* (d), *Aplysina lacunosa* (e), *Callyspongia* sp. (f), *Niphates digitalis* (g), *Callyspongia plicifera* (h) and *Cliona* sp. (i).

V. Discussion

1. Microbial pathogens of corals and sponges

To date, coral diseases have received enormous attention owing to the important role of coral reefs in global biodiversity as well as to the alarming rate at which reefs have been decimated in the context of global warming (Rosenberg *et al.*, 2007; Mao-Jones *et al.*, 2010). In comparison, much less effort has been undertaken to investigate diseases of marine sponges. First reports about sponge bleaching, affecting symbiont-containing individuals like *X. muta*, occurred along with those of coral bleaching over a decade ago (Vicente, 1990). Since then observations on microbial diseases among marine invertebrates have been rising with a fast pace over a broad range of species and geographic areas (Rosenberg and Loya, 2004; Becker *et al.*, 2008), what might have been influenced by an increasing public awareness on coral reef health issues over the last years (Webster, 2007).

Sponge diseases have been documented in all major ocean bodies with the Caribbean representing a particular hot spot (Harvell *et al.*, 1999). They typically start with the appearance of discolored surface patches followed by tissue disintegration and biofouling of the exposed spicule skeleton. The disease usually spreads over the entire sponge body within weeks to months resulting in the death of either single sponge parts, the whole sponge individual or even entire sponge populations. Interestingly, disease progression seems to depend on the growth form of the sponge with massive individuals like *X. muta* being more prone to a fatal course of disease than branching species like *A. compressa*. The latter often reject affected tissue and recover (Wulff, 2006; Angermeier *et al.*, 2011). However, research on sponge diseases has been hampered by the fact that the death of any given sponge is hard to define. On the one hand, it often goes unnoticed. On the other hand, it can be followed, in cases such as *X. muta*, by the outgrowth of offspring at sites, where a sponge body had collapsed before blurring clear definitions of sponge death. However, this phenomenon pinpoints towards the enormous regenerational ability within the phylum *Porifera*, whose disease causing factors are still largely unknown.

Besides corals, also sponges are endangered by direct environmental factors such as climate change (Webster *et al.*, 2008b) and anthropogenic parameters (e.g. pollution), which are assumed to play a role at disease causation. The role of temperature is important in the context of global warming, which impacts the composition of entire ecosystems (Hughes *et al.*, 2003; Hoegh-Guldberg *et al.*, 2007; Whiteman, 2010). Thus, a clear correlation has been

documented between high (Cerrano *et al.*, 2000; Perez *et al.*, 2000; Lopez-Legentil *et al.*, 2008; Webster *et al.*, 2008b; Maldonado *et al.*, 2010) and low temperatures (Perez *et al.*, 2006) and certain sponge diseases. López-Legentil *et al.* (2008) monitored for example the expression of heat shock protein 70 genes as an indicator of stress during the exposition of *X. muta* tissues to different seawater temperatures and found a significant increase at 30°C, stating that stress might negatively influence the size of coral reef sponge populations. A thermal threshold had also been revealed for the GBR sponge *Rhopaloeides odorabile* inbetween 31° and 33°C. Exposition to those temperatures has been leading to tissue necrosis and evoked a shift within the sponge-associated microbial community towards a high proportion of coral bleaching and disease related microorganisms (Webster *et al.*, 2008a). In addition, *R. odorabile*'*s* exposure to the heavy metal copper has been shown as well to elicit a microbial community shift (Webster *et al.*, 2001b). Even though it has been difficult to pinpoint the exact causes, environmental stress, such as elevated seawater temperature or pollution, likely decreases the fitness of marine invertebrates, such as sponges, and renders them more susceptible to disease by influencing the abundance and virulence of potential marine pathogens (Cerrano *et al.*, 2000; Kim and Harvell, 2002; Sutherland *et al.*, 2004).

So far, diverse microorganisms such as *Alphaproteobacteria* (Webster *et al.*, 2002), representatives of the genera *Bacillus* and *Pseudomonas* (Cervino *et al.*, 2006), the phylum *Cyanobacteria* (Rützler, 1988; Olson *et al.*, 2006) as well as fungi (Galstoff, 1942) and viruses (Vacelet and Gallissian, 1978) have been implicated as disease-causing agents among sponges. Some studies in the past even correlated the presence of spongin-boring bacteria within affected sponges of the species *Rhopaloeides odorabile*, *Hippospongia communis*, *Ircinia variabilis*, *Sarcotragus spinosula* and *Spongia officinalis* with disease (Gaino and Pronzato, 1989; Gaino *et al.*, 1992; Vacelet *et al.*, 1994; Webster *et al.*, 2002). However, in only one case Koch's postulates have been upheld, linking the spongin-boring alphaproteobacterial strain NW4327 to necrosis of the Australian GBR sponge *R. odorabile* (Webster *et al.*, 2002). In this study, infection of healthy *R. odorabile* individuals with the spongin-boring strain, that had been isolated from a single necrotic individual before, was shown to trigger severe tissue necrosis within a time interval of two weeks. However, no other study on sponge disease could fulfill the Koch's postulates. In a recent study by Luter *et al.* (2010), that had been simultaneously performed to my study, also no pathogen but a microbial community change has been documented for 'brown lesion necrosis' affecting the Indo-Pacific sponge *Ianthella basta*. The same outcome was validated for 'Aplysina Black Patch disease' affecting the species *Aplysina aerophoba* (Nardo, 1843) at the Slovenian coast

in the Adriatic Sea (Webster *et al.*, 2008a). Therein, a chemical host response going along with a shift in the bacterial community composition during progression of disease has been stated. In contrast, the related Caribbean species *Aplysina cauliformis* has been afflicted by a different phenomenon: 'Aplysina Red Band Syndrome' (ARBS). During its course a distinct reddish band appears on the rope sponge that has been attributed to a yet unidentified cyanobacterial species. However, molecular studies on the etiological role of this strain do not pledge for its state as a single pathogen (personal comment D. Gochfeld, University of Mississippi, 2010; Olson *et al.*, 2006). Table 6 lists the most prominent as well as thoroughly investigated sponge diseases and their assumed infectious agents that I have been referring to within my PhD thesis.

Interestingly, there has been a recent trend in research on marine invertebrate diseases, which pinpoints more towards the importance of microbial community shifts than towards the involvement of single pathogens (Becker *et al.*, 2008; Luter *et al.*, 2010; Angermeier *et al.*, 2011). Though all studies implicated so far microbial pathogens as etiologic agents of sponge disease (Webster, 2007), a bona fide sponge pathogen has rarely been identified underlining my scientific findings. In general, the abundance and geographic distribution of marine sponges is influenced by numerous factors such as inter- and intra-specific competition, predation, sponge nutrition, global climate change (i.e., elevation of seawater temperature or ultraviolet light) as well as sedimentation, pollution and mechanical damage (e.g. by surge or hurricanes) besides the presence of sponge diseases (Lopez-Legentil *et al.*, 2008; McMurray *et al.*, 2010). The suspicion arises that those environmental as well as anthropogenic impacts do not only influence whole sponge populations, but that they are actively involved in the causation of sponge disease. If this suspicion substantiates, long-term detrimental effects on a whole ecosystem level will be the result (Butler *et al.*, 1995) leading to overall shifts within the coral reef community structures (Norström *et al.*, 2009).

Sponge disease	Species affected	Etiologic agent	Reference
Mangrove sponge disease	*Geodia papyracea*	*Oscillatoria* sp. (assumed)	Rützler (1988)
Spongin-boring necrosis	*Rhopaloeides odorabile*	*Alphaproteobacterium NW4327*	Webster *et al.* (2002)
Aplysina Red Band Syndrome	*Aplysina cauliformis*	Not performed	Olson *et al.* (2006)
Aplysina Black Patch disease	*Aplysina aerophoba*	Not detected	Webster *et al.*(2008a)
Brown lesion necrosis	*Ianthella basta*	Not detected	Cervino *et al.* (2006)
Disease-like syndrome	*Ianthella basta*	Not detected	Luter *et al.* (2010)
Sponge Orange Band disease	*Xestospongia muta*	Not detected	Cowart *et al.* (2006); Angermeier *et al.* (2011)
Sponge White Patch disease	*Amphimedon compressa*	Not detected	Angermeier *et al.* (in preparation)

Tab. 6. A selection of sponge diseases mentioned and referred to within this thesis.

2. The pathology of Sponge Orange Band disease affecting *Xestospongia muta*

2.1 Visual observations on Sponge Orange Band disease

This study is based on eleven Sponge Orange Band diseased *X. muta* representatives that were showing characteristic signs of disease yet in an individual manner (Fig. 16). During progression of Sponge Orange Band disease gradual bleaching of the normally brown, symbiont-containing sponge surface tissue takes place causing an orange-band like transition zone in between the non-bleached brown and the completely bleached white sponge surface. Thus, SOB-diseased sponges were grouped into early (solid body texture and little amount of bleaching: Figs. 16b-c, i, l) and advanced stages of disease (high amount of bleaching and sponge erosion: Figs. 16d-h, j-k). Interestingly, I observed that sponges undergoing early stages of disease were still actively pumping (Fig. 17c), whereas no exhalent water current was measurable for the oscula of sponges undergoing advanced stages of disease (Figs. 17b; see also movies on supplementary CD). This latter case has been additionally confirmed by C. Finelli (UNCW; unpublished data) via in situ flow measurements (Fig. 17e). Regarding the fast pace of Sponge Orange Band disease *X. muta* individuals were observed to collapse, entirely bleached, within only 6 to 8 weeks after onset of disease (Cowart *et al.*, 2006) (personal comments N. Lindquist, UNC/CH, 2009 and J. Pawlik, UNCW, 2007). However, at times a regeneration of collapsed sponges occurred by the outgrowth of multiple newly-arising sponge oscula circumventing the former sponge base. The death of those individuals might have been caused by Sponge Orange Band disease as well as described by McMurray *et al.* (2008). Moreover, electron microscopical studies revealed an ongoing surface destruction from the brown via the orange to the white surface tissues of diseased sponges (Figs. 21: SEM; Figs. 24-25: TEM). I found striking differences in between the orange transition zones of sponges undergoing either early or advanced stages of Sponge Orange Band disease. Within the orange surface tissues of early stage diseased sponges (Bahamas collection) a notably increased phagocytosis by sponge cells of the abundantly present cyanobacteria has been revealed via fluorescence (Fig. 29) and electron microscopy (Fig. 25) going along with an extraordinarily high amount of intracellular versus extracellular cyanobacteria (Fig. 28). This seems to indicate an active immune response by the sponge towards the progression of Sponge Orange Band disease. Those observations have been confirmed by Rützler (1988), who documented an active phagocytosis of symbiotic cyanobacteria in diseased tissues of the mangrove sponge *Geodia papyracea* (see Tab. 6: page 98), and by Maldonado *et al.* (2010), who detected the same phenomenon in diseased pustules

of two *Ircinia* species, *Ircinia variabilis* and *Ircinia fasciculata*. In general, for cnidarians with algal symbionts, the intriguing hypothesis has been advanced that tissue bleaching is due to an overly aggressive, innate immune response (e.g. phagocytosis) going along with loss of control over apoptosis and necrosis as the cause of uncontrolled bleaching and ultimately death (Dunn *et al.*, 2004; Weis, 2008). However, the question has still not been answered, what triggers this event. In more advanced stages of Sponge Orange Band disease (sponges of the Florida collection), a extremely high degree of cellular degradation has been visible within the surface tissues, that might have been caused by apoptosis and necrosis of affected sponge cells, cyanobacteria as well as bacterial morphotypes (Figs. 25d-f). Thus, unravelling the mechanisms of interaction between host phagocytes and microbial symbionts (i.e., recognition as well as differentiation between self and non-self) will clearly be instrumental to the understanding of sponge health and disease.

The microscopical examination of the reddish-stained seawater from Ziploc bags, in which the sponge sample had been collected (Fig. 27), showed the presence of large amounts of cyanobacterial symbionts. Those were apparently falling out of the collagen-containing sponge meshwork of healthy *X. muta* individuals, where they are normally located within the surface tissues. However, mechanical destruction seems to cause their loss and results in sponge surface discoloration by staining the surrounding seawater. Thus, the gradual destruction of the sponge tissue and its associated symbionts during bleaching explains the decrease in sponge surface coloration from brown via orange to white, that is going along with the loss of the *X. muta* characteristic secondary metabolites (Fig. 34) and its chlorophyll *a* content (Fig. 35; see annex: Tab. 5). As cyanobacteria harbour chlorophyll *a* within their thylakoid membranes, their decrease is directly correlated with the yield of chlorophyll *a* per sponge sample (Thacker, 2005). Despite the observed decrease in cyanobacteria and sponge cell nuclei, total bacterial cell counts resulted in a higher amount of bacteria within the brown, orange and white surface tissues of Sponge Orange Band diseased *X. muta* individuals (Tab. 1). This might correlate with disease-related, degradative processes, which are setting free normally unavailable nutrients. Those create niches for the settlement of unspecific marine microorganisms that are normally not present within healthy *X. muta* individuals, as they are likely deterred by the present secondary metabolite profile. This explains well, why solely the white surface tissues were interspersed with diverse microbial colonies, filaments and spores (Figs. 21, 23) and why also multicellular animals, like marine amphipods or sea mites, were detected solely within diseased *X. muta* surface tissues (Figs. 18, 23).

2.2 The microbiology of Sponge Orange Band disease

Cultivation efforts as well as microbial fingerprinting were performed on healthy and Sponge Orange Band diseased *X. muta* samples. The diversity of bacteria was much higher within diseased sponge tissues than within healthy sponges. The brown, orange and white surface tissues of SOB-diseased sponges yielded species belonging to the *Alpha-* or *Gammaproteobacteria*, which had been isolated from the healthy or diseased corals *Pseudopterogorgia americana*, *Montastrea annularis* or *Favia* sp. (Barneah *et al.*, 2007; Rypien *et al.*, 2010) (M. Vizcaino, unpublished data) before. For example one clone obtained from white *X. muta* tissue was most similar to a bacterial strain associated with an azooxanthellae coral of the species *Oculina patagonica* (Koren and Rosenberg, 2008). Koren and Rosenberg (2008) documented that the bacterial community within symbiont-free corals, either bleached or growing without light, varies tremendously to the one of healthy corals. From SOB-diseased *X. muta* tissues a *Staphylococcus* strain associated with gill disease of *Salmo salar* (S. Embar-Gopinath; unpublished data) and a *Silicibacter* strain associated with diseased *Pseudopterogorgonia americana* (M. I. Vizcaino; unpublished data) have been obtained besides *Bacillus pumilus* strains. Cervino *et al.* (2006) have found already *Bacillus pumilus* and closely related species within the diseased sponge *Ianthella basta* of the Indo-Pacific. In addition, the *Acinetobacter* sp., that I isolated from the orange surface tissue of diseased *X. muta*, has also been detected by Kefalas *et al.* (2003) within the marine sponge *Spongia officinalis*. They regarded it as an indication for anthropogenic contamination (Lemke and Leff, 1999), that could be responsible for disease causation. However, also Koren and Rosenberg (2008) revealed an *Acinetobacter* cluster that has been dominating as much as 25% of the bacterial clones from bleached corals. This fact underlines the observed microbial community shift that is occurring during bleaching of marine sponges and corals, in which the symbiotic, bacterial phylotypes get replaced by strains most closely related to known coral pathogens (Koren and Rosenberg, 2008; Webster *et al.*, 2008a).

Remarkably, a shift from the stable eubacterial community of healthy *X. muta* sponges towards a heterogeneous mixture of DGGE bands within SOB diseased individuals has been observed during progression of disease. It had its onset within the healthy appearing brown tissues of diseased *X. muta*, but became more prominent during progression of bleaching from orange to white (Fig. 30). Such a microbial community shift preceeding any visual symptom of disease has already been documented by Pantos *et al.* (2003) during bleaching of the coral *Montastrea annularis* and was termed the ‘whole coral response’. In my study I found its

striking relevance also for diseases affecting the phylum *Porifera*. Therefore, I refer in the following context to this phenomenon as the 'holobiont response', as it affects the entire organism of a diseased HMA-sponge.

Looking at the cyanobacterial community within *X. muta*, a distinct shift has been reported to take place during bleaching by Sponge Orange Band disease, which replaces the *Synechococcus/Prochlorococcus* clade of cyanobacterial sponge symbionts with a heterogeneous mixture of unspecific cyanobacterial species just within the white surface tissues. In more detail, it harboured instead of the sponge symbionts representatives belonging to diverse cyanobacterial genera such as the *Gloeocapsa*, *Spirulina*, *Limnothrix*, *Acaryochloris*, *Leptolyngbya*, *Myxosarcina*, *Plectonema* and *Halomicronema* (Fig. 33; see annex: Tabs. 3-4). The sequences of the according DGGE bands have been most closely related to clones obtained from seawater (Goh *et al.*, 2009), microbial mats (M.A. Allen; unpublished data) and slimes (Tracy *et al.*, 2010) as well as artificial (N. Siboni; unpublished data) and healthy coral reefs or sediments (U. Werner; unpublished data). However, they have also been derived from healthy (Klaus *et al.*, 2007; Sunagawa *et al.*, 2009) (L.K. Ranzer, unpublished data) and aquacultured (Sunagawa *et al.*, 2009) or, what is even most striking, from diseased coral tissues (Myers *et al.*, 2007) (S.E. Godwin; unpublished data) and their respective mucopolysaccharide layers (Barneah *et al.*, 2007). Microbial population shifts away from the stable consortium are already well known for coral diseases, where the change has been shown to predate the bleaching event (Cooney *et al.*, 2002; Frias-Lopez *et al.*, 2002; Pantos *et al.*, 2003; Gil-Agudelo *et al.*, 2006; Bourne *et al.*, 2008). Another proof of the correlation inbetween sponge and coral microflora, if both are underoing disease, has been the presence of the normally sponge-affiliated gammaproteobacterial *Spongiobacter* sp. clade as the dominant phylotype during pre- and post-bleaching of the coral *Acropora millepora* (Bourne *et al.*, 2008). Such a microbial community shift likely depends upon the loss of the secondary metabolite profile going along with the sponge's decreased cytotoxicity, which gives the above mentioned bacterial colonizers an unhampered opportunity to invade (Fig. 34). It thus appears that disturbances of the natural microbiota of sponge and coral hosts are involved in the evocation of the 'whole coral-' and the 'holobiont response'. Therefore, they are a common feature and a potential elicitor of marine invertebrate diseases enabling opportunistic bacteria to colonize the newly exposed, chemically undefended invertebrate tissue. Whether these bacteria are simply efficient colonizers or whether they actively contribute to the infection process still remains to be investigated.

Remarkably, attempts at infection with transplanted SOB tissue were not successful. Recipient sponges seemed to recover after up to 11 days by the acceptance and overgrowth of transplanted tissue, no matter whether it has been derived from a diseased or healthy donor sponge (Fig. 36; see annex: Tab. 6). A previous study by Walters & Pawlik (2005) demonstrated already that *X. muta* is able to heal wounds very rapidly. This appears to be true also in my study, whether the wounds were left open (as in the case of Walters & Pawlik, 2005) or filled with exogenous sponge tissue. However, probably most revealing is the unsuccessful infection of healthy individuals at either early or late stages of disease (Fig. 36). Thus, despite a careful characterization of SOB-disease affecting the Caribbean barrel sponge *Xestospongia muta*, this study provided no evidence for the involvement of a specific microbial pathogen as an etiological agent of disease. Consequently, I emphasize that Sponge Orange Band disease of *X. muta* cannot be attributed to a microbial pathogen leaving its ultimate cause still to be explored.

2.3 Conclusions

The causative agents of Sponge Orange Band disease can just be speculated by now, but one potential parameter for its outbreak, at least offshore the US Virgin Islands in 2009, might have been the inflow of the Orinoco and Amazon rivers. This had evoked a plume from March to May 2009 due to the income of turbid, chlorophyll-rich waters off-shore the island (personal comment T. Smith, USVI, 2009). An abnormally high nutrient influx likely correlates with increased productivity of toxic plankton species that might have in turn an effect on the present *X. muta* population. Its intraspecific variation in susceptibility to disease might have been influenced by the genetic heterogeneity among different *X. muta* individuals within a given population that has been causing just single individuals to develop symptoms of disease. Further studies are needed and more than welcome, which include long-term monitoring data of environmental parameters influencing whole *X. muta* populations in situ.

3. The pathology of Sponge White Patch disease affecting *Amphimedon compressa*

3.1 Ecological and visual observations on Sponge White Patch disease

I observed Sponge White Patch disease on *Amphimedon compressa* for the first time in winter 2007 at Dry Rocks Reef, Florida. The total study was based on 171 Sponge White Patch diseased *A. compressa* individuals that were exhibiting white branches or patches on an overall red sponge body (see annex: Tab. 7). Later observations in summer 2009 and 2010 monitored Sponge White Patch disease with a much higher abundance at Conch Reef, Florida, where it has been rarely observed before indicating its increasing importance on coral reefs within the Florida Keys National Marine Sanctuary.

A. compressa appears to possess a regenerational ability by being able to discharge the diseased, white sponge tissue (Fig. 37b). Light- and electron microscopical studies of SWP-diseased *A. compressa* individuals (Figs. 41-44) revealed that the white tissue consists solely out of cellular detritus and spicules interspersed with only few intact sponge cells and bacterial morphotypes. The latter include the spongin-boring bacteria, which are situated inside presumably self-made channels within the spongin matrix. The red *A. compressa* tissue in contrast is comprised of numerous round sponge cells, to all appearance no bacteria, but an intact spongin matrix dispersed by the spicule skeleton only. SEM micrographs show that collagenous fibers are holding the pinacoderm of the sponge surface together (Figs. 42c, f-g), which is comprised to its majority of pinacocytes and accumulated round sponge cells. The latter seem to be responsible for the sponge's overall red coloration by the incorporation of metabolites. As a consequence, if *A. compressa* stops pumping, caused by disease or mechanical damage, it looses its sponge cells and thus becomes subject to bleaching.

3.2 The microbiology of Sponge White Patch disease

Webster *et al.* (2002) had identified the spongin-boring *Alphaproteobacterium* NW4327 within the diseased sponge *Rhopaloides odorabile* and even showed its collagenase activity. Subsequently, they confirmed it to elicit that disease in healthy *R. odorabile* individuals and thus claimed it to be its etiological agent. This is why I was interested in the bacterial affiliation of the spongin-boring strain that I have been observing just within the bleached parts of *A. compressa* and in the role it plays during Sponge White Patch disease.

During isolation on azocoll-containing marine agar I obtained two collagen-degrading strains, that were after first sequencing results most similar to the *Gammaproteobacterium Microbulbifer agarilyticus* strain JAMB A3 (Fig. 45). This fits well to the observation of Koren and Rosenberg (2008), who obtained also during cultivation trials on healthy, cave and bleached corals a highly abundant cluster of *Microbulbifer* sp.. Additional cultivation on Azocoll-containing marine agar yielded no other bacterial isolate capable of degrading collagen. The bacterial diversity was again highest within the white *A. compressa* tissues. Those strains, together with the collagen-degrading strains, have been applied to analysis via restriction fragment length polymorphism (RFLP). In total, nineteen different RFLP banding patterns arose, with the collagen-degrading strains building up one of them (Fig. 46). All of the unique RFLP patterns were subject to denaturing gradient gel electrophoresis (DGGE) for a comparison of their specific bacterial fingerprints to the one of the white *A. compressa* tissue (Figs. 49-50). Consistent fingerprints were of interest for the underwater infection trials. The cultivation trials revealed only few bacterial strains within red *A. compressa* tissues, whether derived from healthy or affected sponges, in contrast to numerous isolates from diseased white *A. compressa* tissues (Tabs. 3 and 5). The bacterial clones isolated during the cultivation trials from the white *A. compressa* tissues were clustering predominantely within the *Alpha-* and *Gammaproteobacteria* as well as within the *Firmicutes* and among *Bacteria* of unknown affiliation. Most striking was the fact that six isolated bacterial strains were the highest related to microbes obtained from other marine invertebrate diseases. Those included *Vibrio* sp. associated with diseased corals (Thompson *et al.*, 2001), *Alpha-* and *Gammaproteobacteria* associated either with body wall lesions of the sea urchin *Tripneustes gratilla* (Becker *et al.*, 2009) or with the black band diseased coral *Siderastrea siderea* (Sekar *et al.*, 2008). Last but not least, the cultivation trials revealed the *Alphaproteobacterium* NW4327, that had been isolated from the diseased GBR sponge *Rhopaloeides odorabile* by Webster *et al.* (2002) before and which was shown to possess collagenolytic activity (Tabs. 5-6).

To elucidate the microbial community during disease progression, I compared the microbial fingerprints of the red versus the white parts of three diseased *A. compressa* sponges. As a result, the bands of high GC-content, present within the red tissues, were absent within the white tissues. However, the latter harbored instead additional bacterial bands. The bacterial affiliation of all excised bands, one band from the red and nine from the white tissues of Sponge White Patch diseased *A. compressa* individuals, was identified. The bacterial clone obtained from the red sponge tissue was with 91% most similar to the sponge

Crambe crambe associated transformant clone 10 (D. Sipkema; unpublished data). LMA sponges have just recently been suspected to possess a specific microbial signature (personal comment Ute Hentschel, 2011). I could confirm via molecular fingerprinting that the healthy LMA-sponge *A. compressa* has its own microbial profile. The fact, that the above mentioned sequence exhibited its maximal similarity with only 91% to any other bacterial strain indicates a lack of sequences in GenBank, that are derived from either this sponge species only or from all low-microbial-abundance (LMA) sponges. In contrast, the DGGE bands derived from the white *A. compressa* tissues were the highest related to microbes obtained from hydrocarbon or oil spill polluted sand (Alonso-Gutierrez *et al.*, 2009), microbial flocs (M. Yuhana; unpublished data), aquarium-kept coral (Sunagawa *et al.*, 2009), the marine sponge *Rhopaloeides odorabile* exposed to elevated temperature at 33°C (Webster *et al.*, 2008a) or from diseased corals either affected by White Plague-like syndrome (Pantos *et al.*, 2003) or by Black Band disease (Sekar *et al.*, 2006; Arotsker *et al.*, 2009). Additional species represented were *Thiothrix* (Cytryn *et al.*, 2006) and coral associated *Clostridiaceae* (W.R. Johnson; unpublished data). All of the above mentioned bacterial phyla present within the white tissues were clustering among the *Alpha*- and *Gammaproteobacteria* and some were of unknown bacterial affiliation, exactly as during the cultivation trials. However, additional representatives obtained via DGGE belonged to the *Flavobacteriaceae*, the *Clostridiaceae* and the *Cyanobacteria* (Tab. 4). Interestingly in contrast to the HMA-sponge *X. muta*, the microbial shift during Sponge White Patch disease of the LMA-sponge *A. compressa* has not been preceeding the bleaching event, as the red tissues of healthy and diseased *A. compressa* were still fairly identical in their bacterial fingerprint. This certainly correlates with *A. compressa's* habitus as a LMA-sponge that goes along with a restricted microbial fingerprint. However, its shift within the microbial community during bleaching of Sponge White Patch disease has likely been influenced by the availability of new nutrients, which were set free by destruction processes, and potentially also by the lack of secondary metabolites such as Amphitoxin (Thompson *et al.*, 2010). However, the latter point deserves further research.

Remarkably, culturable as well as unculturable techniques applied to the bleached tissues of Sponge White Patch diseased *A. compressa* individuals yielded predominantly representatives of the *Alpha*- and *Gammaproteobacteria* that I have found to be frequently associated with diseases affecting diverse marine invertebrate species. Thus, representatives of these strains were of especially high interest for the underwater infection experiments on the transmission of Sponge White Patch disease.

The underwater observation on the progression of Sponge White Patch disease, which was performed for up to seven days on three diseased *A. compressa* individuals, indicated no lesion enlargement over time. In addition also the tissue transplantation trials, which were performed for twenty healthy *A. compressa* individuals to which bleached SWP-tissue had been attached, did not prove any transmission of disease via direct contact. In contrast, this experiment revealed that bleaching can in addition be caused artificially by mechanical impact such as tissue sectioning or cable-tying only. The damaged sponge tissue, which lacks cells and presumably also its secondary metabolite profil, might have simply been rendered susceptible to the settlement of secondary colonizers, that were deterred before. As also Steffens (2003) had detected channel-drilling bacteria throughout the spongin of the healthy sponge species *Axinella verrucosa*, I doubt that spongin-boring bacteria are the etiological agents of sponge disease. I can confirm this comment with the results of the underwater infection experiments, that I have been conducting with five selected bacterial isolates of white *A. compressa* tissue: *Bacillus pumilus* Tbl, *Staphylococcus xylosus* 741, *Gammaproteobacterium* WA_08f, *Alphaproteobacterium* NW4327 and *Vibrio coralliilyticus* strain LMG 10953 (Tab. 5). The applied *Vibrio coralliilyticus* strain LMG 10953 and the gammaproteobacterial strain WA_08f have been representing potential coral pathogens. *Bacillus pumilus* species have already been claimed before by Cervino *et al.* (2006) to be involved in causation of 'Brown lesion necrosis' within the marine sponge *Ianthella basta* off-shore Papua New Guinea. The same has been validated for the *Alphaproteobacterium* NW4327, that has been made responsible for triggering 'Spongin-boring necrosis' within the GBR sponge *R. odorabile* (Tab. 6). Though all of those strains had a highly pathogenic potential, none of them evoked any symptom of Sponge White Patch disease on healthy *A. compressa* individuals during the underwater inoculation trials.

This is why I claim for the, at least within diseased *A. compressa* ubiquitiously present, spongin-boring strain, that it is not involved in the elicitation of Sponge White Patch disease as its etiologic agent. Instead, it likely plays a role as its primary colonizer, who is specialized on bleached sponge tissue and whose presence is dependending upon its availability.

3.3 Conclusions

Pollution is likely a causative agent of Sponge White Patch disease, as about 1/5th of a given population at Dry Rocks Reef has been affected by disease in winter 2007 and the prevalence has been even rising since then affecting additional reefs. Interestingly, Conch Reef has been reported directly before the last field trip in summer 2009, where it was found to be manifested by Sponge White Patch disease, to be drastically affected by strange water conditions, such as upwelling water bodies, cyanobacterial mats in combination with bad underwater vision and the presence of coral bleaching events (personal comment Margaret Miller, NOAA, 2009). At the same time, African dust has been observed to affect the Florida Keys (s comment Niels Lindquist, UNC-CH, 2009 and Gene Shinn, University of South Florida, 2009). Thus, also in this study toxin production by marine algae might have played a role in the development of Sponge White Patch disease due to the high nutrient input. Therefore, I require long-term monitoring studies in the future, that cover the environmental influences *A. compressa* populations are facing in situ, to find an answer to the still open-ended question, what causes healthy *A. compressa* individuals to bleach during the progression of Sponge White Patch disease.

4. Consensus

Comparing Sponge Orange Band disease of the HMA-sponge *X. muta* against Sponge White Patch disease of the LMA-sponge *A. compressa*, reveals the following accordances and discrepancies (Tab. 7): Bleaching of both sponge species has been shown to originate from tissue destruction going along either with the loss of sponge cells, in case of *A. compressa*, or with the loss of the abundantly present symbiotic cyanobacteria, as in terms of *X. muta*. The reduced tissue integrity results in the exposition of the spicule skeleton to the constantly present marine microflora, which is eagerly colonizing newly available, nutrient-rich habitats. As a result shifts within the sponge-associated microbial communities of the white parts have been depicted for both sponge diseases, that were dominated by isolates obtained from other diseased marine invertebrates. However, for the LMA-sponge *A. compressa* diverging microbial fingerprints have been solely observed for the white and not the red parts of diseased individuals, whereas for the HMA-sponge *X. muta* the eubacterial community shift has been already predating the bleaching event. I termed this phenomenon the 'holobiont response'. It seems to be characteristic for HMA-sponges only, as their bacteria rather play a role in maintaining homeostasis of the natural host associated microbiota than in acting as invading pathogens in a clinical sense. Interestingly, by now the majority of the investigated sponge diseases have been affecting HMA-sponges (Webster *et al.*, 2002; Olson *et al.*, 2006; Webster *et al.*, 2008a; Maldonado *et al.*, 2010). For those the sponge associated microorganisms have been clearly shown to undergo fluctuations during disease and to be instrumental to sponge health. Therefore it is not surpising that for *X. muta* an innate immune defense via host cell phagocytosis has been observed in this study. Whether this phenomenon is species-specific or underlying HMA-sponges only, needs to be further investigated, as it was not detected for the LMA-sponge *A. compressa*. Remarkably, the abundance of Sponge Orange Band disease is very limited with a frequency rate of below 1% (Cowart *et al.*, 2006) and a fatal outcome, whereas Sponge White Patch disease affects about 20% of the *A. compressa* population and is characterized by recovery over time. This has been in addition predicted by Wulff (2006), who correlated disease fatality and morphological habitus of sponge species. However, for both sponge diseases investigated I did neither detect responsible pathogens nor contagiousness of disease via direct contact. Consequently, I hypothesize, as Lesser *et al.* (2007) did it for bleached corals, that Sponge Orange Band- as well as Sponge White Patch disease are opportunistic infections secondary to physiological stress. Long-term monitoring data would be appreciated that help to elucidate the environmental parameters acting as stressors during the emergence of sponge disease.

	Sponge Orange Band disease of *Xestospongia muta*	Sponge White Patch disease of *Amphimedon compressa*
Bleaching & Tissue destruction	+	+
Phagocytosis by sponge cells	+	-
Degradation & Loss of cyanobacteria	+	-
Degradation & Loss of sponge cells	+	+
Microbial community shift	+	+
Shift predates the bleaching event	+	-
Invasion of disease related strains	+	+
Evidence for a bacterial pathogen	-	-
Contagiousness of disease	-	-
High abundance of disease	-	+
Recovery from disease	-	+

Tab. 7. A comparison of the characteristics underlying Sponge Orange Band- as well as Sponge White Patch disease as discovered in this study.

VI. Outlook

After thorough molecular and ecological investigations on Sponge Orange Band- as well as Sponge White Patch disease, just few more aspects can be directed to in future research:

- To investigate diligently the early window of infection during sponge disease.

- To isolate and cultivate the ubiquitious spongin-boring strain present within the white *A. compressa* tissues as well as to perform whole-genome-sequencing and specific FISH-probe design to estimate its function during progression of Sponge White Patch disease.

- To tackle the innate immunity, host cell phagocytosis and overall stress response of HMA- versus LMA-sponges involved during disease via TEM as well as apoptosis and necrosis testing applying the tunnel assay on paraffin sections.

- To elucidate the ambient anthropogenic and environmental factors of sponge disease.

- To characterize emerging sponge diseases via combined efforts of marine scientists covering diverse research areas such as ecology, physiology, microbiology, toxicology as well as oceanography. Altogether we might have a chance to understand, what endangers our oceans, and to protect their biodiversity over the long term.

VII. References

Alonso-Gutierrez J., Figueras A., Albaiges J., Jimenez N., Vinas M., Solanas A.M., and Novoa B. (2009) Bacterial communities from shoreline environments (costa da morte, northwestern Spain) affected by the prestige oil spill. *Appl Environ Microbiol* **75:** 3407-3418.

Amann R.I., Ludwig W., and Schleifer K.H. (1995) Phylogenetic identification and in situ detection of individual microbial cells without cultivation. *Microbiol Rev* **59:** 143-169.

Angermeier H., Kamke J., Abdelmohsen U.R., Krohne G., Pawlik J.R., Lindquist N.L., and Hentschel U. (2011) The pathology of sponge orange band disease affecting the Caribbean barrel sponge *Xestospongia muta*. *FEMS Microbiol Ecol* **75:** 218-230.

Armstrong R.A., Singhb H., Torres J., Nemeth R.S., Can A., Roman C. *et al.* (2006) Characterizing the deep insular shelf coral reef habitat of the Hind Bank marine conservation district (US Virgin Islands) using the seabed autonomous underwater vehicle. *Continental Shelf Research* **26:** 194-205.

Arotsker L., Siboni N., Ben-Dov E., Kramarsky-Winter E., Loya Y., and Kushmaro A. (2009) *Vibrio* sp. as a potentially important member of the Black Band Disease (BBD) consortium in *Favia* sp. corals. *FEMS Microbiol Ecol* **70:** 515-524.

Ashelford K.E., Chuzhanova N.A., Fry J.C., Jones A.J., and Weightmann A.J. (2005) At least 1 in 20 16S rRNA sequence records currently held in public repositories is estimated to contain substantial anomalies. *Appl Environ Microbiol* **71:** 7724-7736.

Bakus G.J., Targett N.M., and Schulte B. (1986) Chemical ecology of marine organisms: an overview. *J Chem Ecol* **12:** 951-987.

Bandaranayake W.M., Bemis J.E., and Bourne D.J. (1996) Ultraviolet absorbing pigments from the marine sponge *Dysidea herbacea*: isolation and structure of a new mycosporine. *Comp Biochem Phys C* **115:** 281-286.

Barneah O., Ben-Dov E., Kramarsky-Winter E., and Kushmaro A. (2007) Characterization of black band disease in Red Sea stony corals. *Environ Microbiol* **9:** 1995-2006.

Bayer K., Schmitt S., and Hentschel U. (2008) Physiology, phylogeny and in situ evidence for bacterial and archaeal nitrifiers in the marine sponge *Aplysina aerophoba*. *Environ Microbiol*. **10 (11):** 2942-55.

Becker P.T., Egea E., and Eeckhaut I. (2008) Characterization of the bacterial communities associated with the bald sea urchin disease of the echinoid *Paracentrotus lividus*. *J Invertebr Pathol* **98:** 136-147.

Becker P.T., Gillan D.C., and Eeckhaut I. (2009) Characterization of the bacterial community associated with body wall lesions of *Tripneustes gratilla* (Echinoidea) using culture-independent methods. *J Invertebr Pathol* **100:** 127-130.

Bergquist P.R. (1978) In *Sponges*. University of California Press, Berkeley.

Bergquist P.R. (1985) In *The origins and relationships of lower invertebrates.* The Systematics Association, Clarendon, Oxford.

Bewley C.A., Holland N.D., and Faulkner D.J. (1996) Two classes of metabolites from *Theonella swinhoei* are localized in distinct populations of bacterial symbionts. *Experientia* **52:** 716-722.

Böhm M., Schröder H.C., Müller I.M., Müller W.E., and Gamulin V. (2000) The mitogen-activated protein kinase p38 pathway is conserved in metazoans: cloning and activation of p38 of the SAPK2 subfamily from the sponge *Suberites domuncula*. *Biol Cell* **92:** 95-104.

Bourne D., Iida Y., Uthicke S., and Smith-Keune C. (2008) Changes in coral-associated microbial communities during a bleaching event. *ISME J* **2:** 350-363.

Brusca R.C., and Brusca G.J. (1990) Phylum Porifera: the sponges. Sinauer Press, Sunderland, MA.

Butler M.J., Hunt J.H., Herrnkind W.F., Childress M.J., Bertelsen R., Sharp W. *et al.* (1995) Cascading disturbances in Florida Bay, USA: cyanobacteria blooms, sponge mortality and implications for juvenile spiny lobsters *Panulirus argus*. *Marine Ecology Progress Series* **129:** 119-125.

Cerrano C., Bavestrello G., Bianchi C.N., Cattaneovietti R., Bava S., Morganti C., *et al.* (2000) A catastrophic mass-mortality episode of gorgonians and other organisms in the Ligurian Sea (North-Western Mediterranean), summer 1999. *Ecol Lett* **3:** 284-293.

Cervino J.M., Winiarski-Cervino K., Polson S.W., Goreau T., and Smith G.W. (2006) Identification of bacteria associated with a disease affecting the marine sponge *Ianthella basta*. New Britain, Papua New Guinea. *Mar Ecol Prog Ser* **324:** 139-150.

Collette B.B., and Rützler K. (1977) Reef fishes over sponge bottom off the mouth of the Amazon River. *Proc Third int Coral Reef Symp*: 305-310.

Cooney R.P., Pantos O., Le Tissier M.D., Barer M.R., O'Donnell A.G., and Bythell J.C. (2002) Characterization of the bacterial consortium associated with black band disease in coral using molecular microbiological techniques. *Environ Microbiol* **4:** 401-413.

Cowart J.D., Henkel T.P., McMurray S.E., and Pawlik J.R. (2006) Sponge orange band (SOB): a pathogenic-like condition of the giant barrel sponge, *Xestospongia muta*. *Coral Reefs* **25:** 513.

Cytryn E., Minz D., Gieseke A., and van Rijn J. (2006) Transient development of filamentous *Thiothrix* species in a marine sulfide oxidizing, denitrifying fluidized bed reactor. *FEMS Microbiol Lett* **256:** 22-29.

de Bary A. (1879) Die Erscheinung der Symbiose. In *Tagebl Naturforschung*. Versammlung Cassel, LI.

Dunn S.R., Thomason J.C., Le Tissier M.D., and Bythell J.C. (2004) Heat stress induces different forms of cell death in sea anemones and their endosymbiotic algae depending on temperature and duration. *Cell Death Differ* **11:** 1213-1222.

Duque C., Martinez A., and Penuela G. (1985) Composición esterólica de la esponja marina *Xestospongia muta*. *Rev Colomb Quim* **14:** 81-88.

Enticknap J.J., Kelly M., Peraud O., and Hill R.T. (2006) Characterization of a culturable alphaproteobacterial symbiont common to many marine sponges and evidence for vertical transmission via sponge larvae. *Appl Environ Microbiol* **72**: 3724-3732.

Ereskovsky A.V., Gonobobleva E., and Vishnyakov A. (2005) Morphological evidence for vertical transmission of symbiotic bacteria in the vivaparous sponge *Halisarca dujardini* Johnston (Porifera, Demospongiae, Halisarcida). *Mar Biol* **146:** 869-875.

Erwin P.M., and Thacker R.W. (2008) Cryptic diversity of the symbiotic cyanobacterium *Synechococcus spongiarum* among sponge hosts. *Mol Ecol* **17:** 2937-2947.

Fieseler L., Horn M., Wagner M., and Hentschel U. (2004) Discovery of the novel candidate phylum "Poribacteria" in marine sponges. *Appl Environ Microbiol* **70:** 3724-3732.

Frias-Lopez J., Zerkle A.L., Bonheyo G.T., and Fouke B.W. (2002) Partitioning of bacterial communities between seawater and healthy, black band diseased, and dead coral surfaces. *Appl Environ Microbiol* **68:** 2214-2228.

Friedrich A.B., Fischer I., Proksch P., Hacker J., and Hentschel U. (2001) Temporal variation of the microbial community associated with the Mediterranean sponge *Aplysina aerophoba*. *FEMS Microbiol Ecol* **38:** 105-113.

Friedrich A.B., Merkert H., Fendert T., Hacker J., Proksch P., and Hentschel U. (1999) Microbial diversity in the marine sponge *Aplysina cavernicola* (formerly *Verongia cavernicola*) analyzed by fluorescence in situ hybridization (FISH). *Mar Biol* **134:** 461-470.

Frost T.M. (1978) In situ measurement of clearance rates for the freshwater sponge *Spongilla lacustris*. *Limnol Oceanogr* **23:** 1034-1039.

Gaino E., and Pronzato R. (1989) Ultrastructural evidence of bacterial damage to *Spongia officinalis* fibres (Porifera, Demospongiae). *Dis Aquat Organ* **6:** 67-74.

Gaino E., Pronzato R., Corriero G., and Buffa P. (1992) Mortality of commercial sponges: incidence in two Mediterranean areas. *Bolletino di Zool, publicato dall'unione zool Italiano* **59:** 79-85.

Galstoff P.S. (1942) Wasting disease causing mortality of sponges in the West Indies and Gulf of Mexico. *Proc VIII American Science Congress* **3:** 411-421.

Gammill E.R., and Fenner D. (2005). In *Disease threatens Caribbean sponges: report and identification guide.* http://www.reefbase.org/spongedisease.

Garson M.J., Flowers A.E., Webb R.I., Charan R.D., and McCafferty E.J. (1998) A sponge/dinoflagellate association in the haplosclerid sponge *Haliclona* sp.: cellular origin of cytotoxic alkaloids by Percoll density gradient fractionation. *Cell Tissue* **293:** 365-373.

Gil-Agudelo D.L., Myers C., Smith G.W., and Kim K. (2006) Changes in the microbial communities associated with *Gorgonia ventalina* during aspergillosis infection. *Dis Aquat Organ* **69:** 89-94.

Giovannoni S.J., and Rappe M.S. (2000) In *Evolution, diversity and molecular ecology of marine prokaryotes.* Wiley, New York.

Goh F., Allen M.A., Leuko S., Kawaguchi T., Decho A.W., Burns B.P., and Neilan B.A. (2009) Determining the specific microbial populations and their spatial distribution within the stromatolite ecosystem of Shark Bay. *ISME J* **3:** 383-396.

Hadas E., Marie D., Shpigel M., and Ilan M. (2006) Virus predation by sponges is a new nutrient-flow pathway in coral reef food webs. *Limnol Oceanogr* **51 (3):** 1548–1550.

Hagstrom A., Pommier T., Rohwer F., Simu K., Stolte W., Svensson D., and Zweifel U.L. (2002) Use of 16S ribosomal DNA for delineation of marine bacterioplankton species. *Appl Environ Microbiol* **68:** 3628-3633.

Harvell C.D., Kim K., Burkholder J.M., Colwell R.R., Epstein P.R., Grimes D.J. *et al.* (1999) Emerging marine diseases - climate links and anthropogenic factors. *Science* **285:** 1505-1510.

Haygood M.G., Schmidt E.W., Davidson S.K., and Faulkner D.J. (1999) Microbial symbionts of marine invertebrates: opportunities for microbial biotechnology. *J Mol Microbiol Biotechnol* **1:** 33-43.

Hentschel U., Usher K.M., and Taylor M.W. (2006) Marine sponges as microbial fermenters. *FEMS Microbiol Ecol* **55:** 167-177.

Hentschel U., Schmid M., Wagner M., Fieseler L., Gernert C., and Hacker J. (2001) Isolation and phylogenetic analysis of bacteria with antimicrobial activities from the Mediterranean sponges *Aplysina aerophoba* and *Aplysina cavernicola*. *FEMS Microbiol Ecol* **35:** 305-312.

Hentschel U., Hopke J., Horn M., Friedrich A.B., Wagner M., Hacker J., and Moore B.S. (2002) Molecular evidence for a uniform microbial community in sponges from different oceans. *Appl Environ Microbiol* **68:** 4431-4440.

Hentschel U., Fieseler L., Wehrl M., Gernert C., Steinert M., Hacker J., and Horn M. (2003) Microbial diversity of marine sponges. *Prog Mol Subcell Biol* **37:** 59-88.

Hepperle D. (2002) Align: a multicolor sequence alignment editor. http://science.do-mix.de/software.phd.

Hill R.T. (2004) Microbes from marine sponges: a treasure trove of biodiversity for natural products discovery. In *Microbial Diversity and Bioprospecting*. Bull, A.T. (ed). Washington, DC: ASM Press, pp. 177-190.

Hoegh-Guldberg O., Mumby P.J., Hooten A.J., Steneck R.S., Greenfield P., Gomez E. *et al.* (2007) Coral reefs under rapid climate change and ocean acidification. *Science* **318:** 1737-1742.

Holden C. (2010) Reefs of the Future. In *Science: Random Samples*, p. 253.

Hooper J.N.A., and van Soest R.W.M. (2002) In *Systema Porifera. A guide to the classification of sponges.* New York, NY.

Hughes T.P., Baird A.H., Bellwood D.R., Card M., Connolly S.R., Folke C. *et al.* (2003) Climate change, human impacts, and the resilience of coral reefs. *Science* **301:** 929-933.

Humann P. (1992) In *Reef creature identification*. Jacksonville, Florida: New World Publications, Incorporation.

Imsiecke G. (1993) Ingestion, digestion, and egestion in *Spongilla lacustris* (Porifera, Spongillidae) after pulse feeding with *Chlamydomonas reinhardtii* (Volvocales). *Zoomorphology* **113:** 233-244.

Jung M. (1996) In *Das Handbuch des Tauchsports.* Bielefeld.

Kefalas E., Castritsi-Catharios J., and Miliou H. (2003) Bacteria associated with the sponge *Spongia officinalis* as indicators of contamination. *Ecological Indicators*: 339-343.

Kim K., and Harvell C.D. (2002) Aspergillosis of sea fan corals: disease dynamics in the Florida Keys. In *The Everglades, Florida Bay, and Coral Reefs of the Florida Keys: An Ecosystem Sourcebook*. Porter, J.W., and Porter, K.G. (eds). Boca Raton, FL, USA: CRC Press, pp. 813-824.

Klaus J.S., Janse I., Heikoop J.M., Sanford R.A., and Fouke B.W. (2007) Coral microbial communities, zooxanthellae and mucus along gradients of seawater depth and coastal pollution. *Environ Microbiol* **9:** 1291-1305.

Koren O., and Rosenberg E. (2008) Bacteria associated with the bleached and cave coral *Oculina patagonica*. *Microb Ecol* **55:** 523-529.

Kowalke J. (2000) Ecology and energetics of two Antarctic sponges. *J Exp Mar Biol Ecol* **247:** 85-97.

Kubanek J., Whalen K.E., Engel S., Kelly S.R., Henkel T.-P., Fenical W., and Pawlik J.R. (2002) Multiple defensive roles for triterpene glycosides from two Caribbean sponges. *Oecologia* **131:** 125-136.

Lee O.O., Wang Y., Yang J., Lafi F.F., Al-Suwailem A., and Qian P.Y. (2011) Pyrosequencing reveals highly diverse and species-specific microbial communities in sponges from the Red Sea. *ISME J* **5:** 650-664.

Lemke M.J., and Leff L.G. (1999) Bacterial populations in an anthropogenically disturbed stream: Comparison of different seasons. *Microb Ecol* **38:** 234-243.

Lesser M.P., Bythell J.C., Gates R.D., Johnstone R.W., and Hoegh-Guldberg O. (2007) Are infectious diseases really killing corals? Alternative interpretations of the experimental and ecological data. *Journal of Experimental Marine Biology and Ecology* **346:** 36-44.

Lévi C. (1970) Biology of the *Porifera. Symp Zool Soc Lond Edn* **25:** 353-364.

Li C.W., Chen J.Y., and Hua T.E. (1998) Precambrian sponges with cellular structures. *Science* **279:** 879-882.

Li L.N., Sjöstrand U., and Djerassi C. (1981) Minor and trace sterols in marine invertebrates. 19. Isolation, structure elucidation and partial synthesis of 24-methylene-25-ethylcholesterol (Mutasterol): first example of sterol side-chain bioalkylation at position 25. *J Am Chem Soc* **103:** 115-119.

Lopez-Legentil S., Song B., McMurray S.E., and Pawlik J.R. (2008) Bleaching and stress in coral reef ecosystems: hsp70 expression by the giant barrel sponge *Xestospongia muta*. *Mol Ecol* **17:** 1840-1849.

Ludwig W., Strunk O., Westram R., Richter L., Meier H., Yadhukumar *et al.* (2004) ARB: a software environment for sequence data. *Nucl Acids Res* **32:** 1363-1371.

Luter H.M., Whalan S., and Webster N.S. (2010) Exploring the role of microorganisms in the disease-like syndrome affecting the sponge *Ianthella basta*. *Appl Environ Microbiol* **76:** 5736-5744.

Maldonado M., Sánchez-Tocino L., and Navarro C. (2010) Recurrent disease outbreaks in corneous demosponges of the genus *Ircinia*: epidemic incidence and defense mechanisms. *Marine Biology* **157 (7):** 1577-1590.

Mao-Jones J., Ritchie K.B., Jones L.E., and Ellner S.P. (2010) How microbial community composition regulates coral disease development. *PLoS Biol* **8 (3):** e1000345.

McMurray S.E., Blum J.E., and Pawlik J.R. (2008) Redwood of the reef: growth and age of the giant barrel sponge *Xestospongia muta* in the Florida Keys. *Mar Biol* **155:** 159-171.

McMurray S.E., Henkel T.P., and Pawlik J.R. (2010) Demographics of increasing populations of the giant barrel sponge *Xestospongia muta* in the Florida Keys. *Ecology* **91:** 560-570.

Mincer T.J., Jensen P.R., Kauffman C.A., and Fenical W. (2002) Widespread and persistent populations of a major new marine actinomycete taxon in ocean sediments. *Appl Environ Microbiol* **68:** 5005-5011.

Morinaka B.I., Skepper C.K., and Molinski T.F. (2007) Ene-yne tetrahydrofurans from the sponge *Xestospongia muta*. Exploiting a weak CD effect for assignment of configuration. *Org Lett* **9:** 1975-1978.

Müller W.E., Böhm M., Grebenjuk V.A., Skorokhod A., Müller I.M., and Gamulin V. (2002) Conservation of the positions of metazoan introns from sponges to humans. *Gene* **295:** 299-309.

Müller W.E.G. (1998) Molecular phylogeny of eumetazoa: genes in sponges (*Porifera*) give evidence for the monophyly of animals. *Progr Mol Subcell Biol* **9:** 89-126.

Muyzer G., Brinkhoff T., Nübel U., Santegoeds C., Schäfer H., and Wawer C. (1998) In *Denaturing gradient gel electrophoresis (DGGE) in microbial ecology*. Dordrecht, The Netherlands: Klower.

Myers J.L., Sekar R., and Richardson L.L. (2007) Molecular detection and ecological significance of the cyanobacterial genera *Geitlerinema* and *Leptolyngbya* in black band disease of corals. *Appl Environ Microbiol* **73:** 5173-5182.

Nagelkerken I., Aerts L., and Pors L. (2000) Barrel sponge bows out. *Reef Encounter* **28:** 14-15.

Norström A.V., Nyström M., Lokrantz J., and Folke C. (2009) Alternative states on coral reefs: beyond coral-macroalgal phase shifts. *Marine Ecology Progress Series* **376:** 295–306.

Nübel U., Garcia-Pichel F., and Muyzer G. (1997) PCR primers to amplify 16S rRNA genes from cyanobacteria. *Appl Environ Microbiol* **63:** 3327-3332.

Olson J.B., Gochfeld D.J., and Slattery M. (2006) Aplysina red band syndrome: a new threat to Caribbean sponges. *Dis Aquat Organ* **71:** 163-168.

Pantos O., Cooney R.P., Le Tissier M.D., Barer M.R., O'Donnell A.G., and Bythell J.C. (2003) The bacterial ecology of a plague-like disease affecting the Caribbean coral *Montastrea annularis*. *Environ Microbiol* **5:** 370-382.

Parsons T.R., Maita Y., and Lalli C. (1984) In *A manual of chemical and biological methods for seawater analysis.* New York: Pergamon Press.

Patil A.D., Kokke W.C., Cochran S., Francis T.A., Tomszek T., and Westley J.W. (1992) Brominated polyacetylenic acids from the marine sponge *Xestospongia muta*: inhibitors of HIV protease. *J Nat Prod* **55:** 1170-1177.

Paz M. (1996) New killer disease attacks giant barrel sponge. In *The San Pedro Sun*.

Perez T., Perrin B., Carteron S., Vacelet J., and Boury-Esnault N. (2006) *Celtodoryx morbihanensis* gen. nov. sp. nov., a new sponge species (Poecilosclerida, Demospongiae) invading the Gulf of Morbihan (NE Atlantic-France). *Cah Biol Mar* **47:** 205-214.

Perez T., Garrabou J., Sartoretto S., Harmelin J.G., Francour P., and Vacelet J. (2000) Mortalité massive d'invertébrés marins: un événement sans précédent en Méditerranée nord-occidentale. *C R Acad Sci III* **323:** 853-865.

Pile A.J. (1997) Finding Reiswig's missing carbon: quantification of sponge feeding using dual-beam flow cytometry. In *Proceedings of the 8th International Coral Reef Symposium*, pp. 1403-1410.

Pile A.J., Patterson M.R., and Witman J.D. (1996) *In situ* grazing on plankton < 10µm by the boreal sponge *Mycale lingua*. *Mar Ecol Prog Ser* **141:** 95-102.

Pruesse E., Quast C., Knittel K., Fuchs B.M., Ludwig W., Peplies J., and Glöckner F.O. (2007) SILVA: a comprehensive online resource for quality checked and aligned ribosomal RNA sequence data compatible with ARB. *Nucleic Acids Res* **35:** 7188-7196.

Rai A.N. (1990) In CRC Handbook of symbiotic cyanobacteria. Press, C. (ed). Boca Raton, Florida.

Rappe M.S., and Giovannoni S.J. (2003) The uncultured microbial majority. *Annu Rev Microbiol* **57:** 369-394.

Reiswig H.M. (1971) Particle feeding in natural populations of three marine demosponges. *Biological Bulletin* **141:** 568-591.

Reiswig H.M. (1975) Bacteria as food for temperate-water marine sponges. *Can J Zool* **53:** 582-589.

Reiswig H.M. (1990) *In situ feeding in 2 shallow-water hexactinellid sponges.* Smithonian Institution Press, Washington, DC, USA.

Ribes M., Coma R., and Gili J.M. (1999) Natural diet and grazing rate of the temperate sponge *Dysidea avara* (Demospongiae, Dendroceratida) throughout an annual cycle. *Mar Ecol Prog Ser* **176:** 179-190.

Rosenberg E., and Loya Y. (2004) In *Coral Health and Disease*: Springer Verlag, Berlin-Heidelberg.

Rosenberg E., Koren O., Reshef L., Efrony R., and Zilber-Rosenberg I. (2007) The role of microorganisms in coral health, disease and evolution. *Nat Rev Microbiol* **5:** 355-362.

Ruppert E.E., Fox R.S., and Barnes R.D. (2004) In *Invertebrate Zoology: A functional evolutionary approach. Chapter 5: Porifera and Placozoa.* Brooks/Cole.

Rützler K. (1985) In *Associations between Caribbean sponges and photosynthetic organisms.* Smithsonian Institution Press, Washington, DC, USA.

Rützler K. (1988) Mangrove sponge disease induced by cyanobacterial symbionts: failure of a primitive immune system? *Dis Aquat Organ* **5:** 143-149.

Rypien K.L., Ward J.R., and Azam F. (2010) Antagonistic interactions among coral-associated bacteria. *Environ Microbiol* **12:** 28-39.

Sambrook J., Frischt E.F., and Maniatis T. (1989) In *Molecular cloning: A Laboratory Manual*. Cold Spring Harbor Laboratory Press, New York, NY, USA.

Santavy D.L., Willenz P., and Colwell R.R. (1990) Phenotypic study of bacteria associated with the Caribbean sclerosponge, *Ceratoporella nicholsoni*. *Appl Environ Microbiol* **56:** 1750-1762.

Sara M. (1971) Ultrastructural aspects of the symbiosis between two species of the genus *Aphanocapsa* (Cyanophyceae) and *Ircinia variabilis* (Demospongiae). *Mar Biol* **11:** 214-221.

Schmahl G.P. (1985) In *Community structure and ecology of sponges associated with four southern Florida coral reefs.* Smithsonian Institution Press, Washington, DC, USA.

Schmitt S., Weisz J.B., Lindquist N., and Hentschel U. (2007) Vertical transmission of a phylogenetically complex microbial consortium in the viviparous sponge *Ircinia felix*. *Appl Environ Microbiol* **73:** 2067-2078.

Schmitt S., Angermeier H., Schiller R., Lindquist N., and Hentschel U. (2008) Molecular microbial diversity survey of sponge reproductive stages and mechanistic insights into vertical transmission of microbial symbionts. *Appl Environ Microbiol* **74:** 7694-7708.

Sekar R., Kaczmarsky L.T., and Richardson L.L. (2008) Microbial community composition of black band disease on the coral host *Siderastrea siderea* from three regions of the wider Caribbean. *Mar Ecol Prog Ser* **362:** 85-98.

Sekar R., Mills D.K., Remily E.R., Voss J.D., and Richardson L.L. (2006) Microbial communities in the surface mucopolysaccharide layer and the black band microbial mat of black band-diseased *Siderastrea siderea*. *Appl Environ Microbiol* **72:** 5963-5973.

Sharp K.H., Eam B., Faulkner D.J., and Haygood M.G. (2007) Vertical transmission of diverse microbes in the tropical sponge *Corticium* sp. *Appl Environ Microbiol* **73:** 622-629.

Shick J.M., and Dunlap W.C. (2002) Mycosporine-like amino acids and related Gadusols: biosynthesis, acumulation, and UV-protective functions in aquatic organisms. *Annu Rev Physiol* **64:** 223-262.

Siegl A. (2009) In *Einzelzell-basierte Methoden zur Charakterisierung Schwamm-assoziierter Bakterien*. University of Würzburg, Würzburg, Germany.

Simpson T.L. (1984) In *The cell biology of sponges.* Springer-Verlag, New York, USA.

Soest R.W.M. van (1980) Marine sponges from Curaçao and other Caribbean localities. Part II. Haplosclerida. *Stud Fauna Curaçao Caribb Isl* **62:** 1-173.

Steffens S. (2003) In *Prokaryoten und mikrobielle Eukaryoten aus marinen Schwämmen*. Mathematisch-Naturwissenschaftliche Fakultät, Rheinische Friedrich-Wilhelms-Universität Bonn, Bonn, Germany.

Steindler L., Huchon D., Avni A., and Ilan M. (2005) 16S rRNA phylogeny of sponge-associated cyanobacteria. *Appl Environ Microbiol* **71:** 4127-4131.

Sunagawa S., DeSantis T.Z., Piceno Y.M., Brodie E.L., DeSalvo M.K., Voolstra C.R. *et al.* (2009) Bacterial diversity and White Plague Disease-associated community changes in the Caribbean coral *Montastraea faveolata*. *ISME J* **3:** 512-521.

Sutherland K.P., Porter J.W., and Torres C. (2004) Disease and immunity in Caribbean and Indo-Pacific zooxanthellate corals. *Mar Ecol Prog Ser* **266:** 273–302.

Taylor M.W., Thacker R.W., and Hentschel U. (2007a) Genetics. Evolutionary insights from sponges. *Science* **316:** 1854-1855.

Taylor M.W., Radax R., Steger D., and Wagner M. (2007b) Sponge-associated microorganisms: evolution, ecology, and biotechnological potential. *Microbiol Mol Biol Rev* **71:** 295-347.

Thacker R. (2005) Impacts of shading on sponge-cyanobacteria symbioses: a comparison between host-specific and generalist associations. *Integr Comp Biol* **45:** 369–376.

Thompson F.L., Hoste B., Vandemeulebroecke K., and Swings J. (2001) Genomic diversity amongst *Vibrio* isolates from different sources determined by fluorescent amplified fragment length polymorphism. *Syst Appl Microbiol* **24:** 520-538.

Thompson M.N., Gallimore W.A., Townsend M.M., Chambers N.A., and Williams L.A. (2010) Bioactivity of amphitoxin, the major constituent of the Jamaican sponge *Amphimedon compressa*. *Chem Biodivers* 7: 1904-1910.

Tracy C.R., Streten-Joyce C., Dalton R., Nussear K.E., Gibb K.S., and Christian K.A. (2010) Microclimate and limits to photosynthesis in a diverse community of hypolithic cyanobacteria in northern Australia. *Environ Microbiol* **12:** 592-607.

Unson M.D., Holland N.D., and Faulkner D.J. (1994) A brominated secondary metabolite synthesized by the cyanobacterial symbiont of a marine sponge and accumulation of the crystalline metabolite in the sponge tissue. *Mar Biol* **119:** 1-11.

Uriz M.J., Becerro M.A., Tur J.M., and Tortion X. (1996) Location of toxicity within the Mediterranean sponge *Crambe crambe* (Demospongiae, Poecilosclerida). *Mar Biol* **124:** 583-590.

Usher K.M. (2008) The ecology and phylogeny of cyanobacterial symbionts in sponges. *Marine Ecology* **29:** 178-192.

Usher K.M., Kuo J., Fromont J., and Sutton D.C. (2001) Vertical transmission of cyanobacterial symbionts in the marine sponge *Chondrilla nucula* (Demospongiae). *Hydrobiologica* **461 (1):** 15-23.

Vacelet J. (1970) Description de cellules a bactéries intranucléaires chez des éponges Verongia. *J Microsc* **9:** 333-346.

Vacelet J. (1971) Étude en microscopie électronique de l'association entre une cyanophycée chroococcale et une éponge du genre Verongia. *J Microsc* **12:** 363-380.

Vacelet J. (1975) Étude en microscopie électronique de l'association entre bactéries et spongiaires du genre Verongia (Dictyoceratida). *J Microsc Biol Cell* **23:** 271-288.

Vacelet J., and Donadey C. (1977) Electron microscope study of the association between some sponges and bacteria. *J Exp Mar Ecol* **30:** 301-314.

Vacelet J., and Gallissian M.-F. (1978) Virus-like particles in cells of the sponge *Verongia cavernicola* (Demospongiae, Dictyoceratida) and accompanying tissue changes. *Journal of Invertebrate Pathology* **31 (2):** 246-254.

Vacelet J., Vacelet E., Gaino E., and Gallissian M.-F. (1994) In *Bacterial attack of spongin skeleton during the 1986-1990 Mediterranean sponge disease.* A.A. Balkema, Rotterdam, the Netherlands.

Vicente V.P. (1990) Responses of sponges with autotrophic endosymbionts during the coral-bleaching episode in Puerto Rico (West Indies). *Coral Reefs* **8:** 199-202.

Wagner M., and Horn M. (2006) The *Planctomycetes*, *Verrucomicrobia*, *Chlamydiae* and sister phyla comprise a superphylum with biotechnological and medical relevance. *Curr Opin Biotechnol* **17:** 241-249.

Walters K.D., and Pawlik J.R. (2005) Is there a trade-off between wound-healing and chemical defenses among Caribbean reef sponges? *Integrative and Comparative Biology* **45:** 352-358.

Webster N.S. (2007) Sponge disease: a global threat? *Environ Microbiol* **9:** 1363-1375.

Webster N.S., and Hill R.T. (2001) The culturable microbial community of the Great Barrier Reef sponge *Rhopaloeides odorabile* is dominated by an α-Proteobacterium. *Mar Biol* **138 (4):** 843-851.

Webster N.S., Cobb R.E., and Negri A.P. (2008) Temperature thresholds for bacterial symbiosis with a sponge. *ISME J* **2:** 830-842.

Webster N.S., Wilson K.J., Blackall L.L., and Hill R.T. (2001a) Phylogenetic diversity of bacteria associated with the marine sponge *Rhopaloeides odorabile*. *Appl Environ Microbiol* **67:** 434-444.

Webster N.S., Negri A.P., Webb R.I., and Hill R.T. (2002) A spongin-boring α-proteobacterium is the etiological agent of disease in the Great Barrier Reef sponge *Rhopaloeides odorabile*. *Marine Ecology Progress Series* **232:** 305-309.

Webster N.S., Webb R.I., Ridd M.J., Hill R.T., and Negri A.P. (2001b) The effects of copper on the microbial community of a coral reef sponge. *Environ Microbiol* **3:** 19-31.

Webster N.S., Xavier J.R., Freckelton M., Motti C.A., and Cobb R. (2008a) Shifts in microbial and chemical patterns within the marine sponge *Aplysina aerophoba* during a disease outbreak. *Environ Microbiol* **10:** 3366-3376.

Webster N.S., Taylor M.W., Behnam F., Lucker S., Rattei T., Whalan S. *et al.* (2009) Deep sequencing reveals exceptional diversity and modes of transmission for bacterial sponge symbionts. *Environ Microbiol* **12 (8):** 2070–2082.

Wehner R., and Gehring W. (1995) In *Zoologie.* Thieme Verlag, Stuttgart, New York.

Wehrl M. (2006) In *Bakterielle Aufnahme, Selektivität und interne Prozessierung bei marinen Schwämmen (Porifera)*, Universität Würzburg, Würzburg, Germany.

Wehrl M., Steinert M., and Hentschel U. (2007) Bacterial uptake by the marine sponge *Aplysina aerophoba*. *Microb Ecol* **53:** 355-365.

Weis V.M. (2008) Cellular mechanisms of Cnidarian bleaching: stress causes the collapse of symbiosis. *J Exp Biol* **211:** 3059-3066.

Weisz J.B., Lindquist N., and Martens C.S. (2008) Do associated microbial abundances impact marine demosponge pumping rates and tissue densities? *Oecologia* **155:** 367-376.

Whiteman E. (2010) A fatal switch for corals? *PLoS Biol* **8 (3):** e1000346.

Wilkinson C.R. (1978) Microbial associations in sponges. I. Ecology, physiology and microbial populations of coral reef sponges. *Mar Biol* **49:** 161-167.

Wilkinson C.R. (1983) Net primary productivity in coral reef sponges. *Science* **219:** 410-412.

Wilkinson C.R. (1987) Interocean differences in size and nutrition of coral reef sponge populations. *Science* **236:** 1654-1657.

Wilkinson C.R. (1992) In *Symbiotic interactions between marine sponges and algae*. Biopress, Bristol, UK.

Wilkinson C.R., and Fay P. (1979) Nitrogen fixation in coral reef sponges with symbiotic cyanobacteria. *Nature* **279:** 527-529.

Wilkinson C.R., and Garrone R. (1980) In *Nutrition of marine sponges. Involvement of symbiotic bacteria in the uptake of dissolved carbon.* Pergamon Press, Oxford, UK.

Wilkinson C.R., Garrone R., and Herbage D. (1979) In *Sponge collagen degradation in vitro by sponge-specific bacteria*. CNRS, Paris, France.

Wilkinson C.R., Nowak M., Austin B., and Colwell R.R. (1981) Specificity of bacterial symbionts in Mediterranean and Great Barrier Reef sponges. *Microb Ecol* **7:** 13-21.

Wilkinson C.R., Cheshire A.C., Klumpp D.W., and McKinnon A.D. (1988) Nutritional spectrum of animals with photosynthetic symbionts-corals and sponges. *Proc 6th Internat Coral Reef Symp, Australia* **3:** 27-30.

Willenz P.B., and Van de Vyver G. (1984) Ultrastructural localization of lysosomal digestion in the fresh water sponge *Ephydatia fluviatilis*. *J Ultrastruct Res* **87:** 13-22.

Willmer P. (1990) In *Invertebrate Relationships.* Cambridge University Press, Cambridge, UK.

Wulff J.L. (2006) A simple model of growth form-dependent recovery from disease in coral reef sponges, and implications for monitoring. *Coral Reefs* **25 (3):** 419-426.

Yahel G., Sharp J.H., Marie D., Hase C., and Genin A. (2003) In situ feeding and element removal in the symbiont-bearing sponge *Theonella swinhoei*: bulk DOC is the major source for carbon. *Limnol Oceanogr* **48:** 141-149.

Zea S., Henkel T.P., and Pawlik J.R. (2009) In The Sponge Guide: a picture guide to Caribbean sponges.: http://www.spongeguide.org.

Zhu P., Li Q., and Wang G. (2008) Unique microbial signatures of the alien Hawaiian marine sponge *Suberites zeteki*. *Microb Ecol* **55:** 406-414.

VIII. Annex

1. **Tables 1 to 7:** pictured on the following pages.

Tab. 1: Healthy (n=17) and diseased (n=11) *X. muta* individuals applied to the study of Sponge Orange Band disease.

Tab. 2: Cell counts of healthy (n=4) and Sponge Orange Band diseased (n=1) *X. muta* tissues with a focus on their different surface colorations (brown, orange, white) regarding their amount of sponge cell nuclei, extracellular and intracellular cyanobacteria as well as their ratio and the total amount of cyanobacteria per gram sponge within dilutions of 10^{-3}.

Tab. 3: 16S rRNA gene sequence analysis of the 31 excised bands from the cyanobacterial DGGE gel in Fig. 31a.

Tab. 4: 16S rRNA gene sequence analysis of the 61 excised bands from the cyanobacterial DGGE gel in Fig. 32a.

Tab. 5: Chlorophyll *a* concentration within the surface tissues of healthy (n=9) and Sponge Orange Band diseased (n=3) *X. muta* individuals as listed by tissue coloration.

Tab. 6: *X. muta* individuals used as donor and recipient sponges within the underwater infection experiments at Conch Reef, Florida, in September 2009.

Tab. 7: Healthy (n=538) and diseased (n=171) *A. compressa* individuals applied to the study of Sponge White Patch disease.

Individuals	Tissue coloration	Estimated stage of disease	Sample location	Collection Date	GPS coordinates
Healthy *X. muta* B2	brown	-	Sweetings Cay/Bahamas	17.06.2007	26°33’550’’N; 77°52’650’’W
Healthy *X. muta* B3	brown	-	Sweetings Cay/Bahamas	17.06.2007	26°33’550’’N; 77°52’650’’W
Healthy *X. muta* B4	brown	-	Sweetings Cay/Bahamas	17.06.2007	26°33’550’’N; 77°52’650’’W
Healthy *X. muta* B5	brown	-	Sweetings Cay/Bahamas	17.06.2007	26°33’550’’N; 77°52’650’’W
Healthy *X. muta* B6	brown	-	Sweetings Cay/Bahamas	17.06.2007	26°33’550’’N; 77°52’650’’W
Healthy *X. muta* B7	brown	-	Sweetings Cay/Bahamas	17.06.2007	26°33’550’’N; 77°52’650’’W
Healthy *X. muta* B9	brown	-	Sweetings Cay/Bahamas	19.06.2007	26°33’550’’N; 77°52’650’’W
Healthy *X. muta* KL1	brown	-	Dry Rocks Reef/Key Largo/Florida	29.11.2007	25°07’910’’N; 80°17’555’’W
Healthy *X. muta* KL2	brown	-	Dry Rocks Reef/Key Largo/Florida	29.11.2009	25°07’910’’N; 80°17’555’’W
Healthy *X. muta* KL3	brown	-	Dry Rocks Reef/Key Largo/Florida	29.11.2009	25°07’910’’N; 80°17’555’’W
Healthy *X. muta* KL4	brown	-	Conch Reef/Key Largo/Florida	01.12.2007	24°56’863’’N; 80°27’230’’W
Healthy *X. muta* KL5	brown	-	Dry Rocks Reef/Key Largo/Florida	03.12.2007	25°07’910’’N; 80°17’555’’W
Healthy *X. muta* KL6	brown	-	Dry Rocks Reef/Key Largo/Florida	03.12.2007	25°07’910’’N; 80°17’555’’W
Healthy *X. muta* KL7	brown	-	Dry Rocks Reef/Key Largo/Florida	04.12.2007	25°07’910’’N; 80°17’555’’W
Healthy *X. muta* KL8	brown	-	Dry Rocks Reef/Key Largo/Florida	04.12.2007	25°07’910’’N; 80°17’555’’W
Healthy *X. muta* KL9	brown	-	Dixie Shoals/Key Largo/Florida	07.12.2007	25°04’316’’N; 80°19’074’’W
Healthy *X. muta* KL0	brown	-	Conch Reef/Key Largo/Florida	11.09.2009	24°56’863’’N; 80°27’230’’W
Diseased *X. muta* 1	brown, orange and white	early stage	Stirrup Cays/Bahamas	20.06.2007	25°50’060’’N; 77°54’970’’W
Diseased *X. muta* 2	brown, orange and white	early stage	Plana Cays/Bahamas	25.06.2007	22°36’441’’N; 73°37’555’’W
Diseased *X. muta* 3	white and orange	advanced stage	Conch Reef/Key Largo/Florida	27.11.2007	24°56’863’’N; 80°27’230’’W
Diseased *X. muta* 4	brown, orange and white	advanced stage	Dixie Shoals/Key Largo/Florida	08.12.2007	25°04’316’’N; 80°19’074’’W
Diseased *X. muta* 5	brown, orange and white	advanced stage	Dixie Shoals/Key Largo/Florida	08.12.2007	25°04’316’’N; 80°19’074’’W
Diseased *X. muta* 7	brown and white	advanced stage	San Salvador/Bahamas	05.06.2008	24°01’140’’N; 74°32’680’’W
Diseased *X. muta* 8	brown and white	advanced stage	Plana Cays/Bahamas	07.06.2008	22°36’441’’N; 73°37’555’’W
Diseased *X. muta* 9	brown and white	early stage	Plana Cays/Bahamas	08.06.2008	22°36’441’’N; 73°37’555’’W
Diseased *X. muta* 10	white	advanced stage	Conch Reef/Key Largo/Florida	11.09.2009	24°56’863’’N; 80°27’230’’W
Diseased *X. muta* 11	white	advanced stage	Conch Reef/Key Largo/Florida	11.09.2009	24°56’863’’N; 80°27’230’’W
Diseased *X. muta* 12	brown and white	early stage	Conch Reef/Key Largo/Florida	17.09.2009	24°56’863’’N; 80°27’230’’W

Tab. 1. Healthy (n=17) and diseased (n=11) *X. muta* individuals applied to the study of Sponge Orange Band disease. The samples were derived either from the Bahamas (B) or from Key Largo, Florida (KL). Identical sample numbers were labeled according to their origin.

Average value ± SE	Healthy	SOB1 brown	SOB1 orange	SOB1 white
Sponge cell nuclei	6.3 ± 1.6	3.9 ± 0.5	4.4 ± 0.5	3.6 ± 0.3
Extracellular cyanobacteria	29.9 ± 10.0	7.8 ± 0.8	12.4 ± 0.7	0.9 ± 0.1
Intracellular cyanobacteria	2.8 ± 1.0	6.0 ± 0.7	13.2 ± 3.1	1.1 ± 0.6
Ratio: extracellular/intracellular cyanobacteria	10.7	1.3	0.9	0.8
All cyanobacteria	32.3 ± 10.6	13.8 ± 1.1	25.5 ± 3.5	1.9 ± 0.5

Tab. 2. Cell counts of healthy (n=4) and Sponge Orange Band diseased (n=1) *X. muta* tissues with a focus on their different surface colorations (brown, orange, white) regarding their amount of sponge cell nuclei, extracellular and intracellular cyanobacteria as well as their ratio and the total amount of cyanobacteria per gram sponge within dilutions of 10^{-3}.

Tissue	Band	Closest sequence match in GenBank	Similarity (%)	Length (bp)	Taxonomic affiliation
healthy: brown	1	*X. muta* adult clone XmA109 (EF159841)	99	661/663	*Synechococcus/Prochlorococcus*
	2	*X. muta* adult clone XmA109 (EF159841)	99	661/664	*Synechococcus/Prochlorococcus*
	16	*X. muta* reproductive material clone XmE035 (EF159868)	99	659/662	*Synechococcus/Prochlorococcus*
	17-1	*X. muta* adult clone XmA109 (EF159841)	99	657/663	*Synechococcus/Prochlorococcus*
	17-2	*X. muta* reproductive material clone XmE035 (EF159868)	100	662/662	*Synechococcus/Prochlorococcus*
	17-3	*X. muta* reproductive material clone XmE243 (EF159922)	99	659/663	*Synechococcus/Prochlorococcus*
	18	*X. muta* reproductive material clone XmE035 (EF159868)	99	661/662	*Synechococcus/Prochlorococcus*
diseased: brown	4	*X. muta* adult clone XmA109 (EF159841)	99	661/663	*Synechococcus/Prochlorococcus*
	9	*X. muta* adult clone XmA109 (EF159841)	99	659/663	*Synechococcus/Prochlorococcus*
	11	*X. muta* adult clone XmA124 (EF159843)	98	654/663	*Synechococcus/Prochlorococcus*
	13	*X. muta* reproductive material clone XmE035 (EF159868)	99	661/662	*Synechococcus/Prochlorococcus*
	19	*X. muta* reproductive material clone XmE035 (EF159868)	99	659/662	*Synechococcus/Prochlorococcus*
	29	*X. muta* adult clone XmA109 (EF159841)	99	657/663	*Synechococcus/Prochlorococcus*
	31	*X. muta* adult clone XmA109 (EF159841)	99	661/663	*Synechococcus/Prochlorococcus*
diseased: orange	3	*X. muta* adult clone XmA109 (EF159841)	99	660/663	*Synechococcus/Prochlorococcus*
	10	*X. muta* reproductive material clone XmE035 (EF159868)	99	661/662	*Synechococcus/Prochlorococcus*
	21	*X. muta* reproductive material clone XmE035 (EF159868)	99	659/662	*Synechococcus/Prochlorococcus*
	26	Marine sediment clone Ct-5-36 (AM177424)	97	648/665	*Cyanobacteria*
	30	*X. muta* adult clone XmA151 (EF159845)	98	658/665	*Synechococcus/Prochlorococcus*
diseased: white	5	*X. muta* adult clone XmA109 (EF159841)	99	661/663	*Synechococcus/Prochlorococcus*
	6-1	Pustular microbial mat associated *Gloeocapsa* sp. clone Pc01 (DQ058865)	92	618/671	*Gloeocapsa*
	6-2	Lake Taihu associated clone TH1-52 (AM690850)	97	650/665	*Cyanobacteria*
	7	Hypolithic slime associated clone agateC2 (FJ230783)	92	617/668	*Bacteria*
	8	*X. muta* adult clone XmA109 (EF159841)	99	660/664	*Synechococcus/Prochlorococcus*
	12	CaCO3 deposition on metallic reef associated clone ArtRifE_7 (FJ594839)	98	657/666	*Bacteria*
	14	*Montastraea annularis* associated clone CD207D04 (DQ200596)	99	659/662	*Cyanobacteria*
	15	CaCO3 deposition on metallic reef associated clone ArtRifE_7 (FJ594839)	92	615/668	*Bacteria*
	22-1	BBD affected *S. siderea* associated cyanobacterium SC-1 (EF372582)	96	642/664	*Cyanobacteria*
	22-2	Aquacultured *Montastraea faveolata* clone SGUS386 (FJ202307)	94	634/669	*Bacteria*
	22-3	CaCO3 deposition on metallic reef associated clone ArtRifE_7 (FJ594839)	99	659/662	*Bacteria*
	23-1	*Spirulina* sp. P7 (AF091109)	97	647/663	*Spirulina*
	23-2	Dead skeleton of white syndrome affected *T. mesenterina* clone 4DP1-A17 (EU780373)	95	631/663	*Cyanobacteria*
	24	Marine sediment clone Ct-5-36 (AM177424)	98	653/662	*Cyanobacteria*
	25	Healthy tissue of *Montastraea faveolata* associated clone SHFH594 (FJ203523)	97	646/662	*Bacteria*
	27	*Erythropodium caribaeorum* associated *Limnothrix* sp. clone EC2 (DQ889938)	97	645/664	*Limnothrix*
	28	*Erythropodium caribaeorum* associated *Limnothrix* sp. clone EC2 (DQ889938)	95	633/665	*Limnothrix*

Tab. 3. 16S rRNA gene sequence analysis of the 31 excised bands from the cyanobacterial DGGE gel in Fig. 31a.

Tissue	Band	Accession number	Closest sequence match in GenBank	Similarity (%)	Length (bp)	Taxonomic affiliation
healthy: brown	27	GU590837	*X. muta* symbiont clone XmE035 (EF159868)	97	649/663	*Synechococcus/Prochlorococcus*
diseased: brown	5	GU590805	*X. muta* symbiont clone XmA109 (EF159841)	99	662/663	*Synechococcus/Prochlorococcus*
	6-1	GU590806	*X. muta* symbiont clone XmE243 (EF159922)	99	660/662	*Synechococcus/Prochlorococcus*
	6-2	GU590807	*X. muta* symbiont clone XmA124 (EF159843)	98	656/663	*Synechococcus/Prochlorococcus*
	7	GU590808	*X. muta* symbiont clone XmE243 (EF159922)	99	660/662	*Synechococcus/Prochlorococcus*
	8-1	GU590809	*X. muta* symbiont clone XmA124 (EF159843)	99	659/663	*Synechococcus/Prochlorococcus*
	8-2	GU590810	*X. muta* symbiont clone XmA109 (EF159841)	99	661/663	*Synechococcus/Prochlorococcus*
	8-3	GU590811	*X. muta* symbiont clone XmE035 (EF159868)	99	656/662	*Synechococcus/Prochlorococcus*
	9	GU590812	*X. muta* symbiont clone XmA109 (EF159841)	99	661/664	*Synechococcus/Prochlorococcus*
	17-1	GU590824	*X. muta* symbiont clone XmE035 (EF159868)	99	661/662	*Synechococcus/Prochlorococcus*
	17-2	GU590825	*X. muta* symbiont clone XmA109 (EF159841)	99	657/663	*Synechococcus/Prochlorococcus*
	18	GU590826	*X. muta* symbiont clone XmA151 (EF159845)	99	661/664	*Synechococcus/Prochlorococcus*
	19	GU590827	*X. muta* symbiont clone XmE243 (EF159922)	99	660/662	*Synechococcus/Prochlorococcus*
	20	GU590828	*X. muta* symbiont clone XmA106 (EF159840)	98	652/663	*Synechococcus/Prochlorococcus*
	21	GU590829	*X. muta* symbiont clone XmA109 (EF159841)	99	661/663	*Synechococcus/Prochlorococcus*
	23	GU590830	*X. muta* symbiont clone XmA106 (EF159840)	97	650/664	*Synechococcus/Prochlorococcus*
	24-1	GU590831	*X. muta* symbiont clone XmA124 (EF159843)	98	654/664	*Synechococcus/Prochlorococcus*
	24-2	GU590832	*X. muta* symbiont clone XmE243 (EF159922)	99	656/662	*Synechococcus/Prochlorococcus*
diseased: orange	1	GU590802	*X. muta* symbiont clone XmA109 (EF159841)	99	658/663	*Synechococcus/Prochlorococcus*
	3	GU590803	*X. muta* symbiont clone XmA151 (EF159845)	99	661/664	*Synechococcus/Prochlorococcus*
	4	GU590804	*X. muta* symbiont clone XmA109 (EF159841)	99	658/663	*Synechococcus/Prochlorococcus*
	10	GU590813	*X. muta* symbiont clone XmA109 (EF159841)	99	657/663	*Synechococcus/Prochlorococcus*
	11	GU590814	*X. muta* symbiont clone XmE035 (EF159868)	99	659/663	*Synechococcus/Prochlorococcus*
	12	GU590815	*X. muta* symbiont clone XmE035 (EF159868)	99	659/662	*Synechococcus/Prochlorococcus*
	13-1	GU590816	*X. muta* symbiont clone XmA106 (EF159840)	98	653/664	*Synechococcus/Prochlorococcus*
	13-2	GU590817	*X. muta* symbiont clone XmE035 (EF159868)	99	659/662	*Synechococcus/Prochlorococcus*
	13-3	GU590818	*X. muta* symbiont clone XmA109 (EF159841)	98	656/664	*Synechococcus/Prochlorococcus*
	14	GU590819	*X. muta* symbiont clone XmA151 (EF159845)	99	660/664	*Synechococcus/Prochlorococcus*
	15	GU590820	*X. muta* symbiont clone XmA124 (EF159843)	99	658/663	*Synechococcus/Prochlorococcus*
	16-1	GU590821	*X. muta* symbiont clone XmA151 (EF159845)	97	653/667	*Synechococcus/Prochlorococcus*
	16-2	GU590822	*X. muta* symbiont clone XmA124 (EF159843)	99	657/663	*Synechococcus/Prochlorococcus*
	16-3	GU590823	*X. muta* symbiont clone XmA109 (EF159841)	99	661/663	*Synechococcus/Prochlorococcus*
	25-1	GU590833	*X. muta* symbiont clone XmA106 (EF159840)	98	651/663	*Synechococcus/Prochlorococcus*
	25-2	GU590834	*X. muta* symbiont clone XmA109 (EF159841)	98	656/663	*Synechococcus/Prochlorococcus*
	25-3	GU590835	*X. muta* symbiont clone XmE035 (EF159868)	99	657/662	*Synechococcus/Prochlorococcus*

Tissue	Band	Accession number	Closest sequence match in GenBank	Similarity (%)	Length (bp)	Taxonomic affiliation
diseased: orange	25-4	GU590836	*X. muta* symbiont clone XmA124 (EF159843)	97	651/665	*Synechococcus/Prochlorococcus*
	60	GU590858	*X. muta* symbiont clone XmA109 (EF159841)	99	658/663	*Synechococcus/Prochlorococcus*
diseased: white	28	GU590838	*X. muta* symbiont clone XmE243 (EF159922)	96	639/664	*Synechococcus/Prochlorococcus*
	29	GU590839	Coral reef sediment clone Ct-5-4 (AM177431)	92	623/672	*Cyanobacteria*
	30	GU590840	Lake Taihu clone TH1-52 (AM690850)	95	638/666	*Cyanobacteria*
	31	GU590841	Uncultured *Acaryochloris* sp. (FM995185)	93	626/669	*Bacteria*
	33-1	GU590842	*Montastraea faveolata* healthy tissue clone SHFH401 (FJ203373)	96	642/667	*Bacteria*
	33-2	GU590843	Subtropical white syndrome affected dead *T. mesenterina* skeleton clone 4DP1-A17 (EU780373)	94	633/667	*Cyanobacteria*
	33-3	GU590844	Coral reef sediment clone Ct-5-36 (AM177424)	98	654/662	*Cyanobacteria*
	34	GU590845	*X. muta* symbiont clone XmA109 (EF159841)	98	655/664	*Synechococcus/Prochlorococcus*
	36	GU590846	Microbial mat-associated *Plectonema* sp. clone Sc07 (DQ058836)	92	617/669	*Plectonema*
	37	GU590847	Healthy mucus of Black Band diseased *Favites* sp. associated clone BB2H16S-1 (EF089403)	97	545/561	*Bacteria*
	38	GU590848	*Erythropodium caribaeorum*-associated *Limnothrix* sp. clone EC2 (DQ889938)	94	631/666	*Limnothrix*
	39	GU590849	Black Band diseased *S. siderea*-associated clone SC-1 (EF372582)	97	649/668	*Cyanobacteria*
	40	GU590850	Coral reef sediment clone Ct-4-43 (AM177432)	98	654/664	*Cyanobacteria*
	41	GU590851	*Montastraea faveolata* healthy tissue clone SHFH401 (FJ203373)	96	643/664	*Bacteria*
	42	GU590852	Subtropical white syndrome affected dead *T. mesenterina* skeleton clone 4DP1-A17 (EU780373)	97	647/665	*Cyanobacteria*
	43	GU590853	Hypolithic slime clone agateC2 (FJ230783)	91	618/673	*Bacteria*
	44	GU590854	*Montastraea faveolata* healthy tissue clone SHFH401 (FJ203373)	96	642/667	*Bacteria*
	48	GU590855	Coral reef clone Cb-2-3 (AM177414)	96	640/665	*Cyanobacteria*
	51	GU590856	*X. muta* symbiont clone XmE243 (EF159922)	97	646/664	*Synechococcus/Prochlorococcus*
	57	GU590857	Seawater-associated *Halomicronema* sp. clone SWC9 (EF150805)	94	628/668	*Halomicronema*
	61	GU590859	*X. muta* symbiont clone XmA151 (EF159845)	99	659/664	*Synechococcus/Prochlorococcus*

Tab. 4. 16S rRNA gene sequence analysis of the 61 excised bands of the cyanobacterial DGGE gel in Fig. 32a.

Sponge specimen	**Chlorophyll *a* in µg/g**
X. muta healthy #4: brown	25.6
X. muta healthy #9: brown	14.2
X. muta healthy #1: brown	33.7
X. muta healthy #2: brown	25.1
X. muta healthy #3: brown	22.2
X. muta healthy #5: brown	56.2
X. muta healthy #6: brown	35.4
X. muta healthy #7: brown	35.1
X. muta healthy #8: brown	41.8
X. muta diseased #3: white	15.6
X. muta diseased #3: orange	50.6
X. muta diseased #4: brown	21.7
X. muta diseased #4: white	1.7
X. muta diseased #4: orange	16.8
X. muta diseased #5: brown	44.1
X. muta diseased #5: white	5.3
X. muta diseased #5: orange	19.6

Tab. 5. Chlorophyll *a* concentration within the surface tissues of healthy (n=9) and Sponge Orange Band diseased (n=3) *X. muta* individuals as listed by tissue coloration (brown, orange, white).

Individuals	Role	Donor of implant	Tissue coloration	Estimated stage of disease	Date
Healthy *X. muta* 0	Donor	-	brown	control	11.09.2009
Diseased *X. muta* 10	Donor	-	white	advanced stage	11.09.2009
Diseased *X. muta* 11	Donor	-	white	advanced stage	11.09.2009
Diseased *X. muta* 12	Donor	-	brown and white	early stage	17.09.2009
Healthy *X. muta* 1	Recipient	Diseased *X. muta* 10	brown	-	10.09.2009
Healthy *X. muta* 2	Recipient	Diseased *X. muta* 10	brown	-	10.09.2009
Healthy *X. muta* 3	Recipient	Diseased *X. muta* 10	brown	-	11.09.2009
Healthy *X. muta* 4	Recipient	Healthy *X. muta* 0	brown	-	11.09.2009
Healthy *X. muta* 5	Recipient	Healthy *X. muta* 0	brown	-	11.09.2009
Healthy *X. muta* 6	Recipient	Healthy *X. muta* 0	brown	-	11.09.2009
Healthy *X. muta* 7	Recipient	Diseased *X. muta* 11	brown	-	12.09.2009
Healthy *X. muta* 8	Recipient	Diseased *X. muta* 11	brown	-	12.09.2009
Healthy *X. muta* 9	Recipient	Diseased *X. muta* 11	brown	-	12.09.2009
Healthy *X. muta* 10	Recipient	Diseased *X. muta* 12	brown	-	17.09.2009
Healthy *X. muta* 11	Recipient	Diseased *X. muta* 12	brown	-	17.09.2009
Healthy *X. muta* 12	Recipient	Diseased *X. muta* 12	brown	-	17.09.2009

Tab. 6. *X. muta* individuals used as donor and recipient sponges within the underwater infection experiments at Conch Reef, Florida, in September 2009.

Individual	Tissue coloration	Application	Sample location	Sampling date	GPS coordinates
Healthy *A. compressa* 1	red	Chlorophyll *a*	Dry Rocks Reef/Key Largo/Florida	29.11.2007	25°07'910''N; 80°17'555''W
Healthy *A. compressa* 8	red	Chlorophyll *a*, Molecular, Microsocpy	Dry Rocks Reef/Key Largo/Florida	05.12.2007	25°07'910''N; 80°17'555''W
Healthy *A. compressa* 9	red	Chlorophyll *a,* Molecular, Microscopy	Dry Rocks Reef/Key Largo/Florida	05.12.2007	25°07'910''N; 80°17'555''W
Healthy *A. compressa* 12	red	Cultivation, Molecular, Microscopy	Dry Rocks Reef/Key Largo/Florida	07.12.2007	25°07'910''N; 80°17'555''W
Healthy *A. compressa* 14	red	Molecular, Microscopy	Dry Rocks Reef/Key Largo/Florida	07.12.2007	25°07'910''N; 80°17'555''W
20x Healthy *A.compressa*	red	Infection trials	Conch Reef/Key Largo/Florida	09.2009	24°56'863''N; 80°27'230''W
10 x Healthy *A.compressa*	red	Infection trials	Conch Reef/Key Largo/Florida	09.2009	24°56'863''N; 80°27'230''W
503x Healthy *A.compressa*	red	Disease prevalence	Dry Rocks Reef/Key Largo/Florida	12.2007	25°07'910''N; 80°17'555''W
107x Diseased *A.compressa*	red and white	Disease prevalence	Dry Rocks Reef/Key Largo/Florida	12.2007	25°07'910''N; 80°17'555''W
40x Diseased *A.compressa*	red and white	Manifestation rate per sponge	Dry Rocks Reef/Key Largo/Florida	12.2007	25°07'910''N; 80°17'555''W
10x Diseased *A. compressa*	red and white	Infection trials	Conch Reef/Key Largo/Florida	09.2009	24°56'863''N; 80°27'230''W
Diseased *A. compressa* 1	red and white	Cultivation, Molecular	Conch Reef/Key Largo/Florida	05.2009	24°56'863''N; 80°27'230''W
Diseased *A. compressa* 2	red and white	Cul., Chlorophyll *a*, Molecular, Microscopy	Dry Rocks Reef/Key Largo/Florida	29.11.2007	25°07'910''N; 80°17'555''W
Diseased *A. compressa* 3	red and white	Chlorophyll *a*	Dry Rocks Reef/Key Largo/Florida	29.11.2007	25°07'910''N; 80°17'555''W
Diseased *A. compressa* 4	red and white	Chlorophyll *a,* Microscopy	Dry Rocks Reef/Key Largo/Florida	01.12.2007	25°07'910''N; 80°17'555''W
Diseased *A. compressa* 6	red and white	Microscopy	Dry Rocks Reef/Key Largo/Florida	30.11.2007	25°07'910''N; 80°17'555''W
Diseased *A. compressa* 7	red and white	Underwater observations	Conch Reef/Key Largo/Florida	09.2009	24°56'863''N; 80°27'230''W
Diseased *A. compressa* 8	red and white	Underwater observations	Conch Reef/Key Largo/Florida	09.2009	24°56'863''N; 80°27'230''W
Diseased *A. compressa* 9	red and white	Underwater observations	Conch Reef/Key Largo/Florida	09.2009	24°56'863''N; 80°27'230''W
Diseased *A. compressa* 12	red and white	Microscopy	Dry Rocks Reef/Key Largo/Florida	01.12.2007	25°07'910''N; 80°17'555''W
Diseased *A. compressa* 13	red and white	Cultivation, Molecular, Microscopy	Dry Rocks Reef/Key Largo/Florida	01.12.2007	25°07'910''N; 80°17'555''W
Diseased *A. compressa* 16	red and white	Microscopy	Dry Rocks Reef/Key Largo/Florida	05.12.2007	25°07'910''N; 80°17'555''W
Diseased *A. compressa* 23	red and white	Microscopy	Dry Rocks Reef/Key Largo/Florida	05.12.2007	25°07'910''N; 80°17'555''W
Diseased *A. compressa* 29	red and white	Cultivation, Molecular, Microscopy	Dry Rocks Reef/Key Largo/Florida	07.12.2007	25°07'910''N; 80°17'555''W
Diseased *A. compressa* 30	red and white	Microscopy	Dry Rocks Reef/Key Largo/Florida	07.12.2007	25°07'910''N; 80°17'555''W

Tab. 7. Healthy (n=538) and diseased (n=171) *A. compressa* individuals applied to the study of Sponge White Patch disease: not all experiments are included within this thesis.

2. Abbreviations, Acronyms & Symbols

AIX	Ampicillin-, IPTG- and X-Gal containing medium
Amp	Ampicillin
A. compressa	*Amphimedon compressa*
Appl Environ Microbiol	Applied and Environmental Microbiology
APS	Ammonium persulfate
ARBS	Aplysina Red Band Syndrome
ASW	Artificial seawater
AWI	Alfred-Wegener-Institute
BLAST	Basic Local Alignment Search Tool
bp	Base pair
©	Copyright
°C	Degree Celsius
cm	Centimeter
cm^3	Cubic centimeter
DAPI	Diamino-2-phenyl-indol-dihydrochlorid
dATP	Deoxyadenosine triphosphate
dCTP	Deoxycytidine triphosphate
DGGE	Denaturing Gradient Gel Electrophoresis
dGTP	Deoxyguanosine triphosphate
DNA	Deoxyribonucleic acid
dNTP	Deoxynucleotide triphosphate
DOM	Dissolved organic matter
Dr.	Doctor
DRK	German Red Cross
dTTP	Deoxythymidine triphosphate
E. coli	*Escherichia coli*
EDTA	Ethylenediaminetetraacetic acid
e.g.	*Exempli gratia* (for example)
et al.	*Et altera* (and others)
EtBr	Ethidium bromide
EtOH	Ethanol
EU	European Union
FA	Formaldeyhde
FEMS	Federation of European Microbiological Societies
Fig./Figs.	Figure/Figures
FISH	Fluorescence in situ hybridization
FM	Fluorescence microscopy
g	Gram
GA	Glutaraldehyde
GC	The bases Guanine and Cytosine
GSLS	Graduate School of Life Sciences
h/hrs	Hour/hours
HBOI	Harbour Branch Oceanographic Institution
HMA	High-microbial-abundance sponge
HPLC	High Performance Liquid Chromatography
H_2O	Water
H_2O_{dest}	Distilled water

H_2O_{dd}	Double-distilled water
*hsp*70	Heat shock protein 70
i.e.	*Id est* (that is)
IMIB	Institute for Molecular Infection Biology
Inc.	Incorporated
IPTG	Isopropyl-beta-D-thiogalactopyranoside
ISRS	International Society for Reef Studies
ISS	International Symbiosis Society
kb	Kilobase
kg	Kilogram
l	Liter
LM	Light microscopy
LMA	Low-microbial-abundance sponge
m	Meter
m^2	Square meter
M	Molar/Marker
mA	Milliampere
MeOH	Methanol
mg	Milligram
min	Minute
ml	Milliliter
mm	Millimeter
mM	Millimolar
mo	Microorganism
mol	Mol
MS	Mass Spectrometry
µg	Microgram
µl	Microliter
µm	Micrometer
n	Amount
NCBI	National Center for Biotechnology Information
ng	Nanogram
nm	Nanometer
NOAA	National Oceanic and Atmospheric Administration
NURC	National Undersea Research Center
OTU	Operational Taxonomic Unit
%	Percent
p	Page
pmol	Picomol
PBS	Phosphate buffered saline
PCR	Polymerase Chain Reaction
pH	pH-value
PhD	Philosophiae doctor
PI	Peer investigator
PVC	*Planctomycetes*, *Verrucomicrobia* and *Chlamydiae*
Prof.	Professor
r	Reverse
RFLP	Restriction Fragment Length Polymorphism
rDNA	Ribosomal DNA
RNA	Ribonucleic acid
rpm	Revolutions per minute

rRNA	Ribosomal RNA
Rt	Retention time
RT	Room temperature
RV SJ	Research vessel Seward Johnson
s	Second
SCUBA	Self Contained Underwater Breathing Aparatus
SD	Standard deviation
SDS	Sodium dodecyl sulfate
SE	Standard error
SEM	Scanning electron microscopy
SFB	Collaborative Research Center (Sonderforschungsbereich)
SOB	Sponge Orange Band
sp.	Species
SWP	Sponge White Patch
Tab./Tabs.	Table/Tables
TAE	Tris-acetate-EDTA
TAU	Tel Aviv University
TEM	Transmission electron microscopy
TFA	Trifluoroacetic acid
T_m	Melting temperature
Tris	Tris(hydroxymethyl)aminomethane
U	Enzyme unit
u	Atomic mass unit
UNC/CH	University of North Carolina at Chapel Hill
UNCW	University of North Carolina at Wilmington
USA	United States of America
USVI	United States Virgin Islands
UV	Ultraviolett
UW-PSD	Underwater Photoshop
V	Volt
VAAM	Vereinigung für Allgemeine und Angewandte Mikrobiologie
vol/vol	Volume per volume
w/v	Weight per volume
x	Times
X-Gal	5-Bromo-4-Chloro-3-Indolyl-β-D-galactopyranoside
X. muta	*Xestospongia muta*
ZINF	Research Center for Infectious Diseases
>	Higher
≥	The same or higher
<	Below
#	Number
+	Plus
±	Plus/minus
=	Equals

3. Equipment & General Laboratory Supply

Equipment/Supplies	Manufacturer	Specifications
Autoclaves	Fedegari	Tec 120, 9191E, FV 3.3
	H+P Labortechnik	Varioklav 500, 135S
	Systec	VX 150
Beakers	Kartell, Vitlab	600ml, 800ml, 1000ml
Benchtop centrifuges	Hereaus Instruments	Biofuge Fresco
		Biofuge Pico 17
Binocular microscope	Zeiss	-
Buckets	Kmart	-
Cable ties	Kmart	-
Cannulas	Sterican B/Braun	-
Cellulose nitrate filter	Schleicher & Schuell	0.45µm pore size
Centrifuge	Heraeus Instruments	Megafuge 1.0R
Clean bench	Nunc GmbH	InterMedMicroflow safety cabinet
		HERA safe HS12
	Heraeus	Nuaire
	Varolab	
Coolers	Coleman	100-Qt. wheeled cooler
Cork borer	Bochem Laborbedarf	-
Cover slip	Hartenstein	-
Cryotubes	Greiner	Bio-One (1.5ml), Cryo.S™
Cuvettes (glas)	Hartenstein	-
DGGE-chamber	Biorad	DCode™
DGGE-equipment: glass plates, dummy, clamps & spacer, combs	Biorad	-
DGGE: gradient caster	Biorad	Model 475
Digital camera	Canon	Power Shot S50

Digital camera: waterproof case	Canon	WP-DC300
Dish washer	Miele	Automatic G 7735
	Miele	Miele G 7783
	Miele	Compact Desinfector
Disposable cuvettes	Plastibrand	Halbmikro 1.5ml
Disposable scalpel	Radiomed	-
Disposable syringes	Braun	5ml
Distilling apparatus for H_2O_{dd}	GFL	Bi-Dest 2304
	TKA	TKA-Lab-HP
Dive gear & equipment	IQ, Oceanic, PADI	-
Dive knife	Polaris	Titanium Tauchmesser
Dry ice	Walmart	-
Electroporation apparature	EquiBio	Easyject prima
Electroporation cuvettes	EquiBio	EPC 102
Falcon tubes	Greiner	15ml, 50ml Bio-one CELLSTAR®
FastPrep® instrument	Savant	FP120
	MP Biomedicals	FastPrep®24
Filter apparature	Nalgene	-
Filter disks	Becton Dickinson	-
Filter membranes	Millipore	Millex-GS 0.22µm
Fishing weights	Kmart	-
Flagging tape	Kmart	yellow, red
Fluorescence microscope	Zeiss	Axiolab
Fluorescein dye	Risk Reactor	IFWB-C8 Yellow Green
Freezer (-20°C)	Liebherr	Öko super
	Nunc	QBF 2185V36
Freezer (-80°C)	Hereaus Instruments	Sepatech
	Kendro	Queue Basic QBF 2585V36
Funnels	Hartenstein	-

Gel documentation	BioRad	Gel Doc 2000
	BioRad	Universalhood II
Gel documentation software	BioRad	Software Multi-Analyst 1.1
Gel electrophoresis chambers	BioRad	Sub-Cell® GT
	Pharmacia	-
	Roth	-
Gel electrophoresis slides and combs	BioRad	-
Glass beads	Hartenstein	-
Glass bottles	Schott	Duran® 50ml, 100ml, 250ml, 500ml, 1l, 2l
Glass pipettes	Hartenstein	-
Glass slides	Knittel Gläser	OTMM
Gloves (disposable: Latex)	Nobaglove®Latex	Latex: S
Gloves (disposable: Nitrile)	Ansell	Touch N Tuff
Grid for microscopic counting	Zeiss	10x10 squares, 12.5mm
Hand counter	IVO	-
Handpump for vacuum filtration	Mityvac	MityvacII
Heat block	Laboratory Devices	Digi-Block Jr.
	Roth	Rotilabo® Block-Heater H250
	Liebisch	-
Heating plate with magnetic stirrer	Labinco	L32
	Witeg	MS-20A
HPLC	JASCO System	Pump PU1580
		Gradient unit LG-980-025
		Degasser DG-2080-53
		UV detector MD-2010Plus
HPLC columns	Merck	Chromolith RP-18e
	Merck	Chomolith SemiPrep RP-18e
Ice maker	Scotsman	AF-20

Immersion oil	Roth	X899.3
Incubator	Memmert	TV 40b
	Heraeus	Kelvitron®t
	VWR	Incu-Line
	WTB-Binder	970006
Laptop	Dell	XPS M1330
Light microscope	Zeiss	Axiolab
Lyophilizer	Steris	Lyovac GT2E
Magnetic stirrer	Heidolph	MR3001K
Measuring cylinders	Brand	10ml, 50ml, 100ml, 250ml, 500ml, 1000ml
Microfuge tubes	Thermo scientific	0.5ml Thermo tubes
	Thermo scientific	0.2ml Thermo stripes
Microliter syringe	Hamilton	50µl
Micropipettes	Eppendorf	Research 10 (0.5-10µl)
	Gilson	Pipetman P20 (2-20µl)
	Gilson	Pipetman P200 (20-200µl)
	Gilson	Pipetman P1000 (200-1000µl)
	Sarstedt	1.5ml, 2.0ml
Microplates	Nalgene	Nunclon™
Microscopes	Zeiss	Axiolab, Telaral 31
Microwave	AEG	Micromat
	Severin	700
	Privileg	8020
Mortar & Pestle	Hartenstein	MÖ10/PIS3
MS	Bruker Daltonik	Micromass Q-TOF, MicroTOF
	Finnigan MAT	Triple-stage quadrupole 7000 tandem mass spectrometer system with ESI interface
Multipipette	Eppendorf	Multipipette®Plus

96-well plates	Greiner	Bio-One
Nitex net	Hartenstein	-
Parafilm	Pechiney Plastic Packaging	Parafilm “M”
Pasteur pipettes (glas)	Hartenstein	-
PCR cycler	Biometra®	T3-Thermocycler
	Eppendorf	Mastercycler personal
	Biorad	C 10000^{TM}
Petri dishes (round)	Greiner	633130 (94 x 16mm)
pH meter electrode	WTW	MultiLine P4, SenTix 41
Pipette boy	Brand	Accu-jet® Pro
Pipettes	Greiner	2ml, 10ml, 25ml
Pipettes (plastic)	Noras, Sarstedt	5ml, 10ml, 25ml
Pipette tips	Sarstedt	1000µl: blue
		200µl and 20µl: yellow
		10µl: white
Polycarbonate membrane	Millipore	black, 0.2µm pore size
Power supply for gelelectrophoresis	Consort	E455
	BioRad	Power Pac 300
Reaction tubes	Sarstedt	0.5ml
		1.5ml
		2.0ml
Refrigerator	Privileg	Superöko
	Liebherr	Premium NoFrost
Rotary evaporator	Heidolph	Laborota 4010
Scales	Kern	470-36
	Ohaus	Navigator
Scanning electron microscope	Zeiss	DSM 962
Scissors	Hartenstein	-

Sequencer	Applied Biosystems	ABI Prism™ 310 Genetic Analyzer
SEM tables	Plano	-
Shaker	Edmund Bühler GmbH	TH30
	Infors AG	HR
	New Brunswick Scientific	Innova 4300
Slide for gelelectrophoresis	BioRad	-
Special accuracy scales	Chyo	JL-180
	Kern	770
Spectrophotometer	Pharmacia Biotech	Ultraspec 3000
	PeqLab	NanoDrop ND1000
Speedvac concentrator	Thermo Scientific	Savant
Spray bottle	Roth	500ml
Square for prevalence studies	Homedepot, NURC	-
Sterile filter	Millipore	Millex®GP PCS 0.22µm
Sterile filter units	Nunc	Bottletop filter
Syringe filters	Schleicher & Schuell	0.2µm
Syringes	BD Plastipak	30ml
Tape	TimeMed Labeling Systems, Inc.	-
Tape for autoclaving	Hartenstein	SteriCLIN vp Medical Packaging
Tape measure	Hornbach	20m
TEM grids	Plano	-
Thermal packs	Publix, Walmart	-
Tissues	Fripa	Akito
Transillumination table UV	Brunschwig Chemie	N-90M, 6x15W
Transmission electron microscope	Zeiss	EM10
Typhoon scanner and software	Molecular Dynamics of Amersham Pharmacia Biotech	Typhoon 8600 Variable Mode Imager

Ultramicrotome	RMC	MT-7000
UV-Hood	Desaga Heidelberg	MinUVis
	UVP	UV Transilluminator
UV-Sterilizer	BioRad	UV chamber
Vortexer	Scientific Industries	Vortex-Genie 2
Water bath	GFL®	1083
Water preparation	Millipore	Milli-Q
Ziploc bags	Ziploc	1 gallon, 3 gallons

4. Chemical Reagents

Name of chemical	Manufacturer
Acetone (100%)	Roth
Acetic acid (100%)	AppliChem
Acetonitrile	Sigma
40% Acrylamide/Bisacrylamide Solutions (37.5:1)	Biorad/Roth
Agar granulated	Difco
Agarose ultrapure	Gibco
Ammonium persulfate (APS)	Sigma
Ampicillin	AppliChem
Artificial Sea Salts	Tropic Marin
Azocoll	Sigma
Bacto Peptone	Becton Dickinson
Boric acid (H_3BO_3)	AppliChem
Bromphenol blue	Merck
Bovine serum albumine (BSA)	BioRad
Cacodylic acid sodium salt trihydrate ($C_2H_6AsNaO_2$ x3H_2O)	Roth

Calcium carbonate ($CaCO_3$)	AppliChem
Calcium chloride ($CaCl_2$)	AppliChem
Citifluor	Citifluor Ltd.
Cycloheximide	Sigma
2'-Deoxyadenosine 5'-Triphosphate (dATP)	Sigma
2'-Deoxycytidine 5'-Triphosphate (dCTP)	Sigma
2'-Deoxyguanosine 5'-Triphosphate (dGTP)	Sigma
2'-Deoxythymidine 5'-Triphosphate (dTTP)	Sigma
4', 6-Diamidino-2-phenylindoldihydrochloride (DAPI)	Sigma
Dimethylformamide	AppliChem
Dipotassium hydrogen phosphate (K_2HPO_4)	Roth
Disodium hydrogen phosphate (Na_2HPO_4 x 2 H_2O)	Merck
Epon 812	Serva
Ethidium bromide (1% solution; EtBr)	Roth
Ethanol absolute (100%; EtOH)	Merck
Ethanol denatured (96%; EtOH)	Roth
Ethylenediamine tetraacetic acid dihydrate (Na_2EDTA x $2H_2O$)	Serva
Ficoll Type 400	Sigma
Formaldehyde (37%; FA)	AppliChem
Formamide ($HCONH_2$)	Roth
Glucose	AppliChem
Glutaraldehyde	Sigma
Glycerol (86%; $HOCH_2$-CHOH-CH_2OH)	Roth
Gold palladium	Baltic preparation: Au/Pd Target
Hydrochloric acid (HCl)	AppliChem
1-Isopropyl-β-D-1-thiogalactopyranoside (IPTG)	Sigma
Isopropanol ($(CH_3)_2CHOH$)	Roth
Magnesium chloride hexahydrate ($MgCl_2$ x $6H_2O$)	AppliChem
Marine agar 2216	Difco

Methanol	Sigma, Roth
Osmium tetroxide (2% OsO_4 in ASW)	Sigma
Paraformaldehyde	Serva
PCR-Buffer (10x)	Quiagen
Peptone	Roth
Potassium acetate	AppliChem
Potassium bromide (KBr)	AppliChem
Potassium chloride (KCl)	Fluka
Potassium dihydrogen phosphate (KH_2PO_4)	Roth
Propylene oxide	Roth
Q-Solution	Quiagen
Sequencing buffer (5x)	ABI Prism™ Big Dye™
Sodium acetate trihydrate (NaAc x $3H_2O$)	AppliChem
Sodium chloride (NaCl)	Roth
Sodium dodecyl sulfate (SDS)	AppliChem
Sodium fluoride (NaF)	Fluka
Sodium hydrogen carbonate ($NaHCO_3$)	Merck
Sodium hydroxide (NaOH)	AppliChem
Sodium sulfate (Na_2SO_4)	Merck
Starch (soluble)	Roth
Strontium chloride hexahydrate ($SrCl_2$ x $6H_2O$)	Fluka
SYBR-Gold (10 000 fold)	Invitrogen
TEMED (N,N,N',N'-Tetramethylethylenediamine)	AppliChem
Tris base	AppliChem
Trifluoroacetic acid (0.05%; TFA)	Sigma
Tris (hydroxymethyl) aminomethane hydrochloride (Tris/HCl)	Sigma
Triton X-100	AppliChem
Tryptone/Peptone from Casein	Roth
Uranyl acetate (1% in EtOH)	Sigma

Urea	Roth
Water, distilled (H_2O_{dest})	Uni Würzburg
Water, double-distilled (H_2O_{bidest})	Uni Würzburg
Water, de-ionized (H_2O millipore)	Millipore/Uni Würzburg
Xylene cyanol	AppliChem
X-Gal (5-bromo-4-chloro-3-indolyl-β-D-galactopyranoside)	Sigma
Yeast extract	Becton Dickinson

5. Solutions & Buffers

For sterilization purposes, the solutions and buffers were autoclaved for 20min at 121°C under pressure. After they cooled down, they were supplemented, if necessary, by heat-sensitive and sterile substances such as antibiotics, X-Gal or IPTG. In case they were volatile, pH-sensitive or destructed by heat, they were sterilized by filtration through a 0.22µm filter.

90% Acetone	100% Acetone	450ml
	H_2O_{dest}	50ml
75% Acetone	100% Acetone	375ml
	H_2O_{dest}	125ml
50% Acetone	100% Acetone	250ml
	H_2O_{dest}	250ml
30% Acetone	100% Acetone	150ml
	H_2O_{dest}	350ml
10% Ampicillin solution	Ampicillin sodium salt	1.0g
	H_2O (millipore)	ad 10.0ml
		→sterilize by filter
10% APS	Ammonium persulfate	0.1g
	H_2O (millipore)	1ml

Artificial seawater (ASW)	NaCl	234.7g
	Na_2SO_4	39.2g
	$MgCl_2$ x $6H_2O$	106.4g
	$CaCl_2$	11.0g
	$NaHCO_3$	1.92g
	KCl	6.64g
	KBr	0.96g
	H_3BO_3	0.26g
	$SrCl_2$	0.24g
	NaF	0.03g
	H_2O (millipore)	ad 10l
Cacodylate-buffer (50mM; pH 7.4)	Na-Cacodylate (0.2M; pH 7.2)	1.07g (→pH 7.8 via HCl)
	25% Glutaraldeyde	10ml
	ASW	ad 100ml
Cycloheximide (100µg/ml)	Cycloheximide	100µg
	H_2O_{dest}	1ml
DAPI-Solution (100µg/ml)	DAPI	100µg
	H_2O (millipore)	1ml
100% Denaturing solution at 10% Acrylamide	Acrylamide/Bisacrylamide	25ml
	50xTAE	2ml
	Formamide	40ml
	Urea	42g
	H_2O_{dest}	ad 100ml
90% Denaturing solution at 10% Acrylamide	Acrylamide/Bisacrylamide	25ml
	50xTAE	2ml
	Formamide	36ml
	Urea	37.8g
	H_2O_{dest}	ad 100ml

90% Denaturing solution at 8% Acrylamide	Acrylamide/Bisacrylamide	20ml
	50xTAE	37.8g
	Formamide	36ml
	Urea	2ml
	H_2O_{dest}	ad 100ml
0% Denaturing solution at 10% Acrylamide	Acrylamide/Bisacrylamide	25ml
	50xTAE	2ml
	H_2O_{dest}	73ml
0% Denaturing solution at 8% Acrylamide	Acrylamide/Bisacrylamide	20ml
	50xTAE	2ml
	H_2O_{dest}	78ml
2xDGGE-loading dye	2% Bromphenol blue	0.25ml
	H_2O_{dest}	1.3ml
	2% Xylene cyanol	0.25ml
	86% Glycerol	8.2ml
100bp DNA ladder	100bp DNA ladder	0.2ml
	Stop buffer	0.2ml
	H_2O (millipore)	0.8ml
1kb DNA ladder	1kb DNA ladder	0.2ml
	Stop buffer	0.2ml
	H_2O (millipore)	0.8ml
dNTP mix	dATP	0.1ml
	dCTP	0.1ml
	dGTP	0.1ml
	dTTP	0.1ml
	10x PCR buffer	0.1ml
	H_2O (millipore)	0.5ml
		→partitioning

90% Ethanol	100% Ethanol	450ml
	H_2O_{dest}	50ml
70% Ethanol	100% Ethanol	350ml
	H_2O_{dest}	150ml
50% Ethanol	100% Ethanol	250ml
	H_2O_{dest}	250ml
30% Ethanol	100% Ethanol	150ml
	H_2O_{dest}	350ml
Ethidium bromide dye bath	EtBr 10mg/ml	0.1ml
	H_2O_{dest}	200ml
0.5M EDTA	$Na_2EDTA \times 2H_2O$	136.1g
	H_2O (millipore)	ad 1000ml
		→pH 8 via NaOH (10N)
4% Formaldehyde	Formaldehyde (37%)	10.81ml
	H_2O_{dest} (sterile)	89.19ml
6.25% Glutaraldehyde	25% Glutaraldehyde	25ml
	1x PBS (sterile)	75ml
2.5% Glutaraldehyde	25% Glutaraldehyde	10ml
	1x PBS (sterile)	90ml
20% Glycerol	86% Glycerol	279µl
	Dilution with e.g. liquid culture	921µl
1M IPTG solution	IPTG	2.38g
	H_2O (millipore)	ad 10.0ml
		→sterilize by filter
Lysozyme (10mg/ml)	Lysozyme	10mg
	TNEX	1.0ml
5M NaCl	NaCl	292.2g
	H_2O (millipore)	ad 1000ml

NaOH (10N)	NaOH	240g
	H_2O_{bidest}	ad 1000ml
Paraformaldeyhde (3.7%)	Paraformaldehyde	4.0g
	1x PBS	ad 100ml
Phosphate buffered solution (10x PBS)	NaCl	40.0g
	Na_2HPO_4 x $2H_2O$	6.25g
	KH_2PO_4	1.0g
	KCl	1.0g
	H_2O (millipore)	ad 500ml
		→pH 7.2-7.4 via HCl
1x PBS	10x PBS	10ml
	H_2O_{dest}	90ml
Plasmid mini prep buffer 1	1M Tris/HCl, pH 7.5	5.0ml
	0.5M EDTA, pH 8.0	2.0ml
	RNase 10mg/ml	1.0ml
	H_2O (millipore)	ad 100ml
Plasmid mini prep buffer 2	NaOH	0.8g
	SDS	1.0g
	H_2O (millipore)	ad 100ml
Plasmid mini prep buffer 3	NaAc x $3H_2O$	40.8g
	H_2O (millipore)	ad 100ml
		→pH 4.8 via HCl
Proteinase K	Proteinase K	10.0mg
	H_2O_{dest}	1.0ml
Propylene oxide/Epon 812	Propylene oxide	50ml
	Epon 812	50ml
1% RNase A (10mg/ml)	RNase A	10.0mg
	H_2O (millipore)	1.0ml

1% SDS	SDS	10g
	H_2O_{dest}	ad 1000ml
Soerensen-phosphate-buffer (50mM; pH 7.4)	A) KH_2PO_4	9.078g ad 1000ml H_2O_{dest}
	B) Na_2HPO_4 x 2 H_2O	11.876g ad 1000ml H_2O_{dest}
	→81.8ml B+18.2ml A for pH 7.4	
Stop buffer	Bromphenol blue	25.0mg
	Xylene cyanol	25.0mg
	Ficoll Type 400	2.5g
	H_2O (millipore)	ad 10ml
1x SYBR-Gold dye bath	1x TAE	100ml
	10 000x SYBR-Gold	10µl
50x TAE	Tris/HCl	242.0g
	100% Acetic acid	57.1ml
	0.5M EDTA, pH 8.0	100ml
	H_2O_{dest}	ad 1000ml
1x TAE	50x TAE	20ml
	H_2O_{dest}	980ml
TNE	1M Tris/HCl pH 8.0	1ml
	5M NaCl	0.2ml
	0.5M EDTA, pH 8.0	2ml
	H_2O_{dest}	ad 100ml
TNEX	TNE	99ml
	Triton X-100	1ml
1M Tris/HCl	Tris/HCl	121.0g
	H_2O (millipore)	ad 1000ml
		→pH 7.5-8.0 via HCl
5% X-Gal solution	X-Gal	2.5g
	Dimethylformamide	ad 50.0ml

6. Media

Liquid media and agar-solutions (the according medium plus 1.5% agar) were sterilized by autoclaving for 20min under pressure at 121°C. Heat-sensitive and sterile substances, such as antibiotics, IPTG or X-Gal, were added under the clean bench after the medium/agar had cooled down below 30°C. After thorough mixture the agar was poored into petri-dishes and those were stored, once cold, at 4°C until usage.

Name	Ingredients
Luria-Bertani (LB) medium	8.0g Tryptone/Peptone from Casein 4.0g Yeast extract 4.0g NaCl ad 800ml H_2O_d
Luria-Bertani (LB) medium + Ampicillin	800ml LB medium 800µl Ampicillin (100µg/ml)
Luria-Bertani (LB) agar	8.0g Tryptone/Peptone from Casein 4.0g Yeast extract 4.0g NaCl 12.0g Agar ad 800ml H_2O_d
LB agar+Ampicillin+IPTG+X-gal (AIX)	800ml LB agar 800µl Ampicillin (100µg/ml) 400µl IPTG 0.1M 1.28ml X-Gal (50mg/ml)
M1 agar	8.0g soluble starch 3.2g Yeast extract 1.6g Peptone 14.4g Agar ad 800ml ASW

YPD medium (agar)	16g Glucose 16g Peptone 8g Yeast extract (+12.8g Agar) ad 800ml ASW
GPYNS medium (agar) with/without cycloheximide (100µg/ml)	20g Artifical Sea Salts 0.4g Bacto Peptone 0.08g Yeast Extract 0.8g Glucose (10g Agar) ad 800ml H_2O_{dest} ± Cycloheximide (100µg/ml)
Zobell medium	1.0g Yeast extract 5.0g Peptone 750.0ml ASW ad 1000ml H_2O_{dest}
Marine Agar 2216 + Azocoll	44.08g Marine Agar 2216 0.8g Azocoll ad 800ml H_2O_{dest}

7. Enzymes & Kits

Name of Enzyme	Manufacturer
DNA Polymerase I	New England Biolabs
Restriction enzyme HaeIII and buffer 2	New England Biolabs
Restriction enzyme MspI and buffer 2	New England Biolabs
Restriction enzyme Eco RI and Eco RI buffer	New England Biolabs
Lysozyme	Sigma
Proteinase K	Sigma
REDTaq® ReadyMix™ PCR reaction mix	Sigma
RNase A	Roche
Taq DNA polymerase and buffer	Qiagen
T4 DNA ligase and buffer	New England Biolabs

Name of Kit	Manufacturer
ABI Prism™ Big Dye™ terminator cycle sequencing ready reaction kit: Premix 1.1	Applied Biosystems
FastDNA® spin kit for soil	Q-Biogene
dNTP 100-1KT Deoxynucleotide Set	Sigma
pGEM-T Easy vector system I kit	Promega
QIAquick® PCR purification kit	Qiagen
QIAquick® Gel extraction kit	Qiagen

8. Oligonucleotide Primers

All oligonucleotide primers applied were synthesized by Sigma-Aldrich, Steinheim. Their characteristics are described in the following text:

Primer	5'-3' Sequence	Annealing (°C)	Specificity	Method	Reference
27f	GAG TTT GAT CCT GGC TCA	56	Eubacterial 16S rDNA	PCR	Lane (1991)
1492r	TAC GGC TAC CTT GTT ACG ACT T	57	Eubacterial 16S rDNA	PCR	Lane (1991)
341f	CCT ACG GGA GGC AGC AG	56	Eubacterial 16S rDNA	PCR, DGGE-PCR, Sequencing-PCR	Muyzer *et al.* (1998)
341f+GC	CGC CCG CCG CGC GCG GCG GGC GGG GCG GGG GCA CGG GGG GCC TAC GGG AGG CAG CAG	57	Eubacterial 16S rDNA	DGGE-PCR	Muyzer *et al.* (1998)
907r	CCG TCA ATT CMT TTG AGT TT	52	Eubacterial 16S rDNA	PCR, DGGE-PCR, Sequencing-PCR	Muyzer *et al.* (1998)
106f	CGG ACG GGT GAG TAA CGC GTG A	60	Cyanobacterial 16S rDNA	PCR, DGGE-PCR	Nübel *et al.* (1997)
106f+GC	CGC CCG CCG CGC GCG GCG GGC GGG GCG GGG GCA CGG GGG G CGG ACG GGT GAG TAA CGC GTG A	60	Cyanobacterial 16S rDNA	DGGE-PCR	Nübel *et al.* (1997), Muyzer *et al.* (1998)
781r	GAC TAC WGG GGT ATC TAA TCC CWT T	60	Cyanobacterial 16S rDNA	PCR; DGGE-PCR	Nübel *et al.* (1997)
SP6	ATT TAG GTG ACA CTA TAG	45	pGEM-T (Easy) vector	Colony-PCR, Sequencing-PCR	Promega
T7	GTA ATA CGA CTC ACT ATA GGG	50	pGEM-T (Easy) vector	Colony-PCR, Sequencing-PCR	Promega

Tab. 8. Oligonucleotide primers applied to the study of Sponge Orange Band- as well as Sponge White Patch disease.

9. Markers

The DNA-markers applied during gel electrophoreses were both derived from MBI-Fermentas Life Sciences (Fig. 1). They were either 100bp- or 1kb-DNA-ladders. For denaturing gradient gel electrophoresis the markers DGGE I and DGGE II were applied, which were obtained from Nippon Gene and distributed by WAKO. During a DGGE run 5µl of the respective marker were applied to a single polyacrylamide gel. Staining of the gel was performed as usual for DGGE with either SYBR® Gold or Ethidium Bromide (see Methods: page 30f).

100bp DNA Ladder **1kb DNA Ladder** **DGGE Markers I & II**

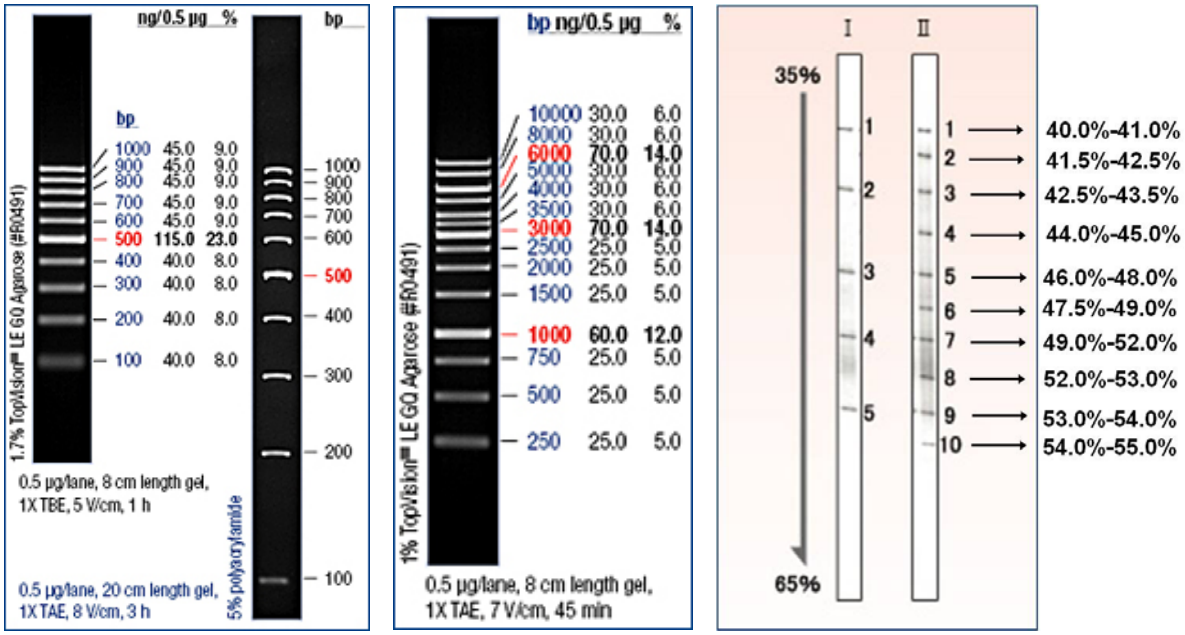

Fig. 1. Markers applied to this thesis: GeneRuler™ 100bp DNA Ladder and GeneRuler™ 1kb DNA Ladder (both Fermentas) were used for normal gel electrophoresis, whereas DGGE Marker I and II (both Nippon Gene) were applied to denaturing gradient gel electrophoresis (DGGE).

10. Vectors & Microorganisms

List of bacterial strains and vector used for the cloning approach:

- ***Escherichia coli*** **Stamm XL1 blue** (for the cloning of PCR-products via electroporation):

  Genotype: *endA1 gyrA96(nal^R) thi-1 recA1 relA1 lac glnV44 F'[::Tn10 proAB$^+$ lacI^q Δ(lacZ)M15] hsdR17(rk$^-$mk$^+$)*

- ***Escherichia coli*** **Stamm Novablue** (for the cloning of PCR-products via heat shock):

  Genotype: *endA1 hsdR17* (r_{K12}^- m_{K12}^+) *supE44 thi-1 recA1 gyrA96 relA1 lac F'*[*proA$^+$B$^+$lacI^q*ZD*M15*::Tn*10*] (Tet^R)

- **Vector pGEM®-T Easy** (Promega, Cat.# A1360) served as cloning vector:

  It consists of 3015bp and harbours an Ampicillin-resistance and a multiple cloning-site that is located within the lacZ-gene (Fig. 2). After vector transformation into the strain *E. coli* Novablue, the culture has been grown on AIX-plates containing Ampicillin, IPTG and X-Gal for growth-selection. If the PCR-product had been integrated successfully within the vector's cloning site, the lacZ-gene was hampered to produce β–galactosidase. The latter is responsible for the destruction of X-Gal under the elicitor IPTG and results in the blue appearance of colony morphology. If therefore the production of blue coloration is disturbed, a white appearance of the respective bacterial colony arises. The white colonies were preferred during this cloning approach, which is commonly called 'Blue-White-Screen'.

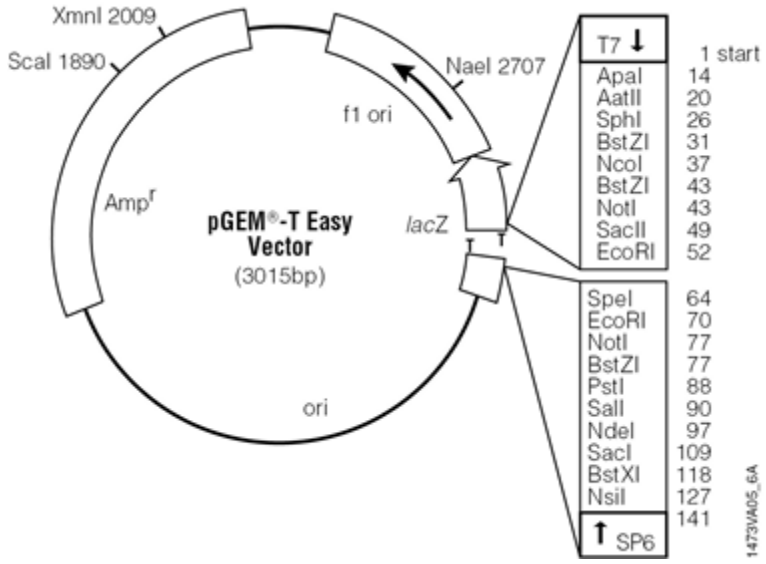

Fig. 2. The Vector pGEM-T Easy and its multiple cloning site framed by the promoters T7 and SP6.

11. Applied Software

Software	Application	Reference
ABI Prism Software	Evaluation and documentation of sequence chromatograms	http://www.appliedbiosystems.com/support/software/3100/conversion.cfm
Adobe Photoshop 7.0	Editing of underwater photographies; scaling of SEM & TEM micrographs	http://www.adobe.com/
Align	Sequence alignment	Hepperle (2002)
ARB	Phylogenetic tree construction based on 16S rDNA genes	Ludwig *et al.* (2004b)
Basic Local Alignment Search Tool (BLAST)	Comparison of self-obtained sequences to the ones deposited in GenBank	http://www.ncbi.nlm.nih.gov/BLAST/
ClustalX	Alignment of sequences	http://www-igbmc.u-strasbg.fr/BioInfo/ClustalX/Top.html
DivX V8.0	Editing of self-made videos	http://www.divx.com
Gel-Pro Express V4.0	Documentation of fluorescence micrographs	http://www.intas.de
HPLC software	Data analysis and documentation	Jasco-Borwin
Microsoft Office 2007 (Excell, Powerpoint, Word)	Data analysis, presentation and documentation	Microsoft Corporation
MovieMaker V5.1	Editing of self-made movies	Microsoft Corporation
Multi Analyst 1.1	Documentation of agarose and polyacrylamide gels	BioRad
NCBI GenBank	For sequence comparison and deposition	http://www.ncbi.nlm.nih.gov/
Pintail	Chimera check of the obtained 16S rDNA	http://www.bioinformatics-toolkit.org/Pintail/index.html
Quantity One	For DGGE banding pattern comparisons among each other	BioRad
SEM software	Documentation and conversion of SEM-images	Soft imaging systems SIS based on analySIS Scandium
SILVA	Phylogenetic tree construction based on 16S rDNA	Pruesse *et al.* (2007a)
Treeview	Visualization of phylogenetic trees	http://taxonomy.zoology.gla.ac.uk/rod/treeview.html
Vector NTI Advance™ 11	ContigExpress for sequence editing	Invitrogen

Tab. 9. Applied computer programs and online-tools as well as their application and references.

IX. Publications

- Schmitt S, **Angermeier H**, Schiller R, Weisz JB, Lindquist N, Hentschel U (2008). Molecular microbial diversity survey of sponge reproductive stages and mechanistic insights into vertical transmission of microbial symbionts. *Appl Environ Microbiol* **74** (24): 7694-708.

- **Angermeier H**, Kamke J, Abdelmohsen UR, Krohne G, Pawlik JR, Lindquist NL, Hentschel U (2011). The pathology of sponge orange band disease affecting the Caribbean barrel sponge *Xestospongia muta*. *FEMS Microbiology Ecology* **75** (2): 218–230.

X. Symposia

Angermeier H, Kamke J, Abdelmohsen UR, Glöckner V, Krohne G, Pawlik JR, Lindquist N, Hentschel U (2011). Sponge Orange Band affecting *Xestospongia muta* and Sponge White Patch affecting *Amphimedon compressa*. 1st International Symposium on Sponge Microbiology, Würzburg, Germany (poster).

Angermeier H, Kamke J, Abdelmohsen UR, Krohne G, Pawlik JR, Lindquist N, Hentschel U (2010). Sponge Orange Band disease affecting the Caribbean sponge *Xestospongia muta*. EURO ISRS symposium 2010: Reefs in a Changing Environment, Wageningen, the Netherlands (invited speaker & representative chair of the session: Reef Health and Reef Rehabilitation).

Angermeier H, Kamke J, Abdelmohsen UR, Krohne G, Pawlik JR, Lindquist N, Hentschel U (2010). Sponge Orange Band disease affecting the Caribbean sponge *Xestospongia muta*. 2nd VAAM Workshop on Symbiotic Interactions 2010, Würzburg, Germany (invited speaker).

Angermeier H, Kamke J, Abelmohsen UR, Krohne G, Pawlik JR, Lindquist N, Hentschel U (2010). Sponge Orange Band disease affecting the Caribbean sponge *Xestospongia muta*. VIII World Sponge Conference 2010, Girona, Spain (invited speaker).

Angermeier H, Kamke J, Pawlik JR, Lindquist N & Hentschel U (2009). Sponge Orange Band and Sponge White Patch: Diseases of Caribbean sponges. Journées européennes de Bactériologie 2009. Lorient, France (invited speaker).

Angermeier H, Pawlik JR, Krohne G & Hentschel U (2009). Caribbean Sponge Diseases: Sponge Orange Band in *X. muta* and Sponge White Patch in *A. compressa.* 6th Congress of the International Symbiosis Society (ISS) 2009. Madison, Wisconsin, USA (poster).

Angermeier H, Pawlik JR, Krohne G & Hentschel U (2009). Sponge Orange Band and Sponge Whitening: Diseases of Caribbean sponges. Doctoral Students Symposium 2009. University of Würzburg, Germany (poster).

Angermeier H, Pawlik JR, Krohne G & Hentschel U (2009). Sponge Orange Band and Sponge Whitening: Diseases of Caribbean sponges. Annual Meeting of the Association for General and Applied Microbiology (VAAM) 2009. Bochum, Germany (poster).

Angermeier H, Pawlik JR, Krohne G & Hentschel U (2008). The pathology of Sponge Orange Band disease in the Caribbean sponge *Xestospongia muta*. 1st GSLS Fellow Retreat of the University of Würzburg 2008, Castle Zeilitzheim, Germany (invited speaker).

XI. Workshops

- *Control of Infectious Tropical Diseases* at the Medical Mission Institute, Würzburg, 23rd-24th November 2010.

- *First Aid Class* including CPR training of the Bavarian Red Cross (DRK) in Würzburg, 10th-11th April 2007

- *Lebensrettende Sofortmaßnahmen (Ersthelfer)* of the Bavarian Red Cross (DRK), Würzburg, August 2009.

- Various classes offered by the Graduate School of Life Sciences (GSLS) at the University of Würzburg: *Giving Academic Talks in English*, *Poster Presentation*, *Scientific Writing*, *Statistics*, *How to apply in English.*

XII. Summer Academies

26th July - 6thAugust 2010: Participation at the **Summer Academy *Global Health*** organized by the Medical Mission Institute, Würzburg, under PD Dr. August Stich.

August 2007 & 2008: Participation including presentation at the **Summer School of BiotecMarin & the Marie Curie Research Training Network (EU)** about the phylum *Porifera* at the Ruđer Bošković Institute in Rovinj, Croatia, under Prof. W.E.G. Müller (University of Mainz, Germany).

XIII. Field Work

September 2009: Field work at the National Undersea Research Center (NURC), based at Key Largo within the Florida Keys National Marine Sanctuary, under instruction of Prof. Christopher Martens and Prof. Niels Lindquist (UNC/CH, USA).

May & June 2008: Research expedition onboard the research vessel RV Seward Johnson (HBOI) under instruction of Prof. Joseph Pawlik (UNCW, USA).

November & December 2007: Field work at the National Undersea Research Center (NURC), based at Key Largo within the Florida Keys National Marine Sanctuary, under instruction of Prof. Joseph Pawlik (UNCW, USA).

June 2007: Research expedition onboard the research vessel RV Seward Johnson (HBOI) under instruction of Prof. Joseph Pawlik (UNCW, USA).